

Double-Layer Systems at Zero Magnetic Field

C. B. Hanna, Dylan Haas*, and J. C. Díaz-Vélez

Department of Physics, Boise State University, Boise, Idaho 83725

(February 1, 2008)

We investigate theoretically the effects of intralayer and interlayer exchange in biased double-layer electron and hole systems, in the absence of a magnetic field. We use a variational Hartree-Fock-like approximation to analyze the effects of layer separation, layer density, tunneling, and applied gate voltages on the layer densities and on interlayer phase coherence. In agreement with earlier work, we find that for very low layer separations and layer densities, an interlayer-correlated ground state possessing spontaneous interlayer coherence (SILC) is obtained, even in the absence of interlayer tunneling. In contrast to earlier work, we find that as a function of total density, there exist four, rather than three, distinct noncrystalline phases for balanced double-layer systems without interlayer tunneling. The newly identified phase exists for a narrow range of densities and has three components and slightly unequal layer densities, with one layer being spin-polarized and the other unpolarized. An additional two-component phase is also possible in the presence of sufficiently strong bias or tunneling. The lowest-density SILC phase is the fully spin- and pseudospin-polarized “one-component” phase discussed by Zheng and co-workers [Phys. Rev. B **55**, 4506 (1997)]. We argue that this phase will produce a finite interlayer Coulomb drag at zero temperature due to the SILC. We calculate the particle densities in each layer as a function of the gate voltage and total particle density, and find that interlayer exchange can reduce or prevent abrupt transfers of charge between the two layers. We also calculate the effect of interlayer exchange on the interlayer capacitance.

PACS numbers: 71.45.Gm, 73.20.Dx, 73.40.Gm, 73.40.Kp

I. INTRODUCTION

In the last several years, double-layer electron and hole systems have provided an exceptionally useful tool for investigating the effects of interparticle Coulomb interactions in two dimensions, particularly at low particle densities where exchange and correlation effects are significant. This has been especially true in the quantum Hall regime,^{1,2} where the combination of a strong perpendicular magnetic field (which quenches the kinetic energy) and very small layer separation (which enhances interlayer exchange) stabilizes remarkable interlayer-coherent quantum Hall states.^{3–9} Even in the absence of any magnetic field, interlayer capacitance and drag measurements in double-layer electron systems (2LES’s) have provided quantitative measures of the effects of electronic interactions on both the thermodynamics¹⁰ and transport (Coulomb drag¹¹) of two-dimensional electron and hole

systems. Unless otherwise specified, we shall take the notation 2LES to also include double-layer hole systems.

Our work is motivated by the rapid pace of advancements in the engineering of double-layer semiconductor devices. We expect that high-mobility double-layer devices will eventually be built with both (1) *separately contactable* layers, and (2) layer separations and carrier densities so small that the *interlayer* correlations between the carriers are substantial, perhaps even without the aid of a strong quantizing magnetic field. Such devices will allow direct measurements of the effects interlayer many-body effects in double-layer systems. As a starting point to analyze the zero magnetic field situation, we have developed a simple mean-field model that incorporates both intralayer and interlayer exchange in biased double-layer electron and hole systems in the absence of a magnetic field. We use the model to calculate theoretically the effect of interlayer exchange on the layer densities and interlayer capacitance as a function of layer spacing, particle density, and applied gate voltage.

Gated double-layer systems have the great advantage of allowing the layer densities of electrons or holes to be varied by the application of a bias (gate voltage). At high densities, the kinetic energy per unit area dominates the exchange and correlation energies, and in a translationally invariant system, the symmetry and properties of the ground state of a many-body system are in one-to-one correspondence with those of a free-electron gas. At lower electron densities, the Coulombic exchange and correlation energies can produce qualitative changes in the nature of the many-particle ground state: numerical work on two- and three-dimensional electron gases show that a spin ferromagnetic state is obtained at low densities, which is eventually supplanted by a Wigner crystal state at the lowest densities. The low-density ferromagnetic state of the interacting electron gas was anticipated some 70 years ago by Bloch;¹² ferromagnetism can be found even within the Hartree-Fock approximation when the exchange interaction energy, which favors occupation of single-particle states of the same spin, dominates the kinetic energy, which favors reducing the Fermi energy by equal occupation of both spin states.

Multilayer semiconductor devices enhance the effects of interparticle interactions through the combination of reduced dimensionality and low particle density, and by the presence of an additional electronic degree of freedom, the layer index.¹³ In double-layer systems, layer occupancy can be specified by introducing a pseudospin variable that points up for one layer and down for the other layer.¹⁴ Extending the notion of an exchange-driven

ferromagnetic transition to double-layer systems suggests that at low enough densities, the electronic ground state should be both spin and pseudospin polarized. Such reasoning, supported by Hartree-Fock calculations, led Ruden and Wu to propose that, at low enough electron densities and for small enough layer separations, the electrons of a 2LES would minimize their ground-state energy by having all electrons occupy a single layer.¹⁵ The Ruden-Wu scenario implies that as the total density of a balanced 2LES is lowered, the electrons should eventually experience an interlayer charge transfer instability that spontaneously empties out one of the two layers. Ruden and Wu also suggested that the inherent bistability of the resulting low-density 2LES (either layer could be the one to lose or gain particles) would constitute an exchange-driven logic gate. The possibility of an exchange-driven interlayer charge-transfer instability has been a subject of both theoretical^{15–18} and experimental^{19–22} interest.

Although pseudospin polarization at sufficiently low densities is likely, it does not require unequal layer densities. This has been demonstrated theoretically in great detail for closely spaced double-layer systems in a strong magnetic field at unit filling factor and appears to give a good explanation of experimental results.^{6–8} The key point is that electrons in double-layer structures are not restricted to occupying only one of two layer eigenstates: quantum mechanics allows states that are superpositions of the two layers. The layer pseudospin must therefore be treated as a Heisenberg variable, as was done in Refs. 6 and 7 in the quantum Hall regime, and by Zheng and co-workers in zero magnetic field,¹⁷ rather than as an Ising variable (where only “up” and “down” allowed) as was done by Ruden and Wu. For example, when interlayer tunneling is present, the single-particle eigenstates are symmetric and antisymmetric combinations of layer states. A major insight of Refs. 6–8 was the concept of “spontaneous interlayer coherence” (SILC): at sufficiently small layer separations, electrons can spontaneously create and occupy linear combinations of layer states in which each layer has the same average number of electrons, *even without any interlayer tunneling*. The spontaneous formation of superposed layer states in double-layer quantum Hall (2LQH) systems can be accomplished by the interlayer exchange interaction alone. SILC in balanced 2LQH systems corresponds to XY pseudospin ferromagnetism in which the pseudospins spontaneously magnetize, but do not point either up or down, since neither layer has (on average) more particles than the other.⁶

The application of SILC to the zero magnetic field case was first made by Zheng and co-workers,¹⁷ who considered the same model system as Ruden and Wu¹⁵ – electrostatically balanced zero-thickness layers of interacting electrons without interlayer tunneling – but came to a very different conclusion. They proved within the Hartree-Fock approximation (HFA) that (1) the 2LES becomes spin ferromagnetic before it becomes pseudospin ferromagnetic for any finite layer separation (this possi-

bility was not considered by Ruden and Wu), and (2) at low enough densities and small enough layer separations, the pseudospin ferromagnetic state possesses SILC, with all electrons occupying one subband composed of a superposition of layer states with equal average density in each layer. Conti and Senatore have also argued that for electrostatically balanced layers, the 2LES ground state cannot be one in which all electrons are eigenstates of the same single layer¹⁸. SILC at sufficiently small layer separations should also follow from earlier calculations presented in Ref. 23, although no explicit inference of SILC was made in that work. Recent work that goes beyond the HFA and includes correlation effects within the STLS approximation²⁴ also finds that SILC is favored over single-layer occupancy for balanced layers that are sufficiently close together.²⁵

When studying a 2LES using a density-functional approach, it is important to note that SILC is a nonlocal effect. Calculations based on local-density approximations will not find SILC if they treat the pseudospin as an Ising-like variable.¹⁷ The same caveat applies to the work of Ruden and Wu, who used a restricted HFA that excluded the possibility of SILC. Once the intralayer separation between electrons becomes comparable to the interlayer separation between layers, the possibility of interlayer correlations (such as SILC) must be considered. The spontaneous charge-transfer state predicted by Ruden and Wu follows quite generally (even beyond the HFA) from the fact that when interlayer correlations are ignored, the negative compressibility of the electron gas guarantees an interlayer charge-transfer instability at sufficiently small layer spacing. But it is precisely at small layer spacings that interlayer correlations become important, and so their effects must be included to obtain physically meaningful results.

We have extended the study the effects of Coulombic exchange in double-layer electron and hole systems to include an applied bias due to front and back gate voltages, while allowing for the possibility interlayer exchange. In the balanced case, we have found that the four- to two-component transition is always interrupted by the presence of a three-component phase with slightly unequal layer densities. There are therefore four possible noncrystalline phases for a 2LES with balanced gates. Under bias or tunneling a second (pseudospin-polarized) two-component state is also possible. We have enumerated the transitions between the five allowed states in the presence of bias, and explored the effects of bias on the one-component state.

The rest of this paper is organized as follows: In Sec. II, we introduce a simplified model for double-layer systems, review the concept of interlayer capacitance, and give a general criterion for stability against spontaneous interlayer charge transfer. In Sec. III, we develop a mean-field approximation for biased double-layer systems that allows for the possibility of interlayer coherence. In Sec. IV, we examine the special case of electrostatically balanced layers, enumerate the resulting four possible noncrys-

talline phases, and explore the onset of interlayer coherence and its effect on the size of the subband splitting. We also obtain a phase diagram for the balanced case, and perform an alternate calculation for the onset of the one-component phase. In Sec. V, we explore the effect of bias on the layer occupancies and interlayer capacitance for large, intermediate, and small layer separations. We develop simple models capable of closely fitting experimental layer-occupancy data, and explore the transitions between different phases induced by layer imbalance. In Sec. VI, we analyze the onset and properties of the one-component state under bias. We summarize our findings and speculate on the possible relevance of these results to the strong magnetic-field regime in Sec. VII.

II. DOUBLE-LAYER MODEL AND INTERLAYER CAPACITANCE

In this section, we introduce an idealized model of double-layer systems. We review the condition for thermodynamic equilibrium between the inner layers, obtain a necessary condition for stability against interlayer charge transfer, and review an experimentally useful measure of the interlayer capacitance, the Eisenstein ratio.¹⁰

Figure 1 illustrates schematically the geometry of the 2LES device. We treat the quantum wells as zero-thickness layers sandwiched between two plates of neutralizing charge, which represent the effects of the front and back gates, which represent the effects of the front and back gates. The distance between the front gate (at far left) and the first layer (layer 1) is D_F ; that between the back gate (at far right) and the second layer (layer 2) is D_B ; the interlayer separation is denoted by d . Typically, $d \sim 10$ nm, $D_F \sim 1\mu\text{m}$, and $D_B \sim 1$ mm, so that $d \ll D_F \ll D_B$; thus, Fig. 1 is not at all to scale.

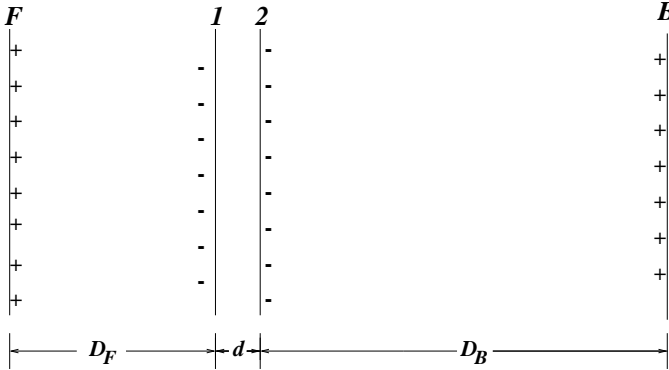


FIG. 1. Schematic figure of a double-layer device with front-gate surface charge density ep_F at left, areal charge densities $-en_1$ and $-en_2$ in the quantum wells, and back-gate surface charge density ep_B at right.

The two inner layers are assumed to be in thermodynamic equilibrium with each other, and the voltage of the front (back) gate relative to the common chemical potential of the inner layers is denoted by V_F (V_B). It is also assumed that small changes δV_α in the gate voltages V_α

$(\alpha = F, B)$ produce small changes in surface charge densities only at the gates ($e\delta p_\alpha$) and in the layers ($-e\delta n_i$, $i = 1, 2$). Overall charge neutrality requires that the total charge density vanish:

$$ep_F + ep_B - en_1 - en_2 = 0. \quad (1)$$

(Strictly speaking, we only require that the *change* in the total charge density vanish: $\delta ep_F + \delta ep_B - \delta en_1 - \delta en_2 = 0$.) In writing Eq. (1), we have assumed that any stray charge not included in Eq. (1) is unchanged when the gate voltages are varied. This implies that the only significant effect of the stray charges is to shift the gate voltages by constant (empirically determined) amounts. Sheet charge densities on the gates and inner layers produce electric fields between the double-layer and the gates (E_α) and between the two layers (E_{12}) according to Gauss's law,

$$\begin{aligned} E_\alpha &= (e/\epsilon)p_\alpha, \\ E_{12} &= (e/\epsilon)(p_F - n_1) = (e/\epsilon)(n_2 - p_B). \end{aligned} \quad (2)$$

We now obtain the conditions for thermodynamic equilibrium and stability between the layers. Regarding the gate charge densities p_α as fixed quantities, we seek the values of the particle density in the inner layers that minimize the total energy per unit area $\mathcal{E}_0/L_x L_y$. Following Ref. 26, we separate the electrostatic part of the total energy per unit area from the rest:

$$\frac{\mathcal{E}_0}{L_x L_y} = \frac{\epsilon}{2} E_{12}^2 d + \varepsilon(n_1, n_2), \quad (3)$$

up to an irrelevant constant, where the first term is the interlayer electrostatic energy density, with E_{12} given by Eq. (2). The quantity $\varepsilon(n_1, n_2)$ represents the total energy per unit area for a fully interacting double-layer system in which each layer contains a uniform neutralizing charge density, for particle densities n_1 and n_2 in layers 1 and 2, respectively. The Fermi, exchange, and correlation energies, both intralayer and interlayer, are contained in $\varepsilon(n_1, n_2)$, and it is this quantity that is calculated using many-body techniques.²⁶ In the next section, we make an approximate calculation of $\varepsilon(n_1, n_2)$ which includes the effects of interlayer and intralayer exchange.

To obtain the condition for thermodynamic equilibrium between the inner layers, we note that for fixed external charge densities p_α , the constraint of overall charge neutrality implies that the particle density in one layer (e.g., n_1) is determined by that in the other layer (e.g., n_2): $n_1 = p_F + p_B - n_2$. We may thus regard the total energy per unit area $\mathcal{E}_0/L_x L_y$ as a function of the layer density n_2 , and extremize $\mathcal{E}_0/L_x L_y$ with respect to n_2 at fixed p_F and p_B to obtain^{10,26}

$$\mu_1 - \mu_2 = eE_{12}d, \quad (4)$$

where

$$\mu_i \equiv \partial \varepsilon(n_1, n_2) / \partial n_i \quad (5)$$

is the chemical potential measured relative to the energy minimum of layer i . Equation (4) states that the difference in the layer values of the chemical potential is equal to the electrostatic potential energy difference between the layers. If the equation of state determining $\mu_i(n_1, n_2)$ were known, then Eqs. (2) and (4) would together determine the values of layer densities n_1 and n_2 for which the total energy $\mathcal{E}_0/L_x L_y$ is an extremum.

We now examine a necessary condition for interlayer thermodynamic stability (i.e., for the local extremum to be a local minimum of the energy). First we follow Ref. 10 and introduce a set of lengths that describe the dependence of the layer chemical potentials μ_i on the layer densities n_j ,

$$s_{ij} \equiv \frac{\epsilon}{e^2} \frac{\partial \mu_i}{\partial n_j} = \frac{\epsilon}{e^2} \frac{\partial^2 \varepsilon}{\partial n_j \partial n_i}. \quad (6)$$

For the extremum condition in Eq. (4) to represent a local minimum of the total energy per unit area, we require that the second derivative of $\mathcal{E}_0/L_x L_y$ with respect to n_2 be positive. (We again regard n_1 as being determined by n_2 for fixed p_α by the requirement for overall charge neutrality.) This gives a necessary condition for stability:

$$d + s_1 + s_2 > 0, \quad (7)$$

where

$$s_1 \equiv s_{11} - s_{12}, \quad s_2 \equiv s_{22} - s_{21}. \quad (8)$$

The above inequality guarantees that the 2LES is at least metastable. If Eq. (7) is violated, then the layer densities constitute a local energetic maximum rather than a local minimum, and there will be an interlayer charge instability that causes charge to flow between the layers until a new energetic minimum is reached.

In the absence of interlayer correlations (the case considered in Refs. 15 and 10), $s_{12} = s_{21} = 0$, and the length s_{ii} is directly related to the electronic compressibility κ_i in layer i according to²⁶

$$s_{ii} = \frac{\epsilon}{e^2 n_i^2 \kappa_i}. \quad (9)$$

Equations (7) and (9) together with the experimentally measured negative compressibility ($\kappa < 0$) of the electrons imply that when interlayer correlations are ignored ($s_{12} = 0$), sufficiently small interlayer separation d will always lead to a charge-transfer instability when the density of either (or both) layer is sufficiently small. This result is true even when intralayer correlations are included beyond the HFA calculation of Ruden and Wu; only interlayer correlations that produce sufficiently negative values of s_{12} to satisfy Eq. (7) can suppress interlayer charge-transfer instabilities at very small interlayer separations.

If the two layers of the 2LES sample can be contacted separately, then the Eisenstein ratio R_E provides a sensitive measure of the interlayer capacitance that avoids the

large gate-distance factors that dominate the gate capacitances per unit area.^{10,26} The Eisenstein ratio is defined as the ratio of the differential change in the electric field E_{12} between the inner layers to that of the electric field E_F between the front gate and the inner layers:

$$R_E \equiv \frac{\delta E_{12}}{\delta E_F} = 1 - \delta n_1 / \delta p_F, \quad (10)$$

where we have made use of Gauss's law, Eq. (2). In the following sections, we calculate the layer occupancies n_i as a function of the gate charges p_α ; we then use Eq. (10) to obtain R_E by computing the derivative of n_1 with respect to p_F . In the classical limit (corresponding to large enough particle densities and layer separations so that only the electrostatic energies are relevant), $n_1 = p_F$ (for $p_F > 0$), so that by Eq. (10), $R_E = 0$. Note also that if $n_1 = 0$ (e.g., due to $p_F < 0$), then $R_E = 1$. By using Eqs. (4) and (6) to express differential changes in E_{12} in terms of the electronic lengths s_{ij} and using Gauss's law, the Eisenstein ratio may be expressed as

$$R_E = \frac{s_1 - s_2 \delta E_B / \delta E_F}{d + s_1 + s_2}. \quad (11)$$

The Eisenstein ratio has an especially simple form for fixed total density since then $\delta E_B = -\delta E_F$; from Eq. (11), $R_E = s/(d + s)$, where $s \equiv s_1 + s_2$. However, most experiments fix the back-gate voltage V_B rather than the total density, and sweep the front-gate voltage V_F . Because of the relatively large size of the back-gate distance D_B , the constraint of fixed back-gate voltage ($\delta V_B = 0$) is very nearly equivalent to that of fixed back-gate sheet charge density ($\delta p_B = 0$ or, by Gauss's law, $\delta E_B = 0$). For $\delta E_B = 0$, Eq. (11) shows that the Eisenstein ratio is very nearly

$$R_E \approx (\delta E_{12} / \delta E_F)_{p_B} = \frac{s_1}{d + s_1 + s_2}. \quad (12)$$

The advantage of measuring R_E rather than the usual gate capacitances per unit area (such as $e\delta p_F / \delta V_F$) is that R_E depends only on the electronic lengths s_i and the interlayer distance d , not on the much larger gate distances D_α . The difficulty in measuring R_E is that (at least one of) layers 1 and 2 must be separately contactable, which becomes increasingly difficult as the layer separation d becomes very small. Nonetheless, measurements of the Eisenstein ratio have been used to demonstrate the negative compressibility of the electron gas,¹⁰ and it is to be expected that devices with separately contactable layers will be built with increasingly narrow layer separations. Note also that R_E is very sensitive to charge-transfer instabilities. In fact, from Eq. (7), the condition for the onset of an instability to interlayer charge transfer, $d + s_1 + s_2 = 0$, shows that R_E formally diverges at the instability. This can also be seen from the relation $R_E = 1 - \delta n_1 / \delta p_F$, since a charge transfer instability would produce an abrupt change in the layer

density n_1 in response to a small change in the gate density p_F . Although evidence for abrupt interlayer charge transfers has been reported based on Shubnikov-de Haas (SdH) measurements,¹⁹ the Eisenstein ratio would be a far more sensitive measure of abrupt interlayer charge transfers.

In subsequent sections, we calculate the layer densities n_i as a function of the front-gate particle density p_F , for fixed back-gate particle density p_B . Fortunately, p_B may be found experimentally from SdH measurements as the value of the layer densities when the system is balanced: i.e., for equal layer densities ($n_1 = n_2$) and minimum subband separation ($n_a - n_b$). Once p_B (which we assume is very nearly constant) is known, p_F may be determined from charge conservation by measuring the total layer density, either by SdH (as the sum of the subband densities) or by Hall effect measurements. It is therefore possible to determine p_F experimentally, without recourse to the gate voltages. Of course, experimentally, it is V_F that is varied directly while V_B is kept fixed, and p_F changes in response to V_F (while p_B changes very little for large D_B). We describe how the gate voltages may be determined from a knowledge of p_F, p_B , and μ_i in Sec. A 1 of the Appendix.

III. MEAN-FIELD APPROXIMATION

In this section, we introduce the microscopic Hamiltonian for the gated double-layer system and make a variational approximation for the ground-state wave function that allows for interlayer coherence. The resulting approximate ground-state energy per unit area depends on both intralayer and interlayer exchange.

We now consider the microscopic Hamiltonian for the double-layer system illustrated in Fig. 1. We idealize the inner layers as being two-dimensional, and treat interlayer tunneling in the tight-binding approximation. The Hamiltonian for the interacting system is then

$$\begin{aligned} \mathcal{H} = & \sum_{j\mathbf{k}s} \varepsilon_k c_{j\mathbf{k}s}^\dagger c_{j\mathbf{k}s} - t \sum_{\mathbf{k}s} (c_{1\mathbf{k}s}^\dagger c_{2\mathbf{k}s} + c_{2\mathbf{k}s}^\dagger c_{1\mathbf{k}s}) \quad (13) \\ & + \frac{1}{2L_x L_y} \sum_{\mathbf{q}} \sum_{j_1 \mathbf{k}_1 s_1} \sum_{j_2 \mathbf{k}_2 s_2} V_{j_1 j_2}(q) \\ & \times c_{j_1 \mathbf{k}_1 + \mathbf{q} s_1}^\dagger c_{j_2 \mathbf{k}_2 - \mathbf{q} s_2}^\dagger c_{j_2 \mathbf{k}_2 s_2} c_{j_1 \mathbf{k}_1 s_1} \\ & - \sum_{j\mathbf{k}s} \sum_{\alpha} V_{j\alpha}(q=0) p_{\alpha} c_{j\mathbf{k}s}^\dagger c_{j\mathbf{k}s} \\ & + \frac{L_x L_y}{2} \sum_{\alpha\beta} V_{\alpha\beta}(q=0) p_{\alpha} p_{\beta}, \end{aligned}$$

where $c_{j\mathbf{k}s}$ ($c_{j\mathbf{k}s}^\dagger$) denotes the second-quantized destruction (creation) operator for an electron or hole in layer j with momentum $\hbar\mathbf{k}$ and spin s . Here $\varepsilon_k = \hbar^2 k^2 / 2m^*$ is the kinetic energy in the effective mass (m^*) approximation, t is the interlayer tunneling amplitude, and the Fourier-transformed Coulomb potential is given by

$$V_{ij}(q) = \frac{e^2}{2\epsilon q} e^{-qd_{ij}}, \quad (14)$$

where d_{ij} is the distance between layer i and layer j . The indices α, β in Eq. (14) take the values F (front gate) or B (back gate), $V_{\alpha\beta}$ is the direct Coulomb interaction between gates α and β , and $V_{\alpha j}$ is the direct Coulomb interaction between gate α and layer j . The last two terms in Eq. (14) represent the direct interaction between the layers and gates, and between front and back gates, respectively.

We use a mean-field approximation (MFA) that is variationally based and that reduces to the Hartree-Fock approximation for the balanced case of equal layer densities. This approximation includes the effects of interlayer correlations in the simplest possible way. The variational ground-state wave function is composed of two subbands, a and b , containing spin up (\uparrow) and spin down (\downarrow) electrons:

$$|\Psi_0\rangle = \prod_{\mathbf{k}_4}^{k_4 \leq k_{b\downarrow}} b_{\mathbf{k}_4\downarrow}^\dagger \prod_{\mathbf{k}_3}^{k_3 \leq k_{b\uparrow}} b_{\mathbf{k}_3\uparrow}^\dagger \prod_{\mathbf{k}_2}^{k_2 \leq k_{a\downarrow}} a_{\mathbf{k}_2\downarrow}^\dagger \prod_{\mathbf{k}_1}^{k_1 \leq k_{a\uparrow}} a_{\mathbf{k}_1\uparrow}^\dagger |0\rangle, \quad (15)$$

where k_{as} and k_{bs} denote the Fermi wave vectors for electrons or holes of spin s in subbands a and b . The creation operators for the subbands are related to the layer creation operators by a canonical transformation that we take to be of the form

$$\begin{aligned} a_{\mathbf{k}s}^\dagger &= \cos(\theta/2) c_{1\mathbf{k}s}^\dagger + \sin(\theta/2) e^{i\phi} c_{2\mathbf{k}s}^\dagger \quad (16) \\ b_{\mathbf{k}s}^\dagger &= -\sin(\theta/2) e^{-i\phi} c_{1\mathbf{k}s}^\dagger + \cos(\theta/2) c_{2\mathbf{k}s}^\dagger \end{aligned}$$

When $\theta = \pi/2$ and $\phi = 0$, subband a is the symmetric subband and subband b is the antisymmetric subband. In the language of pseudospin, the superposition of layer states in Eq. (17) corresponds to treating the layer pseudospin as a Heisenberg, rather than an Ising, spin variable.¹⁷ The form of the canonical transformation in Eq. (17) is not completely equivalent to a fully self-consistent Hartree-Fock calculation because we have taken θ and ϕ to be independent of the wave vector \mathbf{k} and spin s . It would be interesting to explore the effects of including the \mathbf{k} and s dependence of θ and ϕ in a future calculation. Our simpler variational calculation, which is equivalent to Ref. 17 for the special case of balanced layers, offers a reasonable starting point, which is probably qualitatively correct over a large range of layer densities. It certainly gives layer densities that are in close agreement with experimental values obtained from SdH measurements, as we shall show.

The layer occupation numbers may be expressed in terms of the subband occupation numbers by using Eq. (17):

$$\begin{aligned} \langle c_{1\mathbf{k}s}^\dagger c_{1\mathbf{k}s} \rangle &= \cos^2(\theta/2) \langle a_{\mathbf{k}s}^\dagger a_{\mathbf{k}s} \rangle + \sin^2(\theta/2) \langle b_{\mathbf{k}s}^\dagger b_{\mathbf{k}s} \rangle \quad (17) \\ \langle c_{2\mathbf{k}s}^\dagger c_{2\mathbf{k}s} \rangle &= \sin^2(\theta/2) \langle a_{\mathbf{k}s}^\dagger a_{\mathbf{k}s} \rangle + \cos^2(\theta/2) \langle b_{\mathbf{k}s}^\dagger b_{\mathbf{k}s} \rangle \end{aligned}$$

$$\begin{aligned}\langle c_{1\mathbf{k}s}^\dagger c_{2\mathbf{k}s} \rangle &= \sin(\theta/2) \cos(\theta/2) e^{i\phi} (\langle a_{\mathbf{k}s}^\dagger a_{\mathbf{k}s} \rangle - \langle b_{\mathbf{k}s}^\dagger b_{\mathbf{k}s} \rangle) \\ \langle c_{2\mathbf{k}s}^\dagger c_{1\mathbf{k}s} \rangle &= \langle c_{1\mathbf{k}s}^\dagger c_{2\mathbf{k}s} \rangle^*,\end{aligned}$$

where the asterisk denotes complex conjugation, and we have used Eq. (15) to eliminate cross terms such as $\langle a_{\mathbf{k}s}^\dagger b_{\mathbf{k}s} \rangle$. SILC occurs when

$$\langle c_{1\mathbf{k}s}^\dagger c_{2\mathbf{k}s} \rangle \neq 0 \quad (18)$$

in the absence of interlayer tunneling. According to Eqs. (18) and (18), SILC requires that the following occurs: (1) $\theta \neq 0, \pi$ so that the subband densities are different from the layer densities. SILC is therefore excluded when the pseudospin is treated as an Ising variable. (2) $n_a \neq n_b$ so that the subband densities are not equal (nonzero pseudospin polarization). When $n_{as} = n_{bs}$ (completely unpolarized pseudospin), the MFA ground state can be expressed as the product of two uncorrelated single-layer wavefunctions by performing a global pseudospin rotation.

Although it is straightforward to generalize our approach to finite temperature, we calculate numerical results in the limit of zero temperature ($T = 0$), both for the sake of simplicity and because measurements can (and have) been made on double-layer systems at low temperatures, even down to millikelvin temperatures in the quantum Hall regime.⁵ For the zero-magnetic-field case treated here, we expect that finite temperature will not produce significant qualitative changes in the layer densities if the temperature T is below a fraction of the Fermi temperature $T_F \equiv E_F/k_B$, where E_F is Fermi energy and k_B is Boltzmann's constant. For a layer density of $n = 10^{10} \text{ cm}^{-2}$, T_F is roughly 4 K for n -type GaAs, and 1K for p -type GaAs. The scale of the Hartree charge transfer energy, $e^2 d n / 2\epsilon$, is larger than the Fermi energy except for ultrasmall layer separations ($d < 5 \text{ nm}$ for n -type GaAs and $d < 1 \text{ nm}$ for p -type GaAs).

The other reason we work at zero temperature is to address matters of principle, such as whether an interlayer charge transfer instability can occur when the layers are very close together; finite temperatures would presumably smear out such a transfer, if it could occur. In the limit of zero temperature, Eq. (15) implies that

$$\langle a_{\mathbf{k}s}^\dagger a_{\mathbf{k}s} \rangle = \Theta(k_{as} - k), \quad \langle b_{\mathbf{k}s}^\dagger b_{\mathbf{k}s} \rangle = \Theta(k_{bs} - k), \quad (19)$$

where the subband Fermi wave vectors and number densities are related through

$$k_{as} = \sqrt{4\pi n_{as}}, \quad k_{bs} = \sqrt{4\pi n_{bs}}. \quad (20)$$

Summing Equations (18) over wave vector \mathbf{k} relates the number densities of the layers to those of the subbands:

$$\begin{aligned}n_{1s} + n_{2s} &= n_{as} + n_{bs}, \\ n_{1s} - n_{2s} &= (n_{as} - n_{bs}) \cos \theta.\end{aligned} \quad (21)$$

We may use the preceding equations to express the ground-state energy per unit area in terms of the subband occupancies $n_{\alpha s}$ and the angle θ :

$$\begin{aligned}\frac{\mathcal{E}_0}{L_x L_y} &= \frac{1}{\nu_0} \sum_{\alpha s} n_{\alpha s}^2 - t(n_a - n_b) \sin \theta \cos \phi \\ &\quad + \frac{e^2 d}{8\epsilon} [(n_a - n_b) \cos \theta - (p_F - p_B)]^2 \\ &\quad - \frac{1}{2L_x L_y} \sum_{\mathbf{q}\alpha s} V_{11}(q) I_{\alpha\alpha s}(q) \\ &\quad + \frac{\sin^2 \theta}{4L_x L_y} \sum_{\mathbf{q}s} [V_{11}(q) - V_{12}(q)] \\ &\quad \times [I_{aas}(q) + I_{bbs}(q) - 2I_{abs}(q)],\end{aligned} \quad (22)$$

where $\nu_0 = m^*/(\pi\hbar^2)$ is the density of states per unit area for noninteracting spin-1/2 particles in two dimensions, $\mathbf{q} = \mathbf{k}_1 - \mathbf{k}_2$, and

$$\begin{aligned}I_{\alpha\beta s}(q) &\equiv \frac{1}{L_x L_y} \sum_{\mathbf{K}} \Theta(k_{\alpha s} - |\mathbf{K} + \mathbf{q}/2|) \\ &\quad \times \Theta(k_{\beta s} - |\mathbf{K} - \mathbf{q}/2|).\end{aligned} \quad (23)$$

Here $\mathbf{K} = (\mathbf{k}_1 + \mathbf{k}_2)/2$, and the subband indices α and β can be either a or b . Equation (24) says that $I_{\alpha\beta s}(q)$ is $1/(2\pi)^2$ times the common area of two circles of radii $k_{\alpha s}$ and $k_{\beta s}$ whose centers are separated by q . When $\beta = \alpha$, then $k_{\beta s} = k_{\alpha s}$, and the first exchange integral in Eq. (23) may be carried out explicitly:

$$-\frac{1}{2L_x L_y} \sum_{\mathbf{q}} V_{11}(q) I_{\alpha\alpha s}(q) = -\frac{8}{3\sqrt{\pi}} \frac{e^2}{4\pi\epsilon} n_{\alpha s}^{3/2}. \quad (24)$$

Equation (24) is just the exchange energy per unit area for a uniform single-layer spin-polarized two-dimensional electron gas of areal density $n_{\alpha s}$.

The last term in Eq. (23), which contains the interlayer exchange contribution, may be conveniently expressed as

$$\frac{\sin^2 \theta}{4} \frac{e^2 d}{2\epsilon} (n_a - n_b)^2 \Gamma, \quad (25)$$

where Γ is the interlayer exchange parameter, given by

$$\begin{aligned}\Gamma &\equiv \frac{1}{L_x L_y} \sum_{\mathbf{q}s} \left[\frac{V_{11}(q) - V_{12}(q)}{e^2 d / 2\epsilon} \right] \\ &\quad \times \left[\frac{I_{aas}(q) + I_{bbs}(q) - 2I_{abs}(q)}{(n_a - n_b)^2} \right].\end{aligned} \quad (26)$$

The properties of Γ are described in Sec. A 4 of the Appendix. The last term in Eq. (23) must in general be evaluated numerically, although it vanishes at $d = 0$ or when $n_{as} = n_{bs}$. It also vanishes if θ is 0 or π , in which case subband a is the layer (1 or 2) with most particles, while subband b is the layer with the fewest particles. Ruden and Wu implicitly treated the layer pseudospin as an Ising-like variable with 0 and π as the only allowed values for θ ; in their approximation, the last term in Eq. (23) vanishes, and the interlayer effects we shall discuss here do not appear.

For definiteness, we take $n_a \geq n_b$, $n_{\alpha\uparrow} \geq n_{\alpha\downarrow}$, and $0 \leq \theta \leq \pi$. Our procedure consists of finding the values of $n_{\alpha s}$ and θ that minimize the expected energy per unit area, Eq. (23). Within our variational approximation, we find (as in¹⁷ the HFA) that the spins in a given subband are always either completely polarized (ferromagnetic at sufficiently low subband densities) or completely unpolarized (paramagnetic at higher densities). Real systems probably possess intermediate polarization for a range of low densities.^{27,28} For finite $t > 0$, the ground-state energy per unit area, Eq. (23), is minimized for $\phi = 0$. In the absence of interlayer tunneling, the ground-state energy per unit area is independent of ϕ , provided that ϕ is constant; for convenience we set $\phi = 0$. The layer densities n_{1s} and n_{2s} may be obtained from $n_{\alpha s}$ and θ via Eq. (22). We begin our calculations in the next section, by considering the case of electrostatically balanced gates.

IV. BALANCED GATES

In this section, we consider the case of electrostatically balanced gates ($p_F = p_B$), beginning with zero interlayer tunneling. This was the situation originally considered by Ruden and Wu,¹⁵ and more recently in Refs. 17,18, and 23. For balanced gates, our approximation is equivalent to the unrestricted HFA of Zheng and co-workers,¹⁷ and except for our analysis of the three-component phase, most of our results agree with theirs.

A. Zero tunneling

The balanced case raises an important question of principle: can exchange and correlation effects alone, unaided by applied gate biases and unhindered by interlayer tunneling, ever produce a ground state in which the densities of the inner layers are not equal? Based on a restricted HFA (which did not allow for SILC) Ruden and Wu proposed that for small enough layer densities and layer separations, the answer is yes. Zheng and co-workers argued recently that an unrestricted HFA (which allows for, but does not mandate, SILC) gives the opposite answer.¹⁷ We find that, except for a small region in density which supports a three-component phase that has a slight layer imbalance, the layer densities are equal when the gates are balanced.

1. Zero layer separation

In order to classify the four noncrystalline phases that we find for gate-balanced double-layer systems, it is useful to begin with the idealized case of zero layer separation ($d = 0$). For $d = 0$, the Hamiltonian is invariant under spin rotation, pseudospin rotation, and the interchange of spin and pseudospin. It is the same as the Hamiltonian for a four-layer system of spinless fermions

with zero separation between all the layers: layers, subbands, and spins become interchangeable labels for the four components. The $d = 0$ double-layer system is therefore equivalent to a single-layer two-dimensional system of fermions with $CP(3)$ symmetry. At $d = 0$, the interlayer Hartree energy is zero and the interlayer (V_{12}) and intralayer (V_{11}) Coulomb interactions are equal. As a consequence, the variational energy in Eq. (23) is independent of θ and (for $t = 0$) of ϕ when $d = 0$,

$$\frac{\mathcal{E}_0}{L_x L_y} = \sum_{\alpha s} \left[\frac{n_{\alpha s}^2}{\nu_0} - \frac{8}{3\sqrt{\pi}} \frac{e^2}{4\pi\epsilon} n_{\alpha s}^{3/2} \right] \equiv \sum_{\alpha s} \varepsilon(n_{\alpha s}), \quad (27)$$

and the MFA is equivalent to the HFA.

For generality, we first consider an N -component system, where N is twice the number of layers: $N = 4$ for double-layer spin-1/2 systems. At $d = 0$, the MFA lacks intercomponent correlations; thus, the total energy of the system is just the sum of the individual energies $\varepsilon(n_{\alpha s})$ of each component. We can investigate the distribution of component densities in the MFA ground state in an N -component system by taking all but two of component densities to be fixed, and minimizing the energy of the remaining two-component system. If we label the two components we seek to minimize as 1 and 2, then according to Sec. II, the condition for stable equilibrium (local minimum of the total energy) is

$$\mu(n_1) = \mu(n_2), \quad s(n_1) + s(n_2) > 0, \quad (28)$$

where $\mu(n_j) = \partial\varepsilon(n_j)/\partial n_j$ is the chemical potential relative to the minimum energy of component j and $s(n_j) = \partial\mu(n_j)/\partial n_j$ is inversely proportional to the compressibility of component j . When $\varepsilon(n_j)$ is the sum of the kinetic and exchange energies as in Eq. (27), then the MFA energy is minimized only if (1) both layer densities are equal ($n_1 = n_2$), or (2) one or both layers are empty. There are no intermediate possibilities in the MFA. This $d = 0$ result for $N = 2$ gives the results found by Ruden and Wu: when $n_1 + n_2$ is sufficiently large, the component densities are equal; when $n_1 + n_2$ is sufficiently small, there is an exchange-driven intercomponent charge instability that empties out one of the components. In the absence of intercomponent correlations, we expect that at low enough densities the component compressibilities will be negative and that therefore one of the components will empty out, even if intracomponent correlations are included. In the N -component $d = 0$ MFA ground state, any pair of layers either has equal density or has at least one of the layers empty.

There are therefore N possible MFA ground states in an N -component system at $d = 0$, characterized by the number of components p that have nonzero and equal densities. The remaining $N - p$ components have zero density. Defining the dimensionless average interparticle spacing *per component* by $r_s = 1/\sqrt{\pi(n_T/N)a_0^2}$ for an N -component system, where $a_0 = 4\pi\epsilon\hbar^2/m^*e^2$ is the effective Bohr radius, we may write the energy per unit area for the “ p -component” MFA ground state as

$$\frac{\mathcal{E}_p}{L_x L_y} = \frac{e^2}{4\pi\epsilon a_0^3} p \left[\pi \left(\frac{N}{\pi r_s^2 p} \right)^2 - \frac{8}{3\sqrt{\pi}} \left(\frac{N}{\pi r_s^2 p} \right)^{3/2} \right]. \quad (29)$$

In the limit $N \rightarrow \infty$, p becomes a continuous variable that minimizes the energy (29) for $p = p_\infty$, where

$$p_\infty = N \left(\frac{3\pi}{4r_s} \right)^2 = \left(\frac{3\pi}{4} \right)^2 \pi a_0^2 n_T, \quad (30)$$

where we have assumed that $r_s \geq (3\pi/4)$; otherwise, $p_\infty = N$. Equation (30) shows that in the limit $N \rightarrow \infty$, p is proportional to n_T for $r_s \geq (3\pi/4)$, and equal to N otherwise. As expected, the number p of equally occupied components drops as n_T is reduced. Equation (30) is equivalent to saying the dimensionless interparticle separation per component for which $p = p_\infty$ is

$$r_s(p_\infty) = \frac{3\pi}{4} \sqrt{\frac{N}{p_\infty}} \quad (31)$$

when $p_\infty/N \leq 1$. The equilibrium value of the $N \rightarrow \infty$ MFA energy corresponding to Eq. (30) is

$$\varepsilon_\infty = - \left(\frac{4}{3\pi} \right)^2 \frac{e^2}{4\pi\epsilon a_0} n_T. \quad (32)$$

For arbitrary finite N , Eq. (29) can be used to find the interparticle spacing per component $r_s^{(0)}(p, p+1)$ at which the p - and the $(p+1)$ -component phases have the same energies at $d = 0$:

$$r_s^{(0)}(p, p+1) = \frac{3\pi}{8} \left(\sqrt{\frac{N}{p}} + \sqrt{\frac{N}{p+1}} \right). \quad (33)$$

This is the interparticle spacing per component for the MFA transition between the p - and $(p+1)$ -component phases. It is interesting to compare this result to Eq. (31) and to note that

$$r_s^{(0)}(p, p+1) < r_s(p_\infty) < r_s^{(0)}(p-1, p), \quad (34)$$

so that even for finite N , $r_s(p_\infty)$ always gives a value for the interparticle spacing that is in the p -component MFA phase at $d = 0$.

For systems of physical interest containing $N/2$ layers of spin-1/2 particles, it is convenient to work with the interparticle spacing *per layer* (rather than the spacing *per component*). This is accomplished by dividing Eq. (33) by $\sqrt{2}$. For double-layer systems of spin-1/2 particles ($N = 4$),

$$\begin{aligned} r_s^{(0)}(1, 2) &= \frac{3\pi}{8}(\sqrt{2} + 1) \approx 2.844 \\ , r_s^{(0)}(2, 3) &= \frac{3\pi}{8}(1 + \sqrt{2/3}) \approx 2.140 \\ , r_s^{(0)}(3, 4) &= \frac{3\pi}{8}(\sqrt{2/3} + \sqrt{1/2}) \approx 1.795, \end{aligned} \quad (35)$$

where the superscript (0) denotes zero layer separation. Note that the direct four- to two-component MFA transition predicted to occur at

$$r_s(2, 4) = \frac{3\pi}{8}(1 + \sqrt{1/2}) \approx 2.011 \quad (36)$$

does not exist. In fact, we find that when $r_s = r_s(2, 4)$, the gate-balanced ($p_F = p_B$) double-layer system is always in the three-component MFA phase, regardless of the layer separation. The three-component system, which at $d = 0$ has $n_{a\uparrow} = n_{a\downarrow} = n_{b\uparrow} = n_{b\downarrow} = n_T/3$, has a spin-unpolarized subband ($n_{a\uparrow} = n_{a\downarrow}$) with greater density than the other subband ($n_a > n_b$), which is spin-polarized. These features of the three-component phase persist at finite layer separations, although the layer imbalance is greatly reduced.

2. Finite layer separation

Classically (when only the electrostatic energies are considered), balanced layers ($n_1 = n_2$) are obtained when $p_F = p_B$, in order to make the electric field E_{12} between the inner layers vanish. This result gives the asymptotically correct behavior for high layer densities and large layer separations. At sufficiently low densities and layer separations, the exchange energy can dominate the kinetic and electrostatic energies, so that the possibility of strong intralayer exchange leading to an interlayer charge-transfer instability must be considered. However, within the MFA, it can be proved that the inner layer densities are always equal, except in the three-component phase.

If the subband densities are equal ($n_a = n_b$, the case of “pseudospin paramagnetism”), then Eq. (22) shows that $n_1 = n_2$. Thus the four-component ($n_{\alpha s} = n_T/4$) and two-component (with $n_{a\uparrow} = n_{b\uparrow} = n_T/2$) phases have balanced layers. This is because the MFA state constructed by occupying equally the single-particle subband states a and b is equivalent (up to a global pseudospin rotation) to the MFA state constructed by occupying equally the single-particle layer states 1 and 2. The fact that the ground-state energy in Eq. (23) is independent of θ and ϕ when $n_a = n_b$ is due to the invariance of the ground-state energy under global pseudospin rotation.

If the subband densities are not equal ($n_a > n_b$), extremizing the total energy per unit area in Eq. (23) with respect to θ for $p_F = p_B$ and $t = 0$ gives the condition $\sin(2\theta) = 0$. The requirement that the extremum be a minimum (i.e., that the second derivative of the total energy per unit area with respect to θ be positive) gives

$$\sin \theta = \begin{cases} 1 & \text{if } \Gamma < 1 \\ 0 & \text{if } \Gamma > 1 \end{cases} \quad (37)$$

where the interlayer exchange parameter Γ is defined in Eq. (27). The properties of Γ are described in Sec. A 4 of the Appendix. Using the inequality

$$e^2 d / 2\epsilon > V_{11}(q) - V_{12}(q), \quad (38)$$

which is true for $d > 0$, it follows from Eq. (27) that for $d > 0$,

$$\begin{aligned} \Gamma &< \frac{1}{L_x L_y} \sum_{qs} \left[\frac{I_{aas}(q) + I_{bbs}(q) - 2I_{abs}(q)}{(n_a - n_b)^2} \right] \quad (39) \\ &= \sum_s \frac{(n_{as} - n_{bs})^2}{(n_a - n_b)^2}. \end{aligned}$$

Thus the condition

$$(n_{a\uparrow} - n_{b\uparrow})(n_{a\downarrow} - n_{b\downarrow}) \geq 0 \quad (40)$$

is sufficient to guarantee that $\Gamma < 1$ for $d > 0$, so that $\theta = \pi/2$, which balances the layers. The one-component phase ($n_{a\uparrow} = n_T$) satisfies Eq. (40), so $\theta = \pi/2$ and the layers are balanced. No interlayer charge transfer is obtained in the one-component phase because the combined effects of electrostatics and interlayer exchange, which favor balanced layers, always dominate the unbalancing influence of intralayer exchange: $e^2 d / 2\epsilon + V_{12}(q) > V_{11}(q)$.

Within the MFA, the spins in subbands a and b are either completely unpolarized (at higher densities) or fully polarized (at sufficiently low densities). Therefore the only possible MFA configurations of spin and pseudospin which could have unbalanced layers ($n_a > n_b$, $\theta \neq \pi/2$) when $p_F = p_B$ would be three-component states with

$$n_{a\uparrow} = n_{a\downarrow} < n_{b\uparrow}, \quad n_{b\downarrow} = 0. \quad (41)$$

We find numerically that such states always have $\Gamma > 1$ when $t = 0$, so that $\sin \theta = 0$. Hence, there is no interlayer phase coherence and the pseudospins are Ising-like. States with $n_a > n_b$ and $\sin \theta = 0$ have partially unbalanced layers, with the lower-density layer being spin-polarized and the higher-density layer being spin-unpolarized, even for balanced gates ($p_F = p_B$). This is the behavior we find for the three-component MFA phase. For infinitesimal d , one (spin-unpolarized) layer has twice the density of the other (spin-polarized) layer, and the phase exists in the range $r_s^{(0)}(3, 4) < r_s < r_s^{(0)}(2, 3)$. At finite d , the three-component phase has only a slight layer imbalance and exists only in a narrow region of average interparticle spacing around $r_s \approx r_s(2, 4)$.

The equality of the inner layer densities in the balanced case (except for the three-component phase) has also been shown to be true for the one-component phase when intralayer and interlayer correlations are included within the STLS approximation.²⁵ We note that if interlayer exchange were omitted from the total energy per unit area by setting $V_{12}(q) = 0$ in Eq. (23), then four MFA ground states would still be obtained, and the four-, three-, and two-component states would be unchanged. However, Eq. (38) would not be satisfied at small q , and at large interparticle distances (at small values of k_F , or low densities) the vanishing of the second derivative with respect to θ would give the condition $\cos(2\theta) > 0$,

so that $\cos(\theta) = \pm 1$. This would produce the interlayer charge instability of Ruden and Wu for the one-component phase.¹⁵ The fact that the one-component phase has equal densities is due to the effects of interlayer exchange.

Before obtaining the MFA phase diagram for double-layer systems, it is convenient to express lengths and energies as dimensionless quantities. We therefore express the layer separation d and the average density per layer $n_T/2$ in terms of the effective Bohr radius of the sample, $a_0 = 4\pi\epsilon\hbar^2/m^*\epsilon^2$, where ϵ is the dielectric constant in the material, and m^* is the effective mass. For GaAs, the dielectric constant is $\epsilon \approx 13\epsilon_0$. For n -type GaAs, $m^* \approx 0.07m_e$ so that $a_0 \approx 9.8$ nm, while for p -type GaAs, $m^* \approx 0.3m_e$ so that $a_0 \approx 2.3$ nm. The average density per layer can be expressed in terms of dimensionless ratio $r_s = r_0/a_0$ of the interparticle spacing r_0 for a single layer of averaged density $n_T/2$ (defined through $\pi r_0^2 n_T/2 = 1$) to the effective Bohr radius a_0 . Thus, for the same total density, p -type GaAs will have a value for r_s that is about $9.8/2.3 \approx 4.3$ times larger than for n -type GaAs. We define the Fermi wave vector k_F in terms of the total density n_T as

$$k_F = \sqrt{4\pi n_T/p} = \sqrt{\frac{2}{p}} \frac{2}{r_s a_0} \quad (42)$$

for $p = 1, 2, 4$. For the spin-polarized $p = 2a$ state and for the completely unpolarized $p = 4$, k_F is equal to the Fermi wave vector corresponding to the average density per layer ($n_T/2$). The energy scale associated with the effective Bohr radius is $v_0 = e^2/4\pi\epsilon a_0 = \hbar^2/m^* a_0^2$, which gives $v_0 \approx 11$ meV for n -type GaAs, and $v_0 \approx 48$ meV for p -type GaAs.

The HFA phase diagram for balanced double-layers without tunneling was obtained by Zheng and co-workers,¹⁷ except for the three-component phase. Like them, we find that within the MFA, three of the stable phases have equal average inner layer densities. Only the three-component phase has unequal layer densities. To understand the origin of the MFA phases, it is useful to consider the five terms that contribute to the total energy per unit area in Eq. (23). The first term of Eq. (23) is the kinetic (Fermi) energy, which favors distributing the particles equally among the subbands and spins. At the highest densities, the kinetic energy term dominates, and the double-layer system is a four-component spin and pseudospin paramagnet: $n_{a\uparrow} = n_{a\downarrow} = n_{b\uparrow} = n_{b\downarrow} = n_T/4$. The second term of Eq. (23) is the tunneling energy, which we take to be zero for now. In general, it favors $n_a > n_b$ (pseudospin polarization), without regard to the real spin. The third term of Eq. (23) is the electrostatic energy, which vanishes when the gates and inner layers are balanced. In general, the electrostatic term favors complete screening, which would make $n_1 = p_F$ and $n_2 = p_B$, without regard to the real spin.

The fourth term in Eq. (23) is an intrasubband exchange term that dominates at the smallest densities and

layer separations. It has the opposite effect of the kinetic energy, eventually producing a one-component spin and pseudospin ferromagnet at very low densities and small layer separations. The last term (containing the interlayer exchange) favors pseudospin paramagnetism ($n_{as} = n_{bs}$), but is indifferent to the polarization of the real spin, so long as it is the same in both subbands. Thus when $p_F = p_B$ and $d > 0$, the last term and the electrostatic terms are responsible for producing a two-component phase that is ferromagnetic in real spin rather than in pseudospin: $n_{a\uparrow} = n_{b\uparrow} = n_T/2$. (At $d = 0$, two-component states that are ferromagnetic in either the spin or pseudospin are degenerate. For $d > 0$, the pseudospin ferromagnetic $p = 2b$ state is favored only for substantial tunneling t and/or layer imbalance $|p_F - p_B|$.) In the absence of the kinetic energy term (e.g., in the limit $m^* \rightarrow \infty$), the real spin is always polarized due to intralayer exchange. However, because of the interlayer exchange, the two-component state is always obtained at high densities or large layer separations, while the one-component state is favored only for low densities and small layer separations.

Finite layer separation ($d > 0$) differentiates between spin and pseudospin, so that the symmetry of the problem becomes $SU(2) \times U(1)$ rather than the $CP(3)$ symmetry at $d = 0$. At finite layer separation, $V_{12}(q) < V_{11}(q)$, and the last term in the energy per unit area in Eq. (23) is minimized by equal subband densities, rather than by equal real spin densities. This does not effect the $p = 1$ (fully spin- and pseudospin-polarized) or $p = 4$ (completely spin and pseudospin unpolarized) phases. However, when $t = 0$ and $p_F = p_B$, the two-component ($p = 2$) MFA phase has its real spin fully polarized and its pseudospin completely unpolarized.

Finite layer separation also changes the densities at which the transitions between neighboring p -component phases occur. The densities at which the transitions between the phases occur in the MFA can be determined by comparing MFA energies. This task is made easier by the fact that the MFA always makes the real spins in a given subband either completely unpolarized (paramagnetic) or fully polarized (maximally ferromagnetic). This would probably not be true if correlation-energy effects were properly included,²⁷ and it is likely that in real double-layer systems, states with partial polarization may be stable in some regions of density. The same MFA behavior (the restriction to the two extremes of either zero or full polarization) is also found for the pseudospin when the layers are balanced and the interlayer tunneling is zero, except for the three-component phase, which has partial pseudospin polarization.

The four-component and two-component phases both have equal subband densities, so their MFA energies are independent of the layer separation d . If there were a direct transition between these two phases, it would be simply a spin paramagnetic to ferromagnetic transition in each subband or layer. Therefore, within the MFA, such a four-component to two-component transi-

tion would occur at the same layer density as the spin-polarization transition for a single-layer system with a layer density equal to the subband densities: i.e., for $r_s(2, 4) = 3\pi(1 + \sqrt{1/2})/8 \approx 2.011$, independent of the layer separation. As we discuss below, the direct four-to two-component transition is interrupted by a three-component phase, which has one subband (layer) spin-polarized and the other spin-unpolarized. So it is still true that MFA spin polarization transitions occur near $r_s \approx r_s(2, 4)$. However, the actual value of r_s needed to obtain spin-polarization in a real sample is likely to be significantly higher. For single-layer systems, diffusion Monte Carlo simulations show that the low-density ferromagnetic state predicted by the HFA does occur; however, correlation-energy effects move the transition to densities that are probably 100 times lower, to $r_s \approx 20$.²⁸ Such high values of r_s have been achieved in low-density p -type GaAs samples, which possess a larger effective mass (and therefore larger r_s) than n -type samples.²⁹ Large values of the effective mass will favor the existence of the lower-component ($p < 4$) described here, in that they increase r_s .

We find empirically that the three-component MFA phase has $\sin \theta = 0$. In order to analyze this phase, consider a MFA ground state with

$$\begin{aligned} n_{b\uparrow} &= (n_T/3)(1 + x/2), & n_{b\downarrow} &= 0, \\ n_{a\uparrow} &= n_{a\downarrow} = (n_T/3)(1 - x/4), \end{aligned} \quad (43)$$

and $\sin \theta = 0$, for $0 \leq x \leq 1$. Note that the layer imbalance is given by

$$\Delta n \equiv n_a - n_b = (n_T/3)(1 - x). \quad (44)$$

When $d = 0$, the three-component phase distributes the densities equally between the three components (but *not* between the two layers), so that $x = 0$. As $d \rightarrow \infty$, the Coulombic cost of layer imbalance becomes prohibitive, and $x \rightarrow 1$ so that $\Delta n \rightarrow 0$. We plot the layer imbalance ratio $\Delta n/(n_T/3) = (1 - x)$ for $r_s = r_s(2, 4) \approx 2.011$ in Fig. 2.

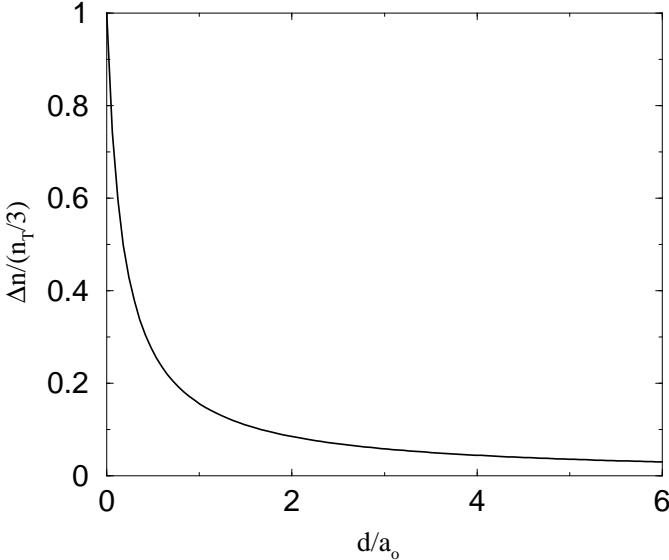


FIG. 2. Layer imbalance ratio $\Delta n/(n_T/3) = 1 - x$ in the three-component phase for $r_s = r_s(2, 4) \approx 2.011$. The imbalance decreases with increasing layer separation.

As $d \rightarrow 0$,

$$x \approx \frac{(4/3)(d/a_0)}{1 - r_s/(\pi\sqrt{2}/3)} \rightarrow 6.174 \frac{d}{a_0}, \quad (45)$$

to linear order in d/a_0 , where the last expression in the equation above is for $r_s = r_s(2, 4)$, which is the only value of r_s for which the double-layer system is in the three-component phase for arbitrary layer separation. As $d \rightarrow \infty$,

$$\frac{\Delta n}{n_T/3} = 1 - x \approx \frac{a_0}{d} \frac{3}{4} \left[\frac{r_s}{(1 + 1/\sqrt{2})\pi/2} \right] \rightarrow \frac{3}{16} \frac{a_0}{d}, \quad (46)$$

to linear order in a_0/d , where the last expression in the equation above is for $r_s = r_s(2, 4)$. Equation (46) says that the layer imbalance Δn in the three-component phase is inversely proportional to d/a_0 for large values of d/a_0 .

For infinitesimal d , the energy per unit area of three-component phase increases by the amount $(e^2 d / 8\epsilon)(n_T/3)^2$ to linear order in d , while that of the four- and two-component phases are unchanged. Equating the three-component energy to the four- and to the two-component energies gives

$$r_s(2, 3) \approx r_s^{(0)}(2, 3) \left(1 - \frac{1}{3} \frac{d}{a_0} \right), \quad (47)$$

$$r_s(3, 4) \approx r_s^{(0)}(3, 4) \left(1 + \frac{2}{3} \frac{d}{a_0} \right),$$

to first order in d/a_0 as $d/a_0 \rightarrow 0$, and

$$r_s(2, 3) \approx r_s^{(0)}(2, 4) \left(1 + \frac{1}{16} \frac{a_0}{d} \right), \quad (48)$$

$$r_s(3, 4) \approx r_s^{(0)}(2, 4) \left(1 - \frac{1}{16} \frac{a_0}{d} \right),$$

to first order in a_0/d as $d/a_0 \rightarrow \infty$. Note that both $r_s(2, 3)$ and $r_s(3, 4)$ approach $r_s(2, 4)$ in the limit $d \rightarrow \infty$. This is because as $d \rightarrow \infty$, the double-layer system consists of two independent layers, and $r_s(2, 4)$ is the interparticle spacing at which the spin-polarized and spin-unpolarized energies are equal in a single-layer system. Thus, as $d \rightarrow \infty$, the energies of the four-, three-, and two-component phases are all equal at $r_s = r_s(2, 4)$.

We now consider the two-component to one-component transition in the MFA. For $d = 0$, the MFA transition to pseudospin ferromagnetism is equivalent to a real-spin paramagnetic to ferromagnetic transition in a single layer having total density n_T (rather than $n_T/2$). Thus for $d = 0$, the MFA critical density per layer for the two-to one-component transition is exactly half the critical density for the four- to two-component transition, so that $r_s^{(0)}(1, 2) = 3\pi(\sqrt{2} + 1)/8 \approx 2.844$. By equating the one- and two-component phase energies per area, the critical density for the one- to two-component transition may be obtained:

$$\begin{aligned} \frac{r_s^{(0)}(1, 2)}{r_s(1, 2)} &= 1 - (1 + 1/\sqrt{2}) \frac{3\pi z}{32} \Gamma_1(z) \\ &= 1 - (1 + 1/\sqrt{2}) [1 - S(z)], \end{aligned} \quad (49)$$

where

$$\begin{aligned} z &= 2k_F d = 2d\sqrt{4\pi n_T} = 4\sqrt{2}d/(r_s a_0) \\ &= (2 - \sqrt{2}) \frac{32}{3\pi} \frac{d}{a_0} \frac{r_s^{(0)}(1, 2)}{r_s}, \end{aligned} \quad (50)$$

$\Gamma_1 = \Gamma(n_{a\uparrow} = n_T)$, and

$$\begin{aligned} S(z) &= \frac{3}{2} \int_0^1 dx e^{-zx} \left[\arccos(x) - x\sqrt{1-x^2} \right] \\ &= \frac{3\pi}{4z} \left\{ 1 - \frac{2}{z} [I_1(z) - L_1(z)] \right\} \\ &\rightarrow \begin{cases} 1 - (3\pi/32)z + (1/5)z^2, & z \rightarrow 0 \\ 3\pi/4z, & z \rightarrow \infty \end{cases} \end{aligned} \quad (51)$$

Here I_1 and L_1 are modified Bessel and modified Struve functions of the first kind, respectively. The derivation of the above formula is discussed in Sec. A 4c of the Appendix. Equations (49) and (50) determine $r_s(1, 2)$, which we have plotted as the upper solid line in Fig. 3.

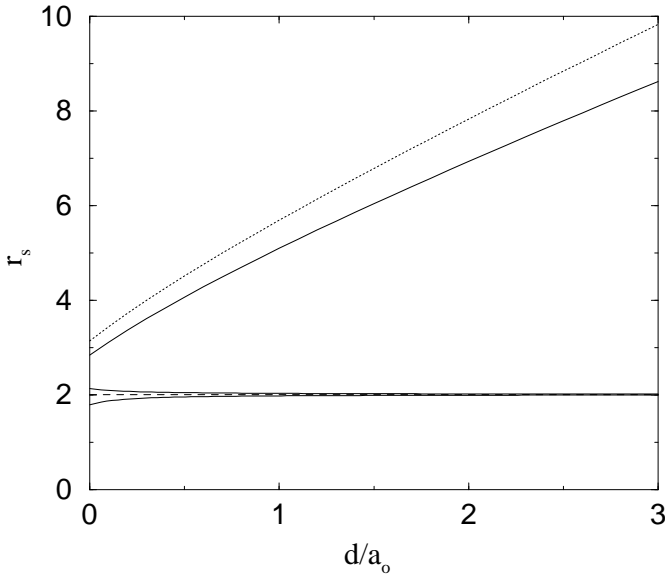


FIG. 3. MFA (solid lines) phase diagram for a gate-balanced ($p_F = p_B$) double-layer system with $t = 0$. At the highest densities (smallest r_s , bottom of figure), the four-component state, which is both spin and pseudospin unpolarized, is energetically favored. In a narrow region around $r_s(2, 4) \approx 2.011$ (dotted line), the three-component state has the lowest energy. At lower densities, a two-component state which is spin polarized but pseudospin unpolarized is favored. At the lowest densities (large r_s , top of figure) a one-component state which is both spin and pseudospin polarized is favored. The dotted line at the top is a GRPA estimate for the onset of the one-component phase.

It follows from Eq. (51) that $r_s(1, 2)/r_s^{(0)}(1, 2) \rightarrow (1 + d/a_0)$ in the limit $d/a_0 \rightarrow 0$. The value of $r_s(1, 2)$ at very large layer separations ($d/a_0 \rightarrow \infty$) can be obtained by setting $r_s(1, 2)/r_s^{(0)}(1, 2) = 0$ in the left-hand side of Eq. (49) and then solving the resulting equation numerically for z . The result is $z \rightarrow 4.015$, or $r_s(1, 2)/r_s^{(0)}(1, 2) \rightarrow 0.495d/a_0$, so that $r_s(1, 2) \rightarrow 1.409d/a_0$. We note that if interlayer exchange were ignored and the pseudospins treated as Ising variables ($\sin \theta = 0$), then the two- to one-component MFA transition would occur at $r_s^{(0)}(1, 2)(1 + d/a_0)$ (for all values of d/a_0) and would put all (spin-polarized) particles in a single layer. Interlayer exchange makes the layer densities equal in the one-component MFA state, and causes the two- to one-component MFA transition to occur at a somewhat lower value of r_s than would be predicted using Ising pseudospins.

B. Infinitesimal tunneling

In this subsection, we discuss the effects of very small interlayer tunneling. The contribution of interlayer tunneling to the MFA energy per unit area is given by $-2t(n_a - n_b)\sin \theta$. Finite interlayer tunneling thus has two important effects. First, it removes the Ising charac-

ter of the spins by making $\sin \theta > 0$. We discuss this in more detail in the next subsection. Second, it always produces some degree of pseudospin polarization ($n_a - n_b > 0$). We have parametrized the dependence of the subband splitting ($n_a - n_b$) on t in terms of the pseudospin Stoner interaction parameter, which we calculate in the second subsection below.

1. Effect of tunneling on phase angle

We first consider the effect of interlayer tunneling on the interlayer phase angle θ . Extremizing the energy per unit area [Eq. (23)] with respect to θ for $t > 0$ gives two possible solutions. The solution

$$\cos \theta = 0 \quad (52)$$

is always an extremum, and is a minimum whenever $\Gamma < 1$, which is true for all phases except $p = 3$ near balance ($p_F \approx p_B$). Of course, if t were large enough to cause full pseudospin polarization ($n_a = n_T$), then $\cos \theta = 0$.

If $\Gamma > 1$ (three-component phase) then the solution

$$\sin \theta = \frac{t}{(\Gamma - 1)e^2 d(n_a - n_b)/2\epsilon} \quad (53)$$

gives the correct minimum, provided that the right-hand side is positive and does not exceed unity. Even in the three-component phase, t will increase ($n_a - n_b$), but since $(n_a - n_b)$ is already finite at $t = 0$, $\sin \theta$ will be proportional to t , to first order in t .

The effect of including a small amount of interlayer tunneling can often be described perturbatively, and produces a smooth increase in the pseudospin polarization ($n_a - n_b$) that is proportional to t . However, the results obtained in the combined limits $t \rightarrow 0$ and $d \rightarrow 0$ can depend on the order of these limits. For example, at $d = 0$, the lowest-energy two-component phase has $n_{a\uparrow} = n_{a\downarrow} = n_T/2$ (pseudospin-polarized but spin-unpolarized) for arbitrarily small but finite t . However, at $t = 0$, the lowest-energy two-component phase has $n_{a\uparrow} = n_{b\uparrow} = n_T/2$ (spin-polarized but pseudospin-unpolarized) for arbitrarily small but finite d . By comparing the MFA energies per unit area of two competing $p = 2$ ground states with $\cos \theta = 0$ (spin-polarized $p = 2a$ versus pseudospin-polarized $p = 2b$), it can be shown that the pseudospin-polarized two-component ($p = 2b$) ground state requires

$$\begin{aligned} t &> \frac{e^2 d n_T}{8\epsilon} \Gamma(n_{a\uparrow} = n_{a\downarrow} = n_T/2) = \frac{e^2 d n_T}{8\epsilon} \Gamma_1(p = 2) \quad (54) \\ &= \frac{e^2 d n_T}{8\epsilon} \frac{16}{3\pi z} [1 - S(z)] \\ &\rightarrow \begin{cases} e^2 d n_T / 16\epsilon, & k_F d \rightarrow 0 \\ (4/3\sqrt{2\pi})^2 \sqrt{n_T} / 4\pi\epsilon, & k_F d \rightarrow \infty \end{cases} \end{aligned}$$

Here $z = 2k_F d = 2d\sqrt{2\pi n_T}$, and $S(z)$ is defined in Eq. (51). Therefore it is the size of t relative to $e^2 d n_T / 16\epsilon$

that must be considered as both t and d approach zero in the two-component phase. A rough estimate of the minimum tunneling energy t_c necessary to obtain the pseudospin-polarized two-component phase may be made by calculating $e^2dn_T/16\epsilon$ for the smallest value of n_T that still gives the two-component phase: i.e., for $r_s \sim r_s^{(0)}(1, 2) \approx 2.844$. For $d = 10$ nm, this gives $t_c \sim 0.7$ meV for n -type GaAs and $t_c \sim 13$ meV for p -type GaAs. The differences between these two values of t_c arise from the fact that n -type GaAs spin-polarizes at a much lower density than p -GaAs, due to the differences in the effective mass (and therefore in r_s). We stress that there exist two $p = 2$ two-component states, which can be either spin- or pseudospin-polarized. The $p = 2$ state that we focus on most will be the spin-polarized state ($p = 2a$).

2. Pseudospin Stoner parameter

The difference $\Delta n \equiv n_a - n_b$ between the subband densities (obtained from SdH measurements) of a balanced double-layer system is often used as a measure of the size of the interlayer tunneling matrix element t by applying the formula $n_a - n_b = (p/2)t\nu_0$, which is valid for noninteracting particles.²³ Here $p = 4$ for spin-unpolarized particles, $p = 2$ for spin-polarized particles, and $\nu_0 = m^*/(\pi\hbar^2)$ is the two-dimensional density of states per unit area. For interacting electrons or holes, the pseudospin Stoner interaction parameter I is defined through²³

$$n_a - n_b = \frac{(p/2)t\nu_0}{1 - I}. \quad (55)$$

For noninteracting particles, $I = 0$. For interacting particles, I is a function of r_s and d/a_0 ; in general, it also a function of t . We do not consider $p = 3$ or $p = 1$, since both the three- and the one-component phases have $n_a > n_b$ at $t = 0$, corresponding to $I = 1$. The onset of SILC ($n_a > n_b$ and $\sin \theta > 0$ even when $t = 0$) occurs at the two- to one-component transition, and corresponds to $I \rightarrow 1$ for $p = 2$.

The Stoner interaction parameter I can be calculated analytically in the limit of vanishing interlayer tunneling ($t \rightarrow 0$), as we show in Sec. A 5 of the Appendix. (For finite t , we calculate I numerically.) The basic idea is to start with equal subband densities ($n_a = n_b$) and infinitesimally small t , and then calculate the change in energy due to moving an infinitesimal amount of charge from subband b to subband a . Minimizing the change in energy with respect to the amount of charge transferred between the subbands gives the linear response to small interlayer tunneling and yields the following expression for the $t \rightarrow 0$ limit of the Stoner interaction parameter:

$$\begin{aligned} I &= \frac{\nu_0 e^2}{2\pi\epsilon k_F} \left(1 - p \frac{\pi}{4} k_F d \Gamma_0 \right) \\ &= \frac{\nu_0}{\pi} \left\{ 2V_{11}(2k_F) - \int_0^1 dx \frac{[V_{11}(2k_Fx) - V_{12}(2k_Fx)]}{\sqrt{1-x^2}} \right\} \end{aligned} \quad (56)$$

$$= \frac{r_s}{\pi} \sqrt{\frac{p}{2}} \left[1 - \frac{1}{2} \int_0^{\pi/2} d\theta \frac{(1 - e^{-2k_F d \sin \theta})}{\sin \theta} \right],$$

where $k_F = \sqrt{4\pi n_T/p}$ for $p = 2, 4$, and $\Gamma_0 \equiv \Gamma(n_a \rightarrow n_b)$. Equation (56) is equivalent to the generalized random-phase approximation (GRPA) result in Eq. (14) of Ref. 23.

Note that $I = 1$ (when $p = 1$) corresponds to SILC, and that the GRPA result for the phase boundary, which is shown as the dashed sloped line in Fig. 3, is different (has larger r_s) than the MFA result. That the GRPA gives a higher value for $r_s(1, 2)$ is not surprising, given that the GRPA goes beyond MFA and contains correlation effects in an approximate way. To lowest order in d , $I(d)/I(0) = (1 - d/a_0)$, so that for $d \rightarrow 0$, the GRPA gives a higher critical value of the interparticle spacing for SILC than the MFA: $r_s(1, 2) \approx \pi(1 + d/a_0)$. As expected, a similar calculation of the linear response of the real spins to a weak Zeeman field shows that a hypothetical four- to two-component GRPA transition would occur at twice the density of the $d = 0$ two- to one-component transition, i.e., at $r_s(1, 2) = \pi/\sqrt{2}$. However, as with the MFA, we expect that a three-component GRPA phase preempts any direct four- to two-component GRPA transition, and that a three-component is always obtained within the GRPA at $r_s = \pi/\sqrt{2}$.

As pointed out in Ref. 23, interactions enhance the subband splitting ($I > 0$) for $k_F d < 1.13$, but reduce the splitting ($I < 0$) for $k_F d > 1.13$. The critical value for r_s at large d that separates the one- and two-component phases is determined by solving Eq. (56) for $I = 1$ and $r_s \rightarrow \infty$. Asymptotically (for $r_s, d/a_0 \rightarrow \infty$), it occurs at the same value of r_s that has $I = 0$ i.e., $k_F d \rightarrow 1.134$ or $r_s(1, 2)/r_s^{(0)}(1, 2) \rightarrow 0.620d/a_0$, which gives $r_s(1, 2) \rightarrow 1.764d/a_0$. Within the GRPA, SILC occurs once the interparticle spacing is roughly twice the interlayer spacing. In the limit $k_F d \rightarrow \infty$, $I(d)/I(0) = 1 - (1/2)[\ln(4k_F d) + \gamma]$, where $\gamma \approx 0.5772$ is Euler's constant. In Ref. 23 it is argued that although $I(d)$ is large and negative as $d \rightarrow \infty$, its apparently divergent behavior is an unphysical artifact of the GRPA.

We have calculated the Stoner interaction parameter I for a few values of the interlayer tunneling t in Figs. 4 (n -type GaAs) and 5 (p -type GaAs), for a hypothetical sample with total density $n_T = 10^{11}\text{cm}^{-2}$. The complete polarization of the pseudospin ($n_a = n_T$) is indicated by the mesa-like regions where I becomes flat: $n_{a\uparrow} = n_{a\downarrow} = n_T/2$ for n -type GaAs and $n_{a\uparrow} = n_T$ for p -type GaAs. Increasing the size of t favors pseudospin polarization and allows it to persist to larger values of $k_F d$. Note that at fixed t , the Stoner interaction is equal to $I_{\max} = 1 - 2t\nu_0/n_T$ as $k_F d \rightarrow 0$, so that I_{\max} decreases with increasing t . The fact that $I_{\max}(t = 0.1) > I_{\max}(t = 0)$ is an artifact of the order in which the limits $t \rightarrow 0$ and $d \rightarrow 0$ are taken: for any finite t , the two-component phase will have $n_{a\uparrow} = n_{a\downarrow} = n_T/2$ as $d \rightarrow 0$, but for any finite d , the two-component

phase will have $n_{a\uparrow} = n_{b\uparrow} = n_T/2$ as $t \rightarrow 0$. For n -type GaAs with $t = 1$ meV (dotted line in Fig. 4), the system goes through three phases as a function of $k_F d$: (1) a pseudospin-polarized two-component phase ($n_{a\uparrow} = n_{a\downarrow} = n_T/2$) for $k_F d \rightarrow 0$, (2) a three-component phase ($n_{a\uparrow} = n_{a\downarrow} < n_{b\uparrow}$) for intermediate values of $k_F d$, indicated in by the “missing piece” on the right side of the mesa in Fig. 4, (3) a real-spin-polarized two-component phase ($n_{a\uparrow} = n_{b\uparrow} = n_T/2$) for larger $k_F d \rightarrow \infty$.

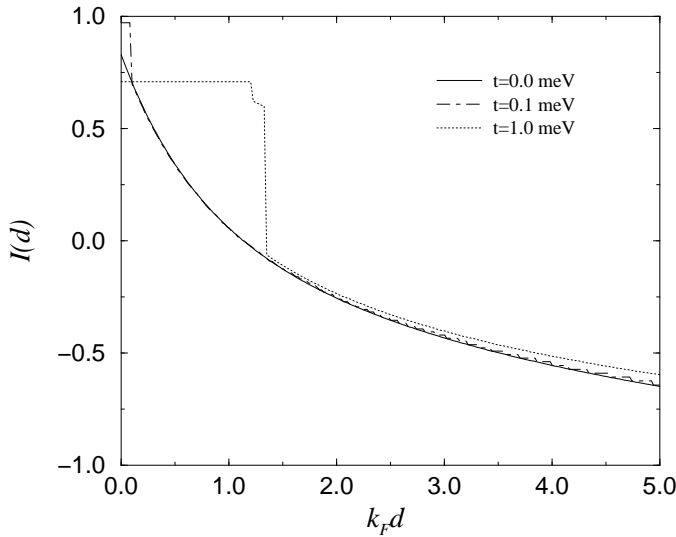


FIG. 4. Stoner interaction parameter $I = 1 - 2t\nu_0/(n_a - n_b)$ versus $k_F d$ for n -type GaAs at total density $n_T = 10^{11} \text{ cm}^{-2}$ for $t = 0, 0.1, 1.0$ meV.

SILC is indicated by having $I(t = 0) = 1$ and occurs only for p -type GaAs (Fig. 5, for $k_F d < 0.7$): $I(t = 0)$ is directly proportional to ν_0 , and therefore to the effective mass of the particles, so that SILC is more likely to be observed in p -type ($m^*/m_e \approx 0.3$) rather than n -type ($m^*/m_e \approx 0.07$) GaAs.

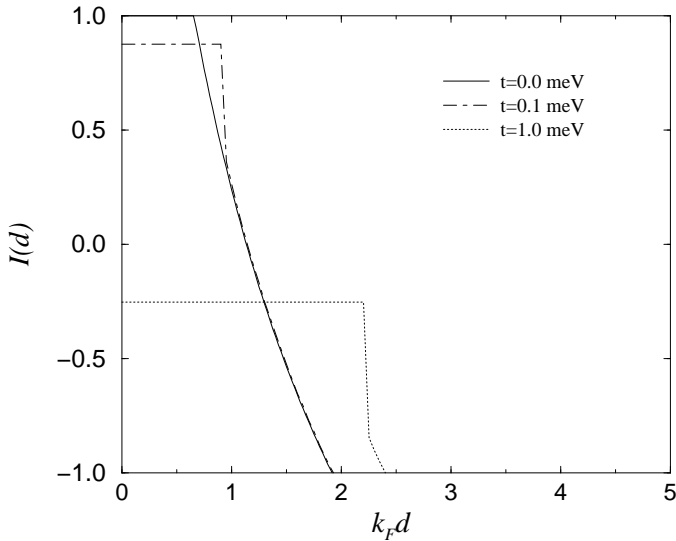


FIG. 5. Stoner interaction parameter $I = 1 - 2t\nu_0/(n_a - n_b)$ versus $k_F d$ for p -type GaAs at total density $n_T = 10^{11} \text{ cm}^{-2}$ for $t = 0, 0.1, 1.0$ meV.

V. EFFECT OF BIAS

In this section, we study the effect of bias ($p_F \neq p_B$, due to applied gate voltages) on the subband and layer densities. The classical results

$$n_1 = p_F \Theta(p_F), \quad n_2 = p_B \Theta(p_B), \quad (57)$$

and

$$V_F = eD_F E_F + edE_{12} + eV_F^{(0)} \quad (58)$$

give the asymptotically correct behavior for high layer densities and large layer separations. Double-layer systems at low densities and small layer separations show measurable deviations from the classical behavior, most notably because of quantum-mechanical exchange. We shall find it convenient to study the effects of layer imbalance by fixing the total density ($n_T = p_F + p_B$) and then varying the gate-imbalance parameter ζ , defined by

$$\zeta \equiv \frac{p_F - p_B}{p_F + p_B} = (p_F - p_B)/n_T. \quad (59)$$

The case of balanced gates ($p_F = p_B$) corresponds to $\zeta = 0$.

In the presence of bias and/or tunneling, there are five possible noncrystalline MFA ground states, which we write in order of increasing r_s in Table I. Only the last ($p = 1$) phase can exhibit SILC. The last two phases are pseudospin-polarized and can have $0 \leq \sin \theta \leq 1$, with the value of θ being determined by the layer separation, density, bias, and tunneling. The first three phases are Ising-like ($\sin \theta = 0$) when $t = 0$, and therefore do not involve interlayer exchange, in the absence of interlayer tunneling. Note that there are two $p = 2$ phases, one that is pseudospin-polarized but spin-unpolarized ($p = 2b$), and another that is spin-polarized but pseudospin unpolarized ($p = 2a$). The pseudospin-polarized $p = 2b$ requires bias and/or tunneling. For all MFA phases, the real spin is either fully polarized or completely unpolarized.

TABLE I. Subband occupancies of the five possible non-crystalline MFA ground states for a double layer system with gate imbalance ($|p_F - p_B| > 0$) or tunneling ($t > 0$).

$p = 4$	$n_{a\uparrow} = n_{a\downarrow} \geq n_{b\uparrow} = n_{b\downarrow} > 0$	
$p = 3$	$n_{a\uparrow} = n_{a\downarrow} \geq n_{b\uparrow} > 0$	$n_{b\downarrow} = 0$
$p = 2a$	$n_{a\uparrow} \geq n_{b\uparrow} > 0$	$n_{a\downarrow} = n_{b\downarrow} = 0$
$p = 2b$	$n_{a\uparrow} = n_{a\downarrow} > 0$	$n_{b\uparrow} = n_{b\downarrow} = 0$
$p = 1$	$n_{a\uparrow} = n_T$	$n_{a\downarrow} = n_{b\uparrow} = n_{b\downarrow} = 0$

We begin this section by studying the case of vanishing interlayer exchange, which is the relevant situation for the majority of double-layer samples that have been studied experimentally, except in the quantum Hall regime.⁵ This is the case when layer separations are sufficiently far apart that interlayer exchange is negligible in zero or weak magnetic fields. A model without interlayer exchange is able to fit existing double-layer data well, and obtains the correct four-, three-, and two-component phases, although it fails to properly describe the one-component phase. We then include the effects of interlayer exchange and solve for the subband and layer densities using our MFA, which allows for the possibility of interlayer exchange, even in the absence of interlayer tunneling. Finally, we give a full treatment of the one-component phase within the MFA, including bias and tunneling.

A. No interlayer exchange

It is simplest to begin our study of the effects of layer imbalance ($p_F \neq p_B$) by first considering the limit of vanishing interlayer exchange. This limit is relevant to most of double-layer samples that have been studied experimentally, except in the quantum Hall regime.⁵ It corresponds to layer separations that are sufficiently far apart that interlayer exchange is negligible in zero or weak magnetic fields. We shall also demonstrate that a very simple model which assumes that the particles are always spin-unpolarized gives a good fit to existing data on the subband occupancies of double-layer systems, except at low densities.

1. No tunneling

Interlayer exchange is negligible when the layer separation is large compared to the interparticle spacing. This condition may be expressed in various ways, e.g., $k_F d \gg 1$ or $r_s \ll d/a_0$, and is satisfied for most samples. In this limit, we ignore interlayer tunneling and correlations and write the exchange-correlation energy in Eq. (3) as

$$\varepsilon(n_1, n_2) \approx \varepsilon(n_1) + \varepsilon(n_2), \quad (60)$$

where $\varepsilon(n)$ is the sum of the kinetic (Fermi), exchange, and correlation (but *not* the electrostatic) energies, for a single-layer two-dimensional electron gas (2DEG) of density n . In the absence of interlayer exchange and tunneling, we can work directly with the layer densities rather than the subband densities because the pseudospins are Ising variables:

$$n_a = \max(n_1, n_2), \quad n_b = \min(n_1, n_2), \quad (61)$$

$$\theta = \pi \Theta(p_B - p_F) = \begin{cases} \pi, & p_F < p_B \\ 0, & p_F > p_B \end{cases}$$

so that $\sin \theta = 0$.

No interlayer exchange is required to correctly describe the four-, three-, and two-component MFA phases at $t = 0$, since all have $\sin \theta = 0$. Our analysis of these phases therefore proceeds as before. It is nonetheless useful to look at the phases of system in terms of the equilibrium and stability conditions of Sec. II, which we do below.

Although it would be straightforward to include intralayer correlation-energy effects in $\varepsilon(n)$, we do not do so here for the sake of simplicity. Even so, the resulting approximate model does a very good job of fitting SdH data until the layer densities get so low that they violate our initial assumption that $k_F d$ is large. We therefore begin with

$$\begin{aligned} \varepsilon(n) &\approx \sum_s \left[\frac{n_s^2}{\nu_0} - \frac{8}{3\sqrt{\pi}} \frac{e^2}{4\pi\epsilon} n_s^{3/2} \right] \\ &= \begin{cases} n^2/2\nu_0 - (8/3\sqrt{2\pi})(e^2/4\pi\epsilon)n^{3/2}, & n > n_c \\ n^2/\nu_0 - (8/(3\sqrt{\pi})(e^2/4\pi\epsilon)n^{3/2}, & n < n_c \end{cases} \end{aligned} \quad (62)$$

where n_c is the critical density for the MFA spin-polarization transition in a single-layer system. The condition $n > n_c$ corresponds to spin-unpolarized electrons and occurs at higher densities, whereas $n < n_c$ corresponds to spin-polarized electrons and occurs at lower densities. When $\sin \theta = 0$ (which is the case we are considering in this section), n_c is the critical density of the MFA (or the HFA) spin-polarization transition for a single layer, which occurs when the single-layer r_s has the value $r_s(2, 4) = (3\pi/8)(1 + \sqrt{1/2}) \approx 2.011$, shown as the dashed line in Fig. 3. Note that $r_s \equiv 1/\sqrt{\pi n a_0^2}$ for a single-layer system of number density n , which gives $n_c a_0^2 = (2/3)(4/\pi)^3(1 - 2\sqrt{2}/3) \approx 0.07870$. In the MFA, which is equivalent to the HFA for balanced layers, the spin polarization is either completely unpolarized (at higher densities) or completely polarized (at lower densities). Correlation-energy effects probably produce a range of intermediate spin polarizations.

The chemical potential measured relative to layer i is $\mu_i = \mu(n_i)$, where

$$\begin{aligned} \mu(n) &= \partial \varepsilon(n) / \partial n \\ &= \begin{cases} n/\nu_0 - (4/\sqrt{2\pi})(e^2/4\pi\epsilon)\sqrt{n}, & n > n_c \\ 2n/\nu_0 - (4/\sqrt{\pi})(e^2/4\pi\epsilon)\sqrt{n}, & n < n_c \end{cases} \end{aligned} \quad (63)$$

where we have used Eqs. (5) and (62). The values of the layer densities can be determined by using Eq. (63) in the equilibrium condition of Eq. (4), $\mu_1 - \mu_2 = eE_{12d}$.

The electronic lengths s_{ij} that determine the Eisenstein ratio R_E [Eq. (11)] and the condition for stability against interlayer charge transfer [Eq. (7)] can be calculated from Eqs. (6) and (63). Ignoring interlayer correlations as in Eq. (60), gives $s_{ij} = 0$ for $i \neq j$, and $s_i = s_{ii} = s(n_i)$, where

$$\begin{aligned} \frac{s(n)}{a_0} &= \frac{\epsilon}{e^2 a_0} \frac{\partial \mu(n)}{\partial n} = \begin{cases} 1/4 - (\sqrt{2/\pi})/(4\pi a_0 \sqrt{n}), & n > n_c \\ 1/2 - (2/\sqrt{\pi})/(4\pi a_0 \sqrt{n}), & n < n_c \end{cases} \\ &= \begin{cases} 1/4 - (\sqrt{2}/4\pi)r_s, & n > n_c \\ 1/2 - (1/2\pi)r_s, & n < n_c \end{cases}. \end{aligned} \quad (64)$$

Note that the MFA compressibility κ can be calculated from the above result using Eq. (9), and that $s(n)$ and therefore κ are negative at sufficiently low densities. The length $s(n)$ and the compressibility κ jump discontinuously at $n = n_c$, where the ground state changes abruptly from spin-unpolarized to spin-polarized. For densities just above n_c , $s(n_c^+)/a_0 \approx 0.0237$, while for densities just below n_c , $s(n_c^-)/a_0 \approx 0.1799$. Sensitive measurements of the interlayer capacitance (e.g., the Eisenstein ratio R_E) could detect the exchange-driven spin polarization of a 2DEG through its effect on the compressibility, especially in *p*-type GaAs samples when the density in a layer could be made small enough to polarize the holes in that layer.

It is straightforward to calculate the effect of spin polarization in a low-density layer on R_E using Eqs. (12) and (64). For the usual case in which the interlayer separation d is substantially larger than the electronic lengths $s(n_i)$ (i.e., for $d/a_0 \gg 0.2$), the MFA gives an abrupt jump in R_E by almost a factor of 8, from approximately $0.0237a_0/d$ for densities just above n_c , to approximately $0.1799a_0/d$ for densities just below n_c . Of course, the MFA overestimates the size of the jump, but it is nonetheless plausible that measurements of R_E could detect changes in the compressibility of a low-density layer due to the exchange-driven polarization of the spins.

2. Unpolarized spins

Ruden and Wu assumed not only that the pseudospins were Ising-like ($\sin \theta = 0$), but also that the real spins were always unpolarized.¹⁵ This limited the phases they found at $p_F = p_B$ to two: pseudospin-unpolarized ($p = 4$) at high density and pseudospin-polarized ($p = 2b$) for low density. It is straightforward to compare the energy of the four-component phase with that of the hypothetical pseudospin-polarized ($p = 2b$) phase of Ruden and Wu and show that they are equal when $r_s/r_s^{(0)}(1, 2) = 1 + 2d/a_0$. Although neither assumption was, strictly speaking, correct, it is an interesting and useful fact that making such assumptions can yield a simple model that fits experimental data for layer densities versus gate bias quite well, except at the lowest densities. Figure 6 shows experimental SdH data³⁰ and a theoretical fit from a simple theory that ignores interlayer exchange and takes the spins to be unpolarized. The value of the interlayer separation d used in the model is taken to be a fitting parameter. The values of d that we obtain with this simplified model always locate the idealized two-dimensional electrons layers inside the confining quantum wells, although d always seems to be somewhat larger than the midwell to midwell distance.

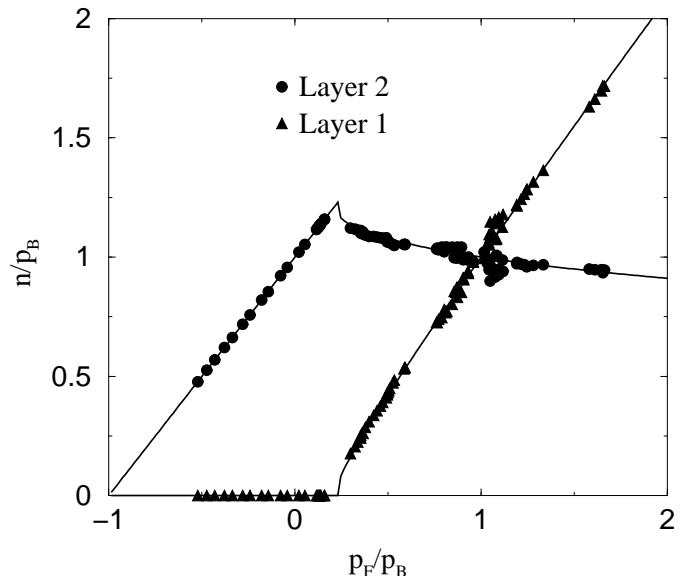


FIG. 6. Plot of the experimental (circles and triangles) and calculated (solid curves) layer densities n_1 and n_2 versus front-gate number density p_F . A simple model which neglects interlayer exchange, intralayer correlations, and spin polarization and assumes zero layer thickness yields a good fit to the experimental densities, except when n_1 becomes small.

Note that the experimental data fits very well almost everywhere, except where the density n_1 is very small when layer 1 is near depletion. Here the simplest theory (which omits the possibilities of spin and pseudospin polarization) erroneously predicts an interlayer charge transfer instability. As we discussed in Sec. II, such an instability is unavoidable when interlayer correlations (s_{12}) are neglected. According to the stability criterion of Eq. (7), the interlayer charge-transfer instability should occur in the simplest theory (spin-unpolarized, no interlayer exchange) when

$$r_{s1} \geq \pi\sqrt{2}(1 + 2d/a_0) - r_{s2}, \quad (65)$$

where $r_{si} = 1/\sqrt{\pi n_i a_0^2}$ is the dimensionless interparticle separation in layer i , and we have taken $n_1 \leq n_2$ (or $r_{s1} \geq r_{s2}$). At balance, setting $r_{s1} = r_{s2}$ in Eq. (65) gives $r_s = (\pi/\sqrt{2})(1 + 2d/a_0)$ as the GRPA version of the critical particle separation for Ruden and Wu's hypothetical pseudospin-polarization ($p = 4 \rightarrow p = 2b$) transition. [In the MFA, $r_s(2b, 4) = r_s^{(0)}(2, 4)(1 + 2d/a_0)$ gives the Ruden-Wu hypothetical pseudospin-polarization transition at balance.]

Note that even in the limit of equal layer densities and zero layer separation, $r_{s1} \geq \sqrt{\pi}/2$, which is the GRPA value of the particle separation for a single layer to spin polarize. Thus even in a theory that neglects interlayer correlations, the particles in the lower-density layer (or both layers, if they are balanced) spin-polarize before the layer empties out. As noted in Ref. 17, the spin polarization of the electrons predicted by the HFA was ignored by Ruden and Wu.¹⁵ However, including the spin polar-

ization does not eliminate the interlayer charge transfer instability, which according to Eqs. (7) and (64) would occur at

$$r_{s1} > 2\pi(3/4 + d/a_0) - r_{s2}/\sqrt{2}, \quad (66)$$

when layer 1 is spin-polarized but layer 2 is not, and at

$$r_{s1} \geq 2\pi(1 + d/a_0) - r_{s2}, \quad (67)$$

when both layers are spin polarized, if interlayer correlations could be ignored.

3. LDF model

We now introduce a tight-binding local density functional (LDF) model, which includes the effects of interlayer tunneling in a simple way. We shall follow the previous section and ignore for now the effects of interlayer exchange, and we shall even take the electron densities to be always spin-unpolarized. Such an elementary model is capable of fitting experimental data quite well, despite its simplicity.

The Kohn-Sham single-particle equations for our tight-binding LDF model is conveniently expressed as a 2×2 matrix equation:

$$\begin{pmatrix} \epsilon_1 & -t \\ -t & \epsilon_2 \end{pmatrix} \begin{pmatrix} z_1^{(\lambda)} \\ z_2^{(\lambda)} \end{pmatrix} = E_\lambda \begin{pmatrix} z_1^{(\lambda)} \\ z_2^{(\lambda)} \end{pmatrix}, \quad (68)$$

where

$$\epsilon_j = (-1)^j \frac{1}{2} eE_{12}d + \mu_{xc}(n_j) \quad (69)$$

represents the “on-site” energy of layer j , and the tunneling matrix element $-t$ is off-diagonal. The amplitude of the wave function for subband λ ($\lambda = a, b$) in layer j is $z_j^{(\lambda)}$, and the subband energy is E_λ . The Hartree contribution to the on-site energy enters via the interlayer electric field E_{12} , as shown in Eq. (2). The intralayer exchange and correlation contributions to the on-site energy are given by the exchange-correlation potential μ_{xc} . In LDF theory, $\mu_{xc}(n)$ is equal to the derivative, with respect to density, of the exchange plus correlation energies per unit area of a two-dimensional single-layer system of uniform areal density n . Equivalently, $\mu_{xc}(n_j)$ is equal to μ_j [see Eq. (5)] minus the kinetic energy contribution to μ_j . For simplicity, we do not include intralayer correlation energy contributions to μ_{xc} , so we write

$$\mu_{xc}(n) \approx -\frac{4}{\sqrt{\pi}} \frac{e^2}{4\pi\epsilon} \sqrt{n}. \quad (70)$$

The density in layer j is given by

$$n_j = \sum_{\lambda=1}^2 N_\lambda |z_j^{(\lambda)}|^2, \quad (71)$$

where

$$N_\lambda \equiv (E_F - E_\lambda)\nu_0 \Theta(E_F - E_\lambda) \quad (72)$$

is the areal-density contribution from subband λ , and $\nu_0 = m^*/\pi\hbar^2$ is the two-dimensional density of states for noninteracting particles. The self-consistency of the Kohn-Sham equations enters via Eqs. (71) and (72), since the layer densities n_j , together with the gate densities p_α , determine the interlayer electric field E_{12} appearing in Eq. (69). The Fermi energy E_F is chosen so that the sum of the subband densities N_λ is equal to the total density $p_F + p_B$.

This simple LDF model, which takes the layers to have zero thickness and assumes that the real spins are unpolarized, is capable of fitting the experimental layer density data closely. This is illustrated in Fig. 7, which shows SdH data taken from sample A of Ref. 20. The front-gate voltages used in Fig. 7 were calculated using Eq. (58).

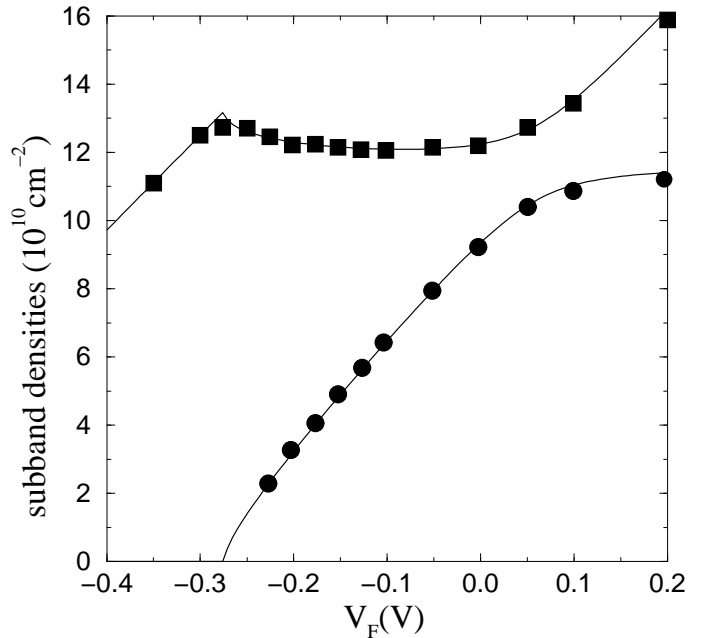


FIG. 7. Experimental subband densities for n_a (squares) and n_b (circles) versus front-gate voltage, together with fit (solid curves) from tight-binding LDF model.

B. Interlayer exchange

We now allow for the possibility of interlayer exchange in biased systems. We found that for balanced systems, interlayer exchange becomes important only at low densities and small layer separations, occurring only in the one-component phase. In this section, we explore the effect of interlayer exchange on biased double layers, and find that it can reduce or suppress interlayer (although not intersubband) charge transfers. We find that bias always increases pseudospin polarization and sometimes reduces the total density required to achieve SILC.

1. Interlayer phase angle

When the interlayer tunneling t is zero, it is possible to determine the equilibrium value of θ that minimizes the total energy per unit area, in terms of the equilibrium subband densities. Extremizing Eq. (23) with respect to θ for $n_a > n_b$ gives

$$\cos \theta = \begin{cases} -1, & X \leq -1 \\ X, & -1 \leq X \leq 1 \\ 1, & X \geq 1 \end{cases} \quad (73)$$

$$X = \frac{(p_F - p_B)/(n_a - n_b)}{1 - \Gamma},$$

where Γ is defined in Eq. (27). In the four-component phase, the kinetic energy dominates over the exchange energy, and $(n_a - n_b) < |p_F - p_B|$, so that $\sin \theta = 0$. In practice, the only time that we find $|\cos \theta| < 1$ (for $t = 0$) is in the one-component phase. For Eq. (73) to minimize the energy with respect to θ , the second derivative of the energy with respect to θ must be positive, which is equivalent to requiring that $\Gamma < 1$. If $\Gamma > 1$ (which is true for the $p = 3$ phase near balance), then $\cos \theta = \pm 1$.

It follows from Eqs. (22) and (73) that

$$(n_1 - n_2) = \begin{cases} -(n_a - n_b), & X \leq -1 \\ (p_F - p_B)/(1 - \Gamma), & -1 \leq X \leq 1 \\ (n_a - n_b), & X \geq 1 \end{cases} \quad (74)$$

In the special case of interest where $|X| < 1$ (which requires $p = 1$), we can calculate the Eisenstein ratio R_E at the point where the layers are balanced:

$$R_E(p_F = p_B) = -\frac{1}{2}(1 - \delta p_B/\delta p_F)\frac{\Gamma}{1 - \Gamma}, \quad (75)$$

where we have used Eqs. (10) and (74). (Recall that $\delta p_B/\delta p_F \approx 0$ if the back-gate voltage V_B is kept fixed, but that $\delta p_B/\delta p_F = -1$ if the total density is kept fixed.)

Within the tight-binding model of tunneling, the MFA model shows that any finite value of the tunneling matrix element t prohibits either layer from completely emptying out, regardless of the gate charges (p_F, p_B). Extremizing the energy per unit area [Eq. (23)] with respect to θ for $t > 0$ and $p_F \neq p_B$ shows that neither $\sin \theta = 0$ nor $\cos \theta = 0$ are ever local extrema. When t is small and $p_F \ll p_B$, including any negative values of p_F (i.e., for $\zeta \leq -1$, roughly speaking), then extremizing the energy per unit area yields

$$\pi - \theta \approx \frac{t/(e^2 d n_T / 2\epsilon)}{[\zeta - (1 - \Gamma)]}, \quad (76)$$

to lowest order in $t/(e^2 d n_T / 2\epsilon)$. This result is a local minimum provided that it is positive, which is true in the limit we are considering here. It follows from Eq. (22) that $n_1/n_T \approx (\phi/2)^2$, so that $n_1 \propto t^2$. Hence n_1 , although small, is always nonzero for $t > 0$. In actual samples, large bias changes the tunneling matrix element t .

Sufficiently large bias shifts the bottom (minimum energy) of the wells relative to one another so greatly that t can be driven (for all practical purposes) to zero.

Interlayer exchange is significant only when the layer densities and their separation are sufficiently small. In order for interlayer exchange to contribute, there must be (1) more particles in one subband than another ($n_a > n_b$), and (2) nonzero $\sin \theta$ ($\theta \neq 0, \pi$). Thus, for example, the case of balanced layers with $\theta = \pi/2$ at very low densities ($n_{a\uparrow} = n_T$) is a situation in which interlayer exchange contributes strongly. We discuss this case in Sec. VI, and we find there that interlayer exchange does indeed suppress interlayer charge transfer. For the case of unbalanced layers at high total density, generally $n_a > n_b$; but when $t = 0$, θ is usually equal to 0 or π , so that in the MFA, interlayer exchange does not contribute. Near depletion, where one of the layers empties out, the situation is not as clear, so we now analyze that situation in some detail later below.

Even with interlayer exchange, it turns out that the MFA model is always unstable with respect to an abrupt exchange-driven intersubband charge transfer from (low-density) subband b to (higher-density) subband a when the particle density in subband b gets small enough. The abrupt intersubband charge transfer is probably an unphysical feature of the MFA model that is not observed in real experiments. We believe that a proper treatment of the correlation energies (which have been entirely omitted here) would help fix this shortcoming. Nevertheless, we can still investigate what the MFA has to say about *interlayer* charge transfer, since the subbands are in general different from the layers, when we include interlayer exchange.

2. Subbands densities nearly equal

We now consider the limit in which $\Delta n \equiv (n_a - n_b) \ll n_T$, so that the double-layer system is only slightly pseudospin-polarized. This will be the case for the two- ($p = 2a$) and four- ($p = 4$) component ground states for small t and $|p_F - p_B|$. We begin by computing the change in the ground-state energy per unit area due to changing Δn from zero to a small but finite value. Expanding Eq. (23) to second order in Δn gives

$$\frac{\Delta \mathcal{E}_0}{L_x L_y} = \frac{(\Delta n)^2}{p \nu_0} - t \Delta n \sin \theta - \frac{e^2}{4\pi\epsilon} \frac{(\Delta n)^2}{\sqrt{p\pi n_T}} + \frac{e^2 d}{8\epsilon} [\Delta n \cos \theta - (p_F - p_B)]^2 + \Gamma_0 \frac{e^2 d}{2\epsilon} \left(\frac{\Delta n}{2} \right)^2 \sin^2 \theta, \quad (77)$$

where

$$\Gamma_0 \equiv \lim_{n_a \rightarrow n_b} \Gamma. \quad (78)$$

The quantity Γ_0 is calculated in Sec. A 4 b of the Appendix. Extremizing Eq. (77) with respect to θ gives

$$\begin{aligned} & -2t \cos \theta + \frac{e^2 d}{2\epsilon} (p_F - p_B) \sin \theta \\ & = (1 - \Gamma_0) \frac{e^2 d}{2\epsilon} \Delta n \sin \theta \cos \theta. \end{aligned} \quad (79)$$

By taking the second derivative of Eq. (77) with respect to θ , we find that Eq. (79) is a local minimum provided that

$$\begin{aligned} & 2t \sin \theta + \frac{e^2 d}{2\epsilon} (p_F - p_B) \cos \theta \\ & - (1 - \Gamma_0) \frac{e^2 d}{2\epsilon} \Delta n \cos(2\theta) > 0. \end{aligned} \quad (80)$$

Except for $p = 3$ near balance, $0 < \Gamma_0 < 1$, so that

$$0 < 1 - \Gamma_0 < 1. \quad (81)$$

Hence Eqs. (79) and (80) imply that if $t > 0$ but $|p_F - p_B| = 0$, then $\cos \theta = 0$ so that $\theta = \pi/2$ (except for $p = 3$.) If, however, $|p_F - p_B| > 0$ but $t = 0$, then $\sin \theta = 0$ so that $\theta = 0, \pi$ (except for $p = 1$.) There is thus a competition between the effects of t and $|p_F - p_B|$. If neither t nor $|p_F - p_B|$ is zero, then $\sin \theta \neq 0$ and $\cos \theta \neq 0$. In the limit that $(e^2 d/2\epsilon)|p_F - p_B| \ll t$, then

$$\cos \theta \approx \frac{(e^2 d/2\epsilon)(p_F - p_B)}{2t} \ll 1 \quad (82)$$

for $\Delta n \rightarrow 0$. On the other hand, in the limit that $t \ll (e^2 d/2\epsilon)|p_F - p_B|$, then

$$\sin \theta \approx \frac{2t}{(e^2 d/2\epsilon)[|p_F - p_B| - (1 - \Gamma_0)\Delta n]} \ll 1. \quad (83)$$

In general, θ must be solved numerically.

Extremizing Eq. (77) with respect to Δn gives

$$\Delta n = \frac{2t \sin \theta + (e^2 d/\epsilon)(p_F - p_B) \cos \theta}{\frac{4}{\rho\nu_0} + \frac{e^2 d}{2\epsilon} (\cos^2 \theta + \Gamma_0 \sin^2 \theta) - \frac{e^2}{4\pi\epsilon} \frac{4}{\sqrt{p\pi n_T}}}, \quad (84)$$

which is a local minimum provided that its denominator is positive, as may be seen by computing the second derivative of Eq. (77) with respect to Δn . Note that both interlayer tunneling (t) and gate bias ($|p_F - p_B|$) produce pseudospin polarization (increase Δn .)

When $p_F = p_B$ and t is (arbitrarily) small but nonzero so that $\theta = \pi/2$, Eq. (84) yields the pseudospin Stoner enhancement factor in Eq. (56). This is discussed in more detail in Sec. IV B 2.

When $\sin \theta = 0$ (which requires $t = 0$), then Eq. (84) gives

$$\frac{\Delta n}{|p_F - p_B|} = \frac{d/a_0}{d/a_0 + (2/p)[1 - r_s/(\pi\sqrt{2/p})]}. \quad (85)$$

This is the case for the $p = 2a$ and $p = 4$ states for $\Delta n/n_T \ll 1$. It follows from this that near balance ($p_F \approx p_B$), the Eisenstein ratio for fixed p_B is given by

$$R_E = \frac{1}{2} \left[1 + \frac{(p/2)d/a_0}{1 - r_s/(\pi\sqrt{2/p})} \right]^{-1}, \quad (86)$$

where we have use of Eq. (10). Equation (85) says that, when $\sin \theta = 0$, then $\Delta n < |p_F - p_B|$ for small $\Delta n/n_T$, provided that

$$r_s < \pi\sqrt{2/p}. \quad (87)$$

Now, the GRPA estimate of the interparticle separation required for spin polarization in a single two-dimensional layer is $r_s = \pi/\sqrt{2}$, which is just the right-hand side of Eq. (87) for $p = 4$. We therefore expect that, as long as the ground state has four components, it will be true that $\Delta n < |p_F - p_B|$, and this is indeed what our MFA calculations find for small r_s .

According to Eq. (85), $\Delta n < |p_F - p_B|$ for small $\Delta n/n_T$ for $p = 2a$ until $r_s > \pi$. The interparticle separation $r_s = \pi$ is also the GRPA estimate of $r_s^{(0)}(1, 2)$ required for pseudospin polarization. Thus for $d > 0$ we expect that at higher densities (small r_s), $\Delta n < |p_F - p_B|$ throughout the $p = 4$ state and in the low- r_s region of the $p = 2a$ state, but that $\Delta n > |p_F - p_B|$ for the high- r_s region of the $p = 2a$ state, at least for small $\Delta n/n_T$. This is in fact what our MFA calculations show. It is also true that in the $p = 3$ phase (which has $\Delta n > 0$ even when $p_F = p_B$), $\Delta n > |p_F - p_B|$ for $\zeta \ll 1$, although not for ζ on the order of one. Of course, for r_s sufficiently small, pseudospin polarization occurs so that $\Delta n = n_T > |p_F - p_B|$.

Figure 8 shows a plot of the subband densities $n_{\alpha s}$ and the ratio $(p_F - p_B)/(n_a - n_b)$ versus r_s for fixed layer separation $d/a_0 = 5$ and fixed layer imbalance $\zeta = 0.2$. For small r_s , the $p = 4$ phase is obtained, and $(p_F - p_B)/(n_a - n_B) > 1$. For $r_s \approx 2.011$, the $p = 4$ phase is obtained, and $(p_F - p_B)/(n_a - n_B) < 1$. For larger r_s , the spin-polarized $p = 2a$ phase is obtained. Note that for $p = 2a$ the ratio $(p_F - p_B)/(n_a - n_B)$ is larger than one for smaller r_s , but smaller than one for larger r_s . For even larger r_s (not shown), the $p = 1$ phase would be obtained with $(p_F - p_B)/(n_a - n_B) = \zeta$, which in this case has $\zeta = 0.2$.

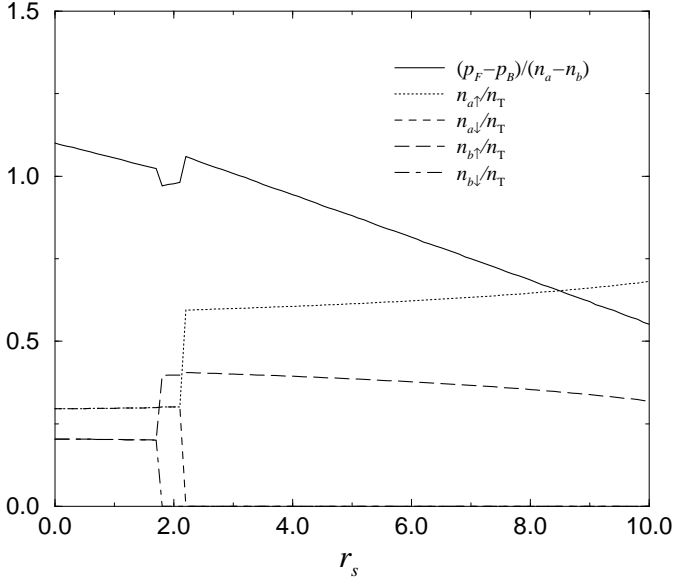


FIG. 8. Normalized subband densities and the ratio $(p_F - p_B)/(n_a - n_b)$, versus average interparticle separation r_s , for fixed $d/a_0 = 5$ and fixed gate imbalance parameter $\zeta = 0.2$. The $p = 4$, $p = 3$, and $p = 2a$ phases are obtained successively as r_s is increased.

If the denominator in Eq. (84) is not positive, then the global minimum for the energy per unit area occurs for $\Delta n = n_T$, corresponding to pseudospin polarization. Thus the GRPA condition for stability against abrupt *intersubband* charge transfer is just the condition that denominator in Eq. (84) be positive, or equivalently

$$\frac{d}{a_0} + \frac{(2/p)[1 - r_s/(\pi\sqrt{2/p})]}{(\cos^2\theta + \Gamma_0\sin^2\theta)} > 0. \quad (88)$$

When $\sin\theta = 0$ (which requires $t = 0$) so that the pseudospin is Ising-like and interlayer exchange does not contribute, then Eq. (88) is equivalent to the stability condition against abrupt *interlayer* charge transfer given in Eq. (7), when the electron lengths $s(n)$ are approximated by Eq. (64). When $\cos\theta = 0$ (e.g., when $p_F = p_B$ and t has any finite positive value), then the violation of the inequality in Eq. (88) is equivalent to the condition that the pseudospin Stoner enhancement factor I , given in Eq. (56), is equal to one, which signals the transition to pseudospin ferromagnetism and SILC. Because $0 < \Gamma_0 < 1$, gate imbalance ($|p_F - p_B| > 0$, so that $\sin^2\theta$ decreases and $\cos^2\theta$ increases) makes the double-layer system more unstable towards pseudospin polarization.

3. Subband densities versus bias

In this section, we show some illustrative calculations of the effect of layer imbalance. We plot the subband densities $n_{\alpha s}$ and the value of Γ versus the gate imbalance parameter $\zeta = (p_F - p_B)/n_T$ at fixed layer separation $d/a_0 = 5$ assuming zero interlayer tunneling ($t = 0$), for different values of r_s . We find that if we fix layer density

(or equivalently, r_s) and vary the gate imbalance parameter ζ , then (for $t = 0$) there are six distinct patterns of transitions between noncrystalline MFA ground states. We list the six possibilities below, in order of increasing layer imbalance (beginning at $\zeta = 0$) from left to right, and in order of increasing average interparticle separation per layer r_s from top to bottom:

1. $r_s < r_s(3, 4)$:
 $(p = 4) \rightarrow (p = 3) \rightarrow (p = 2b)$,
all with $\sin\theta = 0$
2. $r_s(3, 4) < r_s < r_s(2, 3)$:
 $(p = 3) \rightarrow (p = 2b)$,
all with $\sin\theta = 0$
3. $r_s(2, 3) < r_s < \sqrt{2}r_s(2, 4)$:
 $(p = 2a) \rightarrow (p = 3) \rightarrow (p = 2b)$,
all with $\sin\theta = 0$
4. $\sqrt{2}r_s(2, 4) < r_s < r_s(1, 2)$ and $\zeta_c > (1 - \Gamma_1)$:
 $(p = 2a) \rightarrow (p = 1)$,
all with $\sin\theta = 0$
5. $\sqrt{2}r_s(2, 4) < r_s < r_s(1, 2)$ and $\zeta_c < (1 - \Gamma_1)$:
 $(p = 2a) \rightarrow (p = 1)$,
with $\sin\theta > 0$ for $\zeta_c < \zeta < (1 - \Gamma_1)$
6. $r_s > r_s(1, 2)$:
 $(p = 1)$ only,
with $\sin\theta > 0$ for $0 \leq \zeta < (1 - \Gamma_1)$

Here $(p = 2a)$ denotes the spin-polarized two-component state, $(p = 2b)$ denotes the pseudospin-polarized two-component state, and ζ_c is the value of the gate imbalance parameter ζ at which the $(p = 2a) \rightarrow (p = 1)$ transition occurs. The quantity $\sqrt{2}r_s(2, 4)$ appearing in cases (4) and (5) above correspond to the critical density n_c for the MFA spin polarization transition for a single layer, expressed in terms of the average interparticle spacing per layer: $1/\sqrt{\pi(n_c/2)a_0^2}$. (Note that for the same total density n_T , a double-layer system has an average layer $r_s = 1/\sqrt{\pi(n_T/2)a_0^2}$ that is $\sqrt{2}$ larger than the single-layer $r_s = 1/\sqrt{\pi n_T a_0^2}$.) The quantity n_c is discussed below Eq. (62). We shall illustrate the first four of these possibilities in the remainder of this section, and discuss the last two possibilities (which exhibit SILC) in Sec. VI. It is evident from the above list that SILC, which requires $\sin\theta \neq 0$, occurs only for $p = 1$.

Figure 9 is an example of case (1), with $r_s = 1$. This gives a four-component ($p = 4$) phase when the gates are balanced ($\zeta = 0$), and maintains a $p = 4$ state for most of the range of ζ , followed by a $p = 3$ state for ζ near one. If we were to increase ζ beyond one (not shown), corresponding to $p_B < 0$, then a pseudospin-polarized $p = 2b$ state would be obtained.

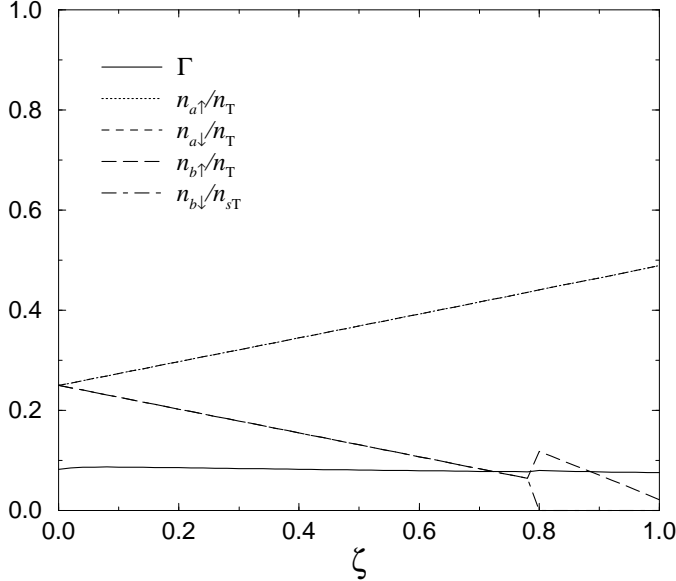


FIG. 9. Normalized subband densities and interlayer exchange parameter Γ , versus layer imbalance parameter $\zeta = (p_F - p_B)/n_T$, for $d/a_0 = 5$ and $r_s = 1$. The $p = 4$ state is obtained except for ζ near one, where the $p = 3$ state is obtained. Beyond $\zeta = 1$ (not shown) the $p = 2b$ state is obtained.

Figure 10 is an example of case (2), with $r_s = r_s(2,4) \approx 2.011$. This gives a three-component ($p = 3$) state when the gates are balanced ($\zeta = 0$), and maintains a $p = 3$ state for most of the range of ζ , followed by a pseudospin-polarized $p = 2b$ state for ζ near one and beyond. Note that for small ζ , $\Gamma(p = 3) > 1$.

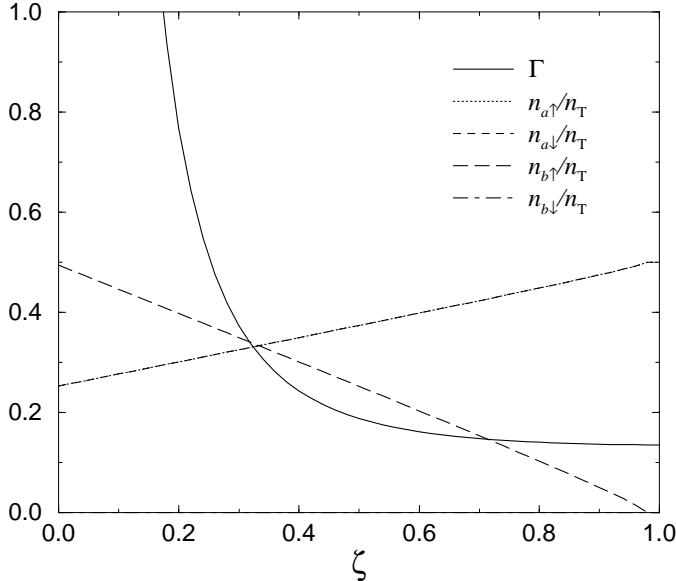


FIG. 10. Normalized subband densities and interlayer exchange parameter Γ , versus layer imbalance parameter $\zeta = (p_F - p_B)/n_T$, for $d/a_0 = 5$ and $r_s = r_s(2,4) \approx 2.011$. The $p = 3$ state is obtained except for ζ near one, where the pseudospin-polarized $p = 2$ state is obtained.

Figure 11 is an example of case (3), with $r_s = 2.5$. This gives a spin-polarized two-component ($p = 2a$) state when the gates are balanced ($\zeta = 0$), and maintains a $p = 2a$ state for $\zeta < 0.55$, followed by a $p = 3$ state for $0.55 < \zeta < 0.95$, and then a pseudospin-polarized $p = 2b$ state for $\zeta > 0.95$.

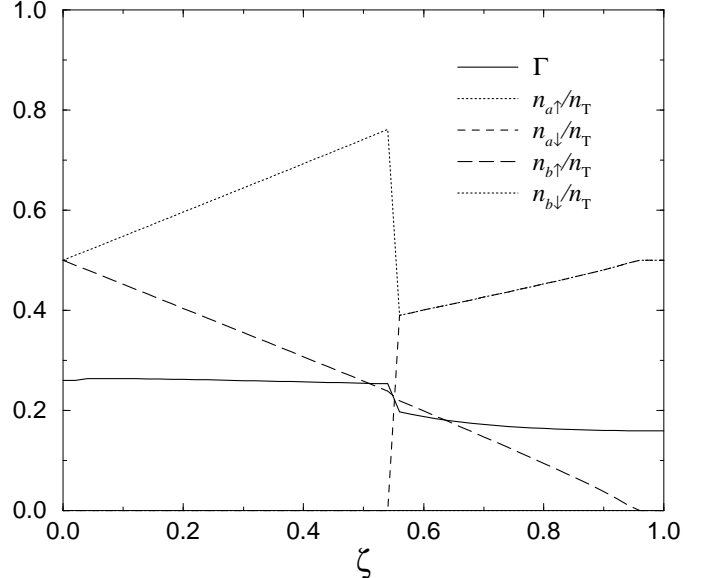


FIG. 11. Normalized subband densities and interlayer exchange parameter Γ , versus layer imbalance parameter $\zeta = (p_F - p_B)/n_T$, for $d/a_0 = 5$ and $r_s = 2.5$. The $p = 2a$ state is obtained for $\zeta < 0.6$, followed by a $p = 3$ state for $0.6 < \zeta < 0.8$, and then a pseudospin-polarized $p = 2b$ state for $\zeta > 0.8$.

Figure 12 is an example of case (4), with $r_s = 9$. This gives a spin-polarized two-component ($p = 2a$) state when the gates are balanced ($\zeta = 0$), and maintains a $p = 2a$ state for $\zeta < \zeta_c \approx 0.45$, followed by a one-component ($p = 1$) state for $\zeta > \zeta_c$. Because $\zeta_c > 1 - \Gamma_1$, $\sin \theta = 0$ throughout, and thus no SILC is found. In the next section, we consider values of r_s large enough that the $p = 1$ state is achieved for $\zeta_c < 1 - \Gamma_1$, thereby producing SILC.

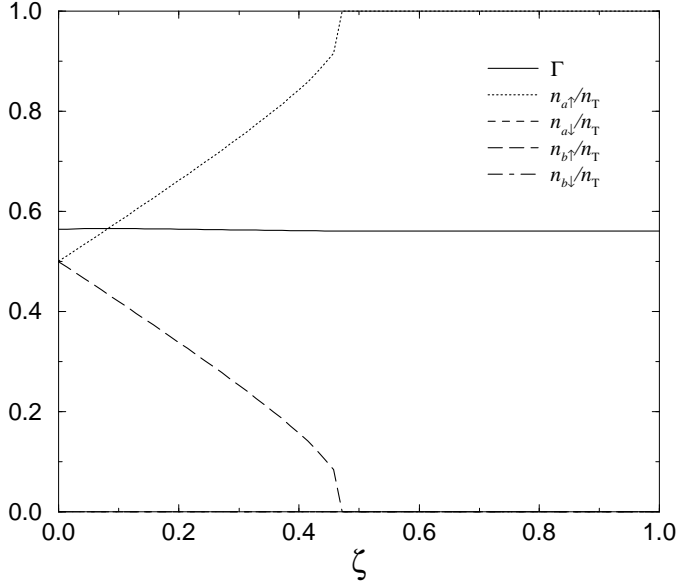


FIG. 12. Normalized subband densities and interlayer exchange parameter Γ , versus layer imbalance parameter $\zeta = (p_F - p_B)/n_T$, for $d/a_0 = 5$ and $r_s = 9$. The $p = 2a$ state is obtained for $\zeta < \zeta_c \approx 0.45$, followed by a $p = 1$ state (without SILC) for $\zeta > \zeta_c$.

VI. PSEUDOSPIN-POLARIZED STATES

In this section, we consider the case in which all the particles are in the lowest-energy subband ($n_a = n_T$), corresponding to full pseudospin polarization. There are two types of pseudospin-polarized MFA ground states: spin-unpolarized ($p = 2b$), and spin-polarized ($p = 1$). The spin-unpolarized case requires either interlayer tunneling ($t > 0$) or gate imbalance $|p_F - p_B| > 0$, or both. In the absence of tunneling, the pseudospin-polarized $p = 2b$ state has $\sin \theta = 0$ (Ising-like pseudospin), and occurs whenever the total density and the layer imbalance are sufficiently large. If the tunneling t is sufficiently large and the total density n_T is not too small, then it is possible in principle to obtain a $p = 2b$ state with $\cos \theta = 0$, for $p_F = p_B$. Tunneling also reduces the value of r_s required to achieve the $p = 1$ state. Because the pseudospin-polarized $p = 2b$ MFA state does not occur without bias or tunneling, we shall focus mainly on the spin-polarized one-component ($p = 1$) phase, which can in principle arise without bias or tunneling. The one-component phase is especially interesting because it can occur as a broken-symmetry ground state of a double-layer system in the absence of tunneling or layer imbalance, at very small particle densities and layer separations.¹⁷

When $n_a = n_T$, the ground-state energy (23) becomes

$$\frac{\mathcal{E}_0}{L_x L_y} = \frac{n_T^2}{p \nu_0} - t n_T \sin \theta - \frac{8}{3\sqrt{p\pi}} \frac{e^2}{4\pi\epsilon} n_T^{3/2} \quad (89)$$

$$+ \frac{e^2 d n_T^2}{8\epsilon} (\cos \theta - \zeta)^2 + \frac{\sin^2 \theta}{4} \frac{e^2 d n_T^2}{2\epsilon} \Gamma_1,$$

where $\Gamma_1 = \Gamma(n_a = n_T)$ and $\zeta = (p_F - p_B)/n_T$. The properties of Γ_1 are described in Sec. A4 of the Appendix. Equation (89) includes the two cases $p = 1$ ($n_{a\uparrow} = n_T$) and $p = 2b$ ($n_{a\uparrow} = n_{a\downarrow} = n_T/2$). For $t = 0$, the $p = 2b$ case has $\cos \theta = \pm 1$, so we will focus on the spin- and pseudospin-polarized one-component ($p = 1$) ground state.

A. Spontaneous interlayer coherence

The pseudospin-polarized ground state offers the possibility of SILC. Recall that SILC occurs when the off-diagonal (or interlayer) density matrix ρ_{12} is nonzero in the absence of interlayer tunneling:

$$\rho_{12} \equiv \sum_{\mathbf{k}s} \langle c_{1\mathbf{k}s}^\dagger c_{2\mathbf{k}s} \rangle = \frac{1}{2}(n_a - n_b) \sin \theta \neq 0, \quad (90)$$

which requires both finite pseudospin polarization ($n_a > n_b$) and $\sin \theta \neq 0$. In the pseudospin-polarized ground state ($n_a = n_T$), ρ_{12} is just the geometric mean of the layer densities:

$$\rho_{12} = \frac{1}{2} n_T \sin \theta = \sqrt{n_1 n_2}, \quad (91)$$

where we have made use of Eq. (18). So if the pseudospin-polarized ground state has some density of particles in each layer, it has interlayer phase coherence, $\rho_{12} \neq 0$. Note that in the one-component phase,

$$\sin \theta = (\rho_{12} + \rho_{21})/n_T \quad (92)$$

measures the interlayer density matrix, normalized by the total density.

For $t = 0$ and $p = 1$, Eq. (73) gives

$$\frac{n_1 - n_2}{n_T} = \cos \theta = \begin{cases} -1, & X \leq -1 \\ X, & -1 \leq X \leq 1 \\ 1, & X \geq 1 \end{cases} \quad (93)$$

$$X = \frac{\zeta}{1 - \Gamma_1} = \frac{\zeta}{1 - (32/3\pi p)[1 - S(z)]/z}$$

$$\rightarrow \frac{\zeta}{(32/45\pi)z - (1/24)z^2},$$

where $z = 2k_F d$, and we have made use of Eq. (22). The last line of Eq. (93) holds in the limit that $z \rightarrow 0$. The layer densities are equal ($n_1 = n_2$) only at exactly $p_F = p_B$; when $p_F > p_B$, layer 1 tends to be occupied, and when $p_F < p_B$, layer 2 tends to be occupied. Thus, the hypothetical bistability of the one-component phase proposed by Ruden and Wu does not exist, due to SILC.¹⁵ Equation (93) gives

$$\sin \theta = \sqrt{1 - [\zeta/(1 - \Gamma_1)]^2} \Theta(1 - \Gamma_1 - |\zeta|) \delta_{n_{a\uparrow}, n_T}, \quad (94)$$

so that $\sin \theta$ is nonzero only for $|\zeta| < 1 - \Gamma_1$ and for $n_{a\uparrow} = n_T$. It is interesting to note that when the ground state is pseudospin-polarized, the dependence of the layer

densities on external parameters (e.g., layer imbalance ζ) does not involve the effective mass m^* of the electrons or holes.

We have found that layer imbalance ($p_F \neq p_B$) can induce SILC at higher total densities than in the balanced case. This is illustrated for $r_s = 11$ in Fig. 13, which is an example of case (5) introduced in Sec. V B 3. Figure 13 shows a spin-polarized two-component ($p = 2a$) state when the gates are balanced ($\zeta = 0$), and maintains a $p = 2a$ state for $\zeta < \zeta_c \approx 0.28$, followed by a one-component ($p = 1$) state for $\zeta > \zeta_c$. Because $\zeta_c < 1 - \Gamma_1$, $\sin \theta > 0$ for $\zeta_c < \zeta < 1 - \Gamma_1$, producing SILC in a finite region of layer imbalance away from $\zeta = 0$, at a smaller value of r_s than is required to achieve SILC for balanced layers.

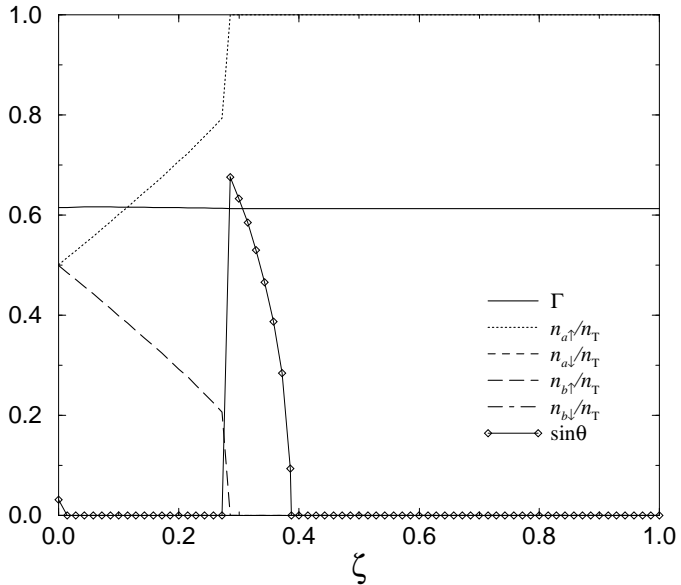


FIG. 13. Normalized subband densities, interlayer exchange parameter Γ , and normalized interlayer density matrix $\sin \theta$, versus layer imbalance parameter $\zeta = (p_F - p_B)/n_T$, for $d/a_0 = 5$ and $r_s = 11$. The $p = 2a$ state is obtained for $\zeta < \zeta_c \approx 0.45$, followed by a $p = 1$ state with SILC for $\zeta_c < \zeta < 1 - \Gamma_1$. SILC is lost for $\zeta > 1 - \Gamma_1$.

When the total density (and layer separation) are sufficiently small, the $p = 1$ phase with SILC is obtained even in the balanced case. This is illustrated for $r_s = 15$ in Fig. 14, which is an example of case (6) introduced in Sec. V B 3. Figure 14 shows a one-component ($p = 1$) state throughout the range of ζ , with $\sin \theta > 0$ for $\zeta < 1 - \Gamma_1$, producing SILC in that region. Note that as $r_s \rightarrow \infty$, then $z = 2k_F d \rightarrow 0$, so that $\Gamma_1(z) \rightarrow 1$, and thus $1 - \Gamma_1 \rightarrow 0$. Therefore the maximum amount of imbalance ζ which allows SILC decreases with the density, at very low densities.

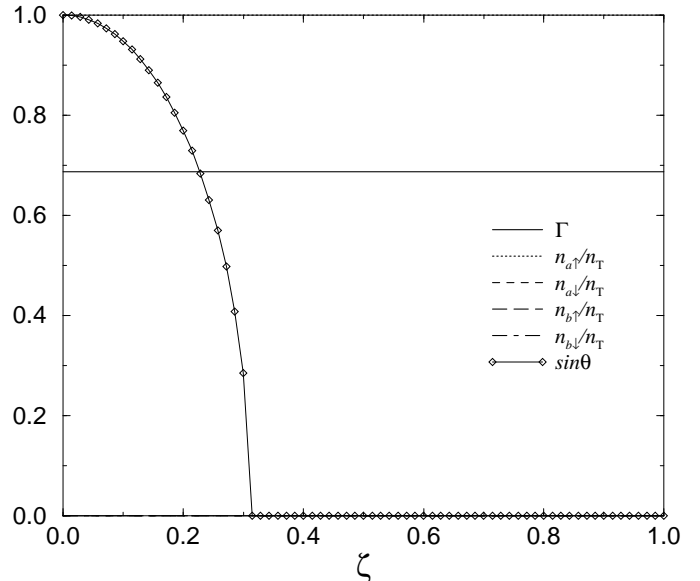


FIG. 14. Normalized interlayer density matrix $\sin \theta$ and interlayer exchange parameter Γ , versus layer imbalance parameter $\zeta = (p_F - p_B)/n_T$ in the one-component phase ($n_{a\uparrow} = n_T$), for $d/a_0 = 5$ and $r_s = 15$. SILC is lost for $\zeta > 1 - \Gamma_1$.

Figure 15 shows $\sin \theta$ versus ζ at $d/a_0 \approx 4.356$ for the three values of r_s , where $\sin \theta$ obeys Eq. (94). At the lowest density shown ($r_s = 11$), the system exhibits SILC when balanced ($\zeta = 0$) and under bias, until $\zeta = 1 - \Gamma_1$. As the density is raised, SILC is lost for the balanced system but appears suddenly around $\zeta \approx 0.2$ for $r_s = 10.5$ when an abrupt intersubband charge transfer produces pseudospin polarization ($p = 1$). For $r_s = 9$ there is only a very small region of layer imbalance ζ that exhibits SILC, and for r_s slightly smaller than this value, SILC disappears completely.

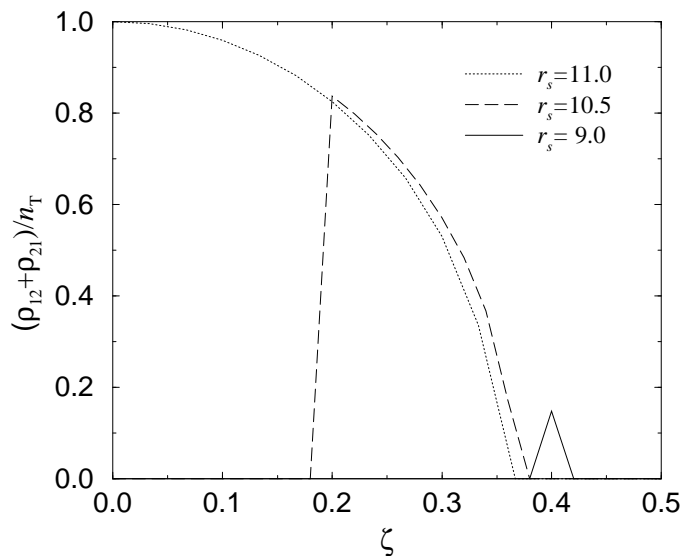


FIG. 15. Interlayer exchange strength $(\rho_{12} + \rho_{21})/n_T = \sin \theta$ as a function of the gate-imbalance parameter $\zeta = (p_F - p_B)/n_T$ for fixed $d/a_0 \approx 4.356$.

Using Eqs. (89), (91), and (93), we may calculate the energy per unit area $\varepsilon(n_1, n_2)$ defined in Eq. (3), for the one-component phase:

$$\varepsilon(n_1, n_2) = \frac{n_T^2}{\nu_0} - \frac{8}{3\sqrt{\pi}} \frac{e^2}{4\pi\epsilon} n_T^{3/2} + \frac{e^2 d n_1 n_2}{2\epsilon} \Gamma_1, \quad (95)$$

where $n_T = n_1 + n_2$. Recall that ε does not include the electrostatic contribution to the energy per unit area. We may use Eqs. (5) and (95) to calculate μ_1 , the chemical potential measure relative to the energy minimum of layer 1,

$$\begin{aligned} \mu_1 = & \frac{2n_T}{\nu_0} - \frac{4}{\sqrt{\pi}} \frac{e^2}{4\pi\epsilon} \sqrt{n_T} \\ & + \frac{e^2 d n_2}{2\epsilon} \left(\Gamma_1 + n_1 \frac{d\Gamma_1}{dn_T} \right), \end{aligned} \quad (96)$$

where we have used the fact that in the one-component phase, Γ_1 depends on n_1 and n_2 only through $n_T = n_1 + n_2$. The quantity μ_2 may be obtained by interchanging n_1 and n_2 in Eq. (96) and can be used to compute the front-gate voltage V_F using Eq. (A3) in the Appendix. It is straightforward to check that the difference between μ_1 and μ_2 satisfies the equilibrium condition in Eq. (4). Equations (6) and (96) may be used to calculate the electronic length s_{ij} defined in Sec. II:

$$\frac{s_{11}}{a_0} = \frac{1}{2} - \frac{r_s}{2\pi\sqrt{2}} + \frac{1}{2} \frac{d}{a_0} n_2 \left(2 \frac{\partial\Gamma_1}{\partial n_T} + n_1 \frac{\partial^2\Gamma_1}{\partial n_T^2} \right). \quad (97)$$

The quantity s_{22} may be obtained by interchanging n_1 and n_2 in Eq. (97).

Interlayer correlations produce a nonzero value of the electron length s_{12} . From Eqs. (6), (8), and (96) we have

$$s_{12} = s_{11} + \frac{d}{2} \left[\Gamma_1 + (n_1 - n_2) \frac{\partial\Gamma_1}{\partial n_T} \right]. \quad (98)$$

Note that $s_{21} = s_{12}$, and that

$$s_1 \equiv s_{11} - s_{12} = -\frac{d}{2} \left[\Gamma_1 + (n_1 - n_2) \frac{\partial\Gamma_1}{\partial n_T} \right]. \quad (99)$$

The length s_2 can be obtained from s_1 by interchanging n_1 and n_2 . Note that

$$s \equiv s_1 + s_2 = -\Gamma_1 d, \quad (100)$$

so that, from Eq. (11), the Eisenstein ratio for fixed total density (constant n_T) is

$$R_E = \frac{s}{d+s} = \frac{-\Gamma_1}{1-\Gamma_1} \rightarrow \frac{-1}{(32/45\pi)z}, \quad (101)$$

where $z = 2k_F d$, and the right-hand side holds in the limit $z \rightarrow 0$. It is interesting to note that $R_E \propto -1/z$,

as $d \rightarrow 0$, just as was found in Ref. 26 for the $\nu_T = 1$ 2LQH state. For fixed p_B (nearly equivalent to keeping the back-gate voltage V_B constant),

$$R_E = \frac{s_1}{d+s} = -\frac{[\Gamma_1 + (n_1 - n_2)\partial\Gamma_1/\partial n_T]}{2(1-\Gamma_1)}, \quad (102)$$

which in the balanced case ($p_F = p_B$ so that $n_1 = n_2$) gives Eq. (75), which is exactly half of Eq. (101).

Figure 16 shows an example of the one-component phase under bias for fixed back-gate density p_B (essentially fixed back-gate voltage V_B). The normalized layer densities n_1 and n_2 are shown, together with the interlayer density matrix ρ_{12}/p_B and Γ , and also the Eisenstein ratio R_E . For $p_F/p_B < 0.5$, layer 2 contains all the charge ($n_2 = n_T$) and layer 1 is empty, so that Eq. (10) gives $R_E = 1$. For $0.5 < p_F/p_B < 2.25$, both n_1 and n_2 are partially occupied, $\rho_{12} = \sqrt{n_1 n_2}$ is nonzero, and R_E has dropped abruptly and become negative, reflecting the presence of SILC, with its value in this region given by Eq. (102). For $p_F/p_B > 2.25$, layer 2 is empty, $n_1 = n_T$, and $R_E = 0$. Figure 16 illustrates an interesting hypothetical situation in which bias and the exchange interaction have completely emptied out layer 2, despite the fact that p_B is nonzero. It turns out that within the MFA, sufficiently large p_F would eventually repopulate layer 2. We analyze this issue further below, when we calculate the energy gap Δ_{ab} in a pseudospin-polarized state ($n_a = n_T$) to an otherwise empty subband ($n_b = 0$).

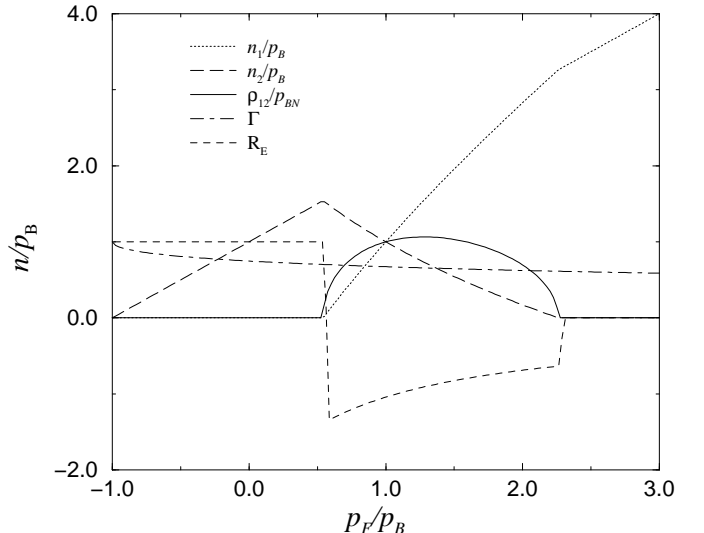


FIG. 16. Layer densities n_1, n_2 and normalized interlayer density matrix $2\rho_{12}/n_T = \sin \theta$, in the one-component phase, versus front-gate density p_F/p_B , for fixed back-gate density p_B .

Although Zheng and co-workers showed (within an unrestricted HFA) that an abrupt *interlayer* charge transfer does not occur when the gates are electrostatically balanced ($p_F = p_B$), one may ask if an abrupt interlayer charge transfer can occur if the system is biased. According to the MFA developed here, the answer is yes,

except at sufficiently small densities. (We are speaking here of zero tunneling; otherwise, neither layer is strictly empty, according to the MFA.) In the MFA, sufficiently strong bias or tunneling or sufficient lowering of the densities eventually produces an abrupt *intersubband* charge transfer, i.e., at some point, n_a suddenly jumps. Whether this translates into abrupt *interlayer* charge transfers depends on what happens with the phase angle θ . If $\sin \theta \neq 0$ (SILC), then the interlayer charge transfer is suppressed, or at least somewhat reduced. If the density is so high that strong bias produces the $p = 2b$ pseudospin-polarized phase with $\sin \theta = 0$, then the MFA does give an abrupt interlayer charge transfer, because then $\cos \theta = \pm 1$, and there is no difference between subband densities and layer densities. So, for example, a system with a density that would correspond to $p = 4$ when balanced will not exhibit SILC. It is likely that including correlation-energy effects eliminates the abruptness of the transition, but these effects have not been included here.

B. Intersubband gap

The intersubband energy gap Δ_{ab} for the pseudospin-polarized ($p = 1$ or $p = 2b$) phase is defined as the energy required to move a particle from the occupied a subband with $n_a = n_T$ to the (otherwise empty) b subband:

$$\Delta_{ab} = \frac{\delta}{\delta n} \left(\frac{\mathcal{E}_0}{L_x L_y} \right), \quad (103)$$

for

$$\begin{aligned} n_{a\uparrow} &\rightarrow (1/p)(n_T - \delta n), & n_{b\uparrow} &\rightarrow \delta n, \\ n_{a\downarrow} &\rightarrow (1 - 1/p)(n_T - \delta n), & n_{b\downarrow} &= 0. \end{aligned} \quad (104)$$

An outline of the MFA calculation of Δ_{ab} is given in Sec. A 6 of the Appendix. In units of the energy scale $v_0 = e^2/4\pi\epsilon a_0$, the MFA intersubband gap is

$$\begin{aligned} \frac{\Delta_{ab}}{v_0} &= \frac{2t}{v_0} \sin \theta - \frac{4}{r_s^2} \left[\frac{1}{p} + \frac{d}{a_0} \cos \theta (\cos \theta - \zeta) \right] \quad (105) \\ &+ \sqrt{\frac{2}{p}} \frac{4}{\pi} \frac{1}{r_s} - \sin^2 \theta \sqrt{\frac{2}{p} \frac{1}{r_s}} \left\{ \frac{[e^{-z/2} - (1 - z/2)]}{z/2} \right. \\ &\quad \left. + \frac{2}{\pi} \int_0^1 dx (1 - e^{-zx}) \arccos(x) \right\} \end{aligned}$$

where $\zeta = (p_F - p_B)/n_T$, and $z = 2k_F d$ is the layer imbalance.

The intersubband gap Δ_{ab} is useful for at least two purposes. First, it provides an estimate for the location of the pseudospin-polarization transition. The condition $\Delta_{ab} > 0$ means the pseudospin-polarized ground state is stable against intersubband charge transfers, whereas $\Delta_{ab} < 0$ implies the opposite. Thus, solving the equation $\Delta_{ab} = 0$ in the MFA yields an estimate of the location of the pseudospin-polarization transition. It turns

out that this procedure gives a lower value of r_s for the $p = 1$ transition than the GRPA estimate (obtained using the pseudospin Stoner enhancement factor I): at $d = 0$, the MFA Δ_{ab} calculation (for $t = \zeta = 0 = \cos \theta = 0$) gives $r_s^{(0)}(1, 2) = \pi/\sqrt{2}$, compared to $r_s^{(0)}(1, 2) = \pi$ from the GRPA. Figure 17 shows Δ_{ab} versus d/a_0 when $t = \zeta = \cos \theta = 0$ for $r_s = 1, 2, 3, 6$. It is evident that $\Delta_{ab} > 0$ only for sufficiently large r_s , and that it decreases with layer separation d/a_0 . Negative values of Δ_{ab} indicate regions where the pseudospin-polarized state is not stable.

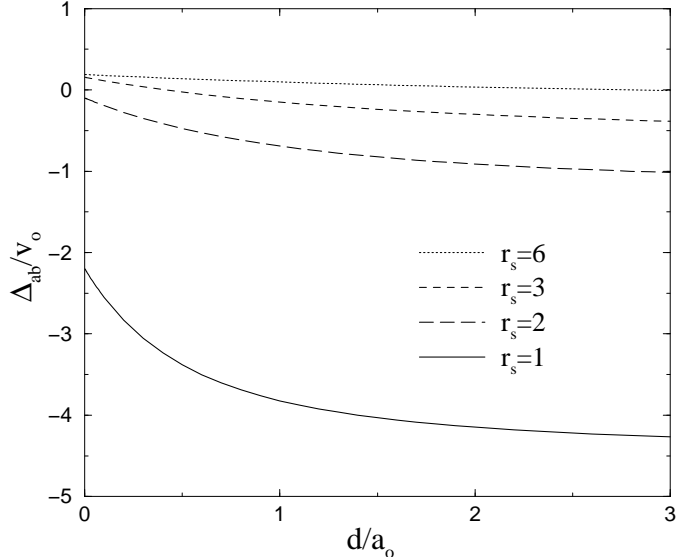


FIG. 17. Normalized intersubband energy gap Δ_{ab} for transferring particles from the occupied lower-energy subband a to the (assumed empty) higher-energy subband b , for $r_s = 1, 2, 3, 6, 10$.

The intersubband gap has a simple form when $t = \sin \theta = 0$:

$$\frac{\Delta_{ab}}{v_0} = -\frac{4}{r_s^2} \left[\frac{1}{p} + \frac{d}{a_0} (1 - |\zeta|) \right] + \sqrt{\frac{2}{p}} \frac{4}{\pi} \frac{1}{r_s}. \quad (106)$$

Equation (106) provides an estimate of when one of the layers contains all the particles. It tells us that for sufficiently high total density (small r_s), $\Delta_{ab} < 0$ and both layers must be occupied, provided that $1/2 + (d/a_0)(1 - |\zeta|) > 0$ (which includes $\zeta = 1$, corresponding to $p_B = 0$). This is because the kinetic energy (and the Coulomb energy, for $|\zeta| < 1$), which favors occupying both layers, dominates over the exchange energy, which favors occupying a single layer, at higher densities. For example, for $p = 2$ and $\zeta = 1$, Eq. (106) shows that both layers will be occupied even when $p_B = 0$, provided that $r_s < \pi/2$. On the other hand, for $p = 1$ and $\sin \theta = 0$ (i.e., $|\zeta| > 1 - \Gamma_1$), only one layer will be occupied, provided that $r_s > (\pi/\sqrt{2})[1 + (d/a_0)(1 - |\zeta|)]$. This is the situation shown in Fig. 16, which shows that layer 2 has completely emptied for $p_F/p_B > 2.25$. At higher values

of p_F/p_B (e.g., $r_s < \pi/2$, not shown), layer 2 would no longer be empty.

The second use of the MFA calculation of Δ_{ab} is as a rough estimate of the minimum energy (thermal, or from photons) required to excite particles from the occupied to the unoccupied subband in the one-component state. Perhaps this could be detected with sensitive heat-capacity measurements or by measuring microwave absorption.

C. Coulomb drag

One very interesting feature of the one-component state with SILC is that it is expected to exhibit interlayer drag (finite dc transresistance), even at zero temperature. Ordinarily, if the layers are not correlated in the ground state, current in one layer can drag along particles in the other layer (due to the Coulomb interaction between the layers) only at finite temperature.¹¹ But if $\rho_{12} \neq 0$, due to either tunneling or, more interestingly, to SILC, then interlayer correlations present in the 2LES ground state will produce interlayer drag even at zero temperature, as has been predicted for interlayer-correlated 2LQH states.^{7,31} Based on the Kubo formula with the ground state of Eq. (15), we expect that a calculation of the zero-temperature dc transconductivity σ_d will give

$$\sigma_d \propto \frac{e^2 \rho_{12}}{m^*} \propto \frac{e^2 (n_a - n_b) \sin \theta}{m^*}. \quad (107)$$

Calculations of the drag conductivity for a pseudospin-polarized ground state are currently being carried out by other researchers.³² According to Eqs. (91) and (107), we expect that in the $p = 1$ phase ($n_a = n_T$), $\sigma_d \sim \sqrt{n_1 n_2}$, approximately (i.e., within an MFA calculation of σ_d .)

It would be interesting to clarify the relationship between s_{12} , ρ_{12} , and σ_d . We conjecture that finite interlayer drag at zero temperature requires $\rho_{12} \neq 0$ at zero temperature (although we have not proved this) and that $\rho_{12} \neq 0$ (or at least $\rho_{12}\rho_{21} \neq 0$) at zero implies finite interlayer drag at zero temperature. It is certainly true that $\rho_{12} \neq 0$ and $\sigma_d \neq 0$ occur together at zero temperature in the interlayer-correlated 2LQH effect.⁷ We also think it likely that a similar relation holds between s_{12} and ρ_{12} , and hence between s_{12} and σ_d , although we have not proved this either.

VII. CONCLUSIONS

We investigated the effects of intralayer and interlayer exchange in biased double-layer systems, in the absence of a magnetic field. This was accomplished using a mean-field approximation (MFA) which, in the limit of balanced layers (no bias), is equivalent to the unrestricted HFA of Zheng and co-workers¹⁷

A. Findings

We found that a balanced 2LES possesses four possible noncrystalline MFA ground states. The spin- and pseudospin-unpolarized four-component ($p = 4$) state is obtained at the highest densities. In contrast to earlier work, we found that as the density is lowered, a three-component ($p = 3$) state with slightly unequal layer densities is obtained. Thus, we find that there is no direct four- to two-component transition. At finite layer separation ($d > 0$) and zero interlayer tunneling ($t = 0$), the $(p = 4) \rightarrow (p = 3)$ MFA transition involves a small but abrupt interlayer charge transfer. Any such abrupt interlayer charge transfer will in principle result in a large (formally infinite) value of the Eisenstein ratio R_E at the transition. The Eisenstein ratio is a sensitive measure of the interlayer capacitance discussed in Sec. II.

Like Zheng and co-workers, we found that as the total density was lowered, a spin-polarized two-component ($p = 2a$) state preceded a low-density one-component ($p = 1$) state possessing SILC, provided that the gates were balanced ($p_F = p_B$). This $p = 1$ state is different from that of Ruden and Wu, whose proposed one-component state occupied a single layer, rather than a single subband consisting of a linear combination of both layers. We obtained a MFA phase diagram for the noncrystalline phases of the 2LES, shown in Fig. 3. This phase diagram is similar to that of Ref. 17, except for the presence of the $p = 3$ phase between the $p = 4$ and $p = 2$ phases. Only the $p = 1$ phase was found to possess SILC — i.e., a nonzero interlayer density matrix ($\rho_{12} \neq 0$) even with zero interlayer tunneling ($t = 0$). We also defined the pseudospin Stoner interaction parameter I , and considered the linear response of the MFA ground state to interlayer tunneling, equivalent to a GRPA calculation. We used I to obtain an alternate (GRPA) estimate of the location of the $(p = 2) \rightarrow (p = 1)$ transition, shown as the dotted line at the top of Fig. 3. Of course, in the limit of vanishing total density ($r_s \rightarrow \infty$), we expect that a Wigner crystal state is obtained (in the absence of disorder). We did not consider the effects of disorder here, except to note that it limits the maximum r_s for a state with mobile particles.

Under bias ($|p_F - p_B| > 0$), we found that there are five possible noncrystalline ground states. In every case, the MFA gave subbands, which, when occupied, were either completely spin-unpolarized or fully spin-polarized. Including correlation-energy effects would likely produce ground states with intermediate spin polarizations, as is apparently the case in three dimensions.²⁷ The additional state that can appear under sufficiently large bias and/or interlayer tunneling is a pseudospin-polarized two-component ($n_{a\uparrow} = n_{a\downarrow} = n_T/2$) state, which we labeled $p = 2b$. The $p = 2b$ state requires bias and/or tunneling, and has $\sin \theta = 0$ (and thus no SILC) for $t = 0$. In Sec. V we studied the effect of bias by considering systems at fixed total density n_T , for a range of values of the layer-imbalance parameter $\zeta = (p_F - p_B)/n_T$. We enu-

merated the six possible scenarios for bias-driven transitions between the (five possible) noncrystalline MFA ground states for $t = 0$. We also showed that a very simple model that assumes no interlayer exchange and no spin polarization is capable of fitting experimental SdH data quite well (see Fig. 6), and that a simple LDF model can do the same in the presence of interlayer tunneling (see Fig. 7).

We studied the one-component phase under applied bias, finding that bias lowers the r_s required for SILC (see Fig. 15). Within the MFA, SILC occurs only in the one-component phase: when $t = 0$, $\sin \theta$ is nonzero only when $n_{a\uparrow} = n_T$. Perhaps including correlation-energy effects would allow SILC for states with partial pseudospin polarization. But $p = 1$ is only a necessary condition for SILC, not a sufficient one. We found that if the layer imbalance parameter was too large ($\zeta > 1 - \Gamma_1$), then SILC was lost. When SILC occurs, the MFA gave a value of the interlayer density matrix equal to the geometric mean of the layer densities: $\rho_{12} = \sqrt{n_1 n_2}$. For the case that SILC is present, we calculated the layer densities (n_i), local values of the chemical potential (μ_i), electronic lengths (s_{ij}), and Eisenstein ratio (R_E) (see Fig. 16).

Ruden and Wu originally predicted an abrupt interlayer charge transfer for $t = 0$ at sufficiently low densities and layer separations, in the balanced case ($p_F = p_B$).¹⁵ Like Zheng and co-workers, we found that an abrupt *interlayer* charge transfer does not occur in the balanced case, due to SILC. However, the MFA (and the unrestricted HFA of Ref. 17) does produce abrupt *intersubband* charge transfers, even for the balanced case. This is a feature of the HFA that requires correlation-energy effects to remedy. In the case of nonzero bias, intersubband transfers are equivalent to interlayer transfers if $\sin \theta = 0$, which is the usual case, except possibly for $p = 1$. Interlayer subband transfers at $t = 0$ are reduced or suppressed in the MFA only for the $(p = 2a) \rightarrow (p = 1)$ transition, and only if $\zeta < (1 - \Gamma_1)$ in the $p = 1$ phase. So SILC, when present, does reduce or eliminate abrupt interlayer subband transfers, but the MFA does not always eliminate them under bias ($p_F \neq p_B$). If the system is at sufficiently low density and layer separation that it stays in the $p = 1$ state, then there are no abrupt interlayer charge transfers under bias in the MFA, despite the fact that the layers can empty out as p_F is changed (see Fig. 16).

We also calculated the intersubband gap Δ_{ab} for the pseudospin-polarized ($p = 1$ or $p = 2b$) phases within the MFA, defined as the energy to move a particle from the lower energy a subband to the higher energy (empty) b subband. This energy provides an estimate of the single-particle intersubband gap in the pseudospin-polarized $p = 1$ and $p = 2b$ phases, and can be used to estimate the stability of those phases. If the $p = 1$ phase can be obtained experimentally, Δ_{ab} might be measured using heat-capacity or microwave/optical techniques. A very interesting feature of the one-component phase with SILC is that it should have nonzero interlayer drag, even

at zero temperature, with the size of the interlayer drag conductivity being proportional to the interlayer density matrix ρ_{12} .

Pseudospin polarization can be detected by SdH measurements, which exhibit oscillations that are periodic in $1/H$ (where H is the applied magnetic field). The periods of the SdH oscillations are given by

$$\Delta_{\alpha s}(1/H) = \frac{2\pi e}{\hbar} \frac{1}{A_{\alpha s}} = \frac{2\pi e}{\hbar} \frac{1}{\pi k_{\alpha s}^2} = \frac{e}{h} \frac{1}{n_{\alpha s}}, \quad (108)$$

where $A_{\alpha s}$ is the cross-sectional area of the Fermi surface perpendicular to the applied magnetic field for electrons in subband α with spin s . Knowing the total density n_T (e.g., from Hall measurements), SdH measurements of the subband densities $n_{\alpha s}$ could allow a determination of the degree of spin and pseudospin polarization. For example, in the case of equally balanced layers ($n_1 = n_2 = n_T/2$) having a p -component ground state ($p = 1, 2, 4$) in the absence of tunneling ($t = 0$), there is a single (p -fold degenerate) SdH oscillation period,

$$\Delta_p(1/H) = \frac{2\pi e}{\hbar} \frac{1}{A_p} = \frac{2\pi e}{\hbar} \frac{1}{\pi k_F^2} = \frac{e}{h} \frac{p}{n_T}, \quad (109)$$

which allows p to be determined directly from SdH measurements.

B. Can it exist?

Can the one-component state be realized in the balanced case? The $p = 1$ state is a legitimate solution of in the HFA, but we have not examined its stability here. It is hypothetically possible that the $p = 1$ state might always be preempted by a Wigner crystal state. Conti and Senatore¹⁸ carried out diffusion Monte Carlo (DMC) simulations in the $d = 0$ limit, calculating the $p = 4$ ground-state energy as a function of r_s and using previous single-layer DMC results²⁸ to estimate the $p = 2$ and $p = 1$ energies. They also estimated the ground-state energy for a Wigner crystal state, and found that the $p = 4$ state is obtained for $r_s < 42$, and that the Wigner crystal state is obtained for larger values of r_s . In their calculation, neither the $p = 2$ nor the $p = 1$ states are ever favored energetically.

Although the DMC results in Ref. 18 show the need to examine the existence and stability of the $p = 1$ state beyond the HFA, they do not rule out its existence. This is because at $d = 0$ the fermions possess $CP(3)$ symmetry (spin and pseudospin fully rotateable and interchangeable), and estimating the $p = 2$ and $p = 1$ energies using single-layer results misses part of the correlation energy, which lowers the $p = 1$ and $p = 2$ ground-state energies. Ideally, a DMC simulation of $CP(3)$ fermions would be most useful to determine theoretically if the $p = 1$ state can be obtained, but such calculations might be prohibitively difficult to carry out. As a start, allowing for the possibility of Wigner crystallization (broken translational symmetry) within the MFA calculation would

be helpful. Alternatively, a time-dependent MFA calculation of the collective mode would indicate where (for what density and layer separation) the collective mode of the 2LES goes soft ($\omega \rightarrow 0$), signaling the onset of Wigner crystallization. We are currently developing such a calculation of the collective mode. Better yet would be a double-layer STLS calculation allowing for the possibility of Wigner crystallization, or at least a determination of when the STLS collective mode goes soft in a double-layer system.

More important is the question of whether SILC can be achieved experimentally in the absence of a strong magnetic field, which serves to quench the kinetic energy of the particles. The MFA and HFA underestimate the value of r_s required for the transitions, perhaps by a factor of 10. For example, the spin-polarization transition for a single layer has been estimated to occur for $r_s \sim 20$.²⁸ Although such high values of r_s have been achieved in *p*-type GaAs samples, even higher values of r_s will be required to achieve spontaneous pseudospin polarization. Disorder imposes further constraints, because it limits the maximum r_s for which the particles are still mobile. However, given the impressive progress in producing double-layer systems with ever-lower particle densities and ever-higher mobilities, it does not seem prudent to rule out the possibility that such a state might someday be realized.

As pointed out by Zheng and co-workers¹⁷ and by Conti and Senator,¹⁸ most of the considerations presented in Ref. 7 for SILC in the quantum Hall regime should be relevant to the $p = 1$ phase (with SILC) in the absence of a magnetic field. In both cases, there is a ground state with broken $U(1)$ symmetry (when $t = 0$), due to interlayer exchange at small layer separations and particle densities. It is therefore expected that the $p = 1$ state will exhibit many of the novel features of the 2LQH state with SILC, including zero-temperature interlayer drag, vortex excitations [of the angle ϕ in Eq. (23)] and an associated a finite-temperature Kosterlitz-Thouless transition (for $t = 0$), and interesting many-body effects in tilted magnetic fields for finite interlayer tunneling.^{6–8}

C. Speculations regarding the 2LQH regime

It is interesting to speculate about the applicability of these ideas to the 2LQH effect at total filling factor unity.⁷ For sufficiently small distances ($d < d_c \approx 1.2\ell$, where $\ell = \sqrt{\hbar/eB}$ is the magnetic length⁶), the 2LQH system exhibits a quantum Hall effect.⁵ Theoretically, the small- d 2LQH state has nonzero ρ_{12} even for $t = 0$ (SILC), and the 2LQH system exhibits strong Coulomb drag.^{7,31} At sufficiently large layer separations, it is found experimentally that the quantum Hall effect disappears,⁵ and it has been proposed that there is a quantum phase transition to a state without SILC.⁷ The nature of the ground state for $d > d_c$ is a topic of active investigation. It has been analyzed as a system of two weakly coupled

layers of $\nu = 1/2$ composite fermions (CF's). Theoretical calculations of the drag at low temperatures predict that the drag resistivity should scale with temperature as $T^{4/3}$, based on calculating the effects of gauge fluctuations on two CF layers in the metallic state.^{33–35} It has also been proposed that the weak coupling between the CF's in different layers produces BCS pairing between them at sufficiently low temperatures,³⁶ and that this paired state leads to a finite drag resistivity at zero temperature.^{37,38}

We point out here that besides the apparent BCS instability between CF's in different layers, double-layer CF systems might be unstable to pseudospin polarization. In the limit $d \rightarrow \infty$, the double-layer $\nu_T = 1$ system may be regarded as a $p = 2a$ phase (i.e., spin-polarized but pseudospin-unpolarized) of CF's in zero effective magnetic field ($\nu = 1/2$ per layer). Naively, the presumably large effective mass of the CF's would correspond to a much larger effective value of r_s than for the zero-field case, perhaps producing a value of r_s sufficiently large to obtain a pseudospin-polarized $p = 1$ phase. Another way of saying this is that the large magnetic field experienced in each $\nu = 1/2$ layer quenches the kinetic energy of the particles, and that this quenching might strongly enhance exchange instabilities – in this case towards pseudospin polarization ($n_a > n_b$), presumably with $\sin \theta = 1$ (when $p_F = p_B$), since no spontaneous interlayer transfer has been found to occur for $p_F \approx p_B$. One appealing feature of a hypothetical $p = 1$ CF state is that it would have small or zero resistivity in the pseudospin channel (i.e., for oppositely directed currents), the same channel in which the 2LQH state exhibits superfluidity at sufficiently small layer separations.⁷ Such a $p = 1$ state of CF's would exhibit SILC ($\rho_{12} \neq 0$ even when $t = 0$) and therefore possess zero-temperature Coulomb drag. Recent experiments with double-layer systems corresponding to filling factor $\nu = 1/2$ in each layer provide evidence for the possibility of zero-temperature drag.³⁹ We are currently investigating the possibility and consequences of pseudospin polarization in double-layer CF systems.

We also note that a perpendicular magnetic field \mathbf{B} will generally enhance spin and pseudospin polarization because it tends to quench the kinetic energy. This effect enhances the exchange and correlation effects that lead to polarization. We therefore expect that SILC can in principle be found at *any* filling factor $\nu_T = (h/e)n_T/B$, provided that the total density n_T and the layer separation d are sufficiently small. In particular, if it exists in the one-component phase for zero magnetic field, SILC will probably persist, and even grow stronger, when a perpendicular magnetic field is applied. Finally, we remark that it may prove instructive to view the $\nu_T = 1$ 2LQH state as a Chern-Simons bosonic condensate of spin- and pseudospin-polarized ($p = 1$) electrons bound to unit flux quanta.

It has recently been found that double-layer systems in strong magnetic fields near total filling factor unity

exhibit a huge resonant enhancement of the interlayer tunneling conductivity when SILC is present.⁴⁰ It would be interesting to measure the tunneling conductivity for a tilted sample, since many-body effects in a state with SILC strongly suppress the interlayer tunneling amplitude when the parallel component of the magnetic field exceeds a critical value. This suppression is much stronger than for a system without SILC. We expect a similar strong enhancement of the tunneling conductivity at zero magnetic field, provided that the system possesses SILC. Such tunneling measurements could prove very useful for measuring the strength of SILC in double-layer systems at zero (or higher) magnetic field.

VIII. ACKNOWLEDGMENTS

We thank F. David Núñez in deep appreciation of his patience and enthusiasm, and for his invaluable assistance. We thank A. R. Hamilton for providing us with SdH data for a double-layer hole system, and for patiently answering several questions regarding experimental measurements on double-layer systems. Special thanks are also owed to S. Das Sarma and A.H. MacDonald for useful discussions. C.B.H. thanks the Institute for Theoretical Physics (University of California, Santa Barbara), where part of this work was carried out, and for their support through the ITP Scholars Program. This work was supported by a grant from the Research Corporation, and by the National Science Foundation under grant 9972332.

APPENDIX:

1. Gate voltages

The layer densities (n_1, n_2) are determined theoretically by minimizing the total ground-state energy per unit area [Eq. (23)] for fixed gate densities (p_F, p_B). Experimentally however, it is the gate voltages which are tuned. If needed, the gate voltages for a given value of (p_F, p_B) can be calculated using

$$\begin{aligned} eV_F &= eD_F E_F + \mu_1 + eV_F^{(0)}, \\ eV_B &= eD_B E_B + \mu_2 + eV_B^{(0)}, \end{aligned} \quad (\text{A1})$$

and Eq. (5). Here the gate electric fields depend on the gate sheet densities through Gauss's law, $E_\alpha = (e/\epsilon)p_\alpha$, and $eV_\alpha^{(0)}$ are sample-dependent constant gate-voltage shifts. Although eV_α is approximately equal to $eD_\alpha E_\alpha$, Eq. (A1) shows that the layer values μ_i of the chemical potential also contribute to the gate voltages.

The layer values of the chemical potential μ_i can be computed numerically from the variation of the equilibrium value of the total energy per unit area (regarded as a function of the front- and back-gate densities p_F and p_B) with respect to infinitesimal changes in gate densities:

$$\delta\bar{\mathcal{E}}_0/L_x L_y = \mu_1 \delta p_F + \mu_2 \delta p_B. \quad (\text{A2})$$

For the typical case in which the back-gate voltage V_B is kept constant and the back-gate distance D_B is much larger than the interparticle and interlayer separation so that p_B is nearly constant, it is convenient to use Eq. (4) and write

$$eV_F = eD_F E_F + edE_{12} + \mu_2 + eV_F^{(0)}, \quad (\text{A3})$$

where Eq. (A2) gives

$$\mu_2 \approx \frac{\partial}{\partial p_B} \left(\frac{\bar{\mathcal{E}}_0}{L_x L_y} \right)_{p_F}. \quad (\text{A4})$$

Equation (A3) has the advantage of being applicable even when layer 1 empties out. Equations (A3) and (A4) can be used to calculate theoretically the front-gate voltage. In the limit where the interlayer separation is larger than the intralayer particle separation and (which usually amounts to the same thing) interlayer correlations can be neglected, then variations of μ_2 with p_F are small in comparison with edE_{12} , so that the effects of μ_2 can be absorbed into the voltage shift $eV_F^{(0)}$, thus giving

$$V_F \approx E_F D_F + E_{12} d + V_F^{(0)}. \quad (\text{A5})$$

2. Hartree-Fock approximation

In the Hartree-Fock Approximation (HFA) the two-body interaction is factored so that the ground-state energy per unit area is

$$\begin{aligned} \frac{\mathcal{E}_{HF}}{L_x L_y} &= \frac{1}{L_x L_y} \sum_{\mathbf{k}s} \varepsilon_k \langle c_{1\mathbf{k}s}^\dagger c_{1\mathbf{k}s} + c_{2\mathbf{k}s}^\dagger c_{2\mathbf{k}s} \rangle \\ &\quad - \frac{t}{L_x L_y} \sum_{\mathbf{k}s} \langle c_{1\mathbf{k}s}^\dagger c_{2\mathbf{k}s} + c_{2\mathbf{k}s}^\dagger c_{1\mathbf{k}s} \rangle \\ &\quad - \frac{1}{2(L_x L_y)^2} \sum_{j_1 \mathbf{k}_1 s_1} \sum_{j_2 \mathbf{k}_2 s_2} V_{j_1 j_2}(|\mathbf{k}_2 - \mathbf{k}_1|) \\ &\quad \times \langle c_{j_1 \mathbf{k}_2 s_1}^\dagger c_{j_2 \mathbf{k}_2 s_2} \rangle \langle c_{j_2 \mathbf{k}_1 s_2}^\dagger c_{j_1 \mathbf{k}_1 s_1} \rangle \\ &\quad + \frac{1}{2} \sum_{j_1} \sum_{j_2} V_{j_1 j_2}(q=0) n_{j_2} n_{j_1} \\ &\quad - \sum_j \sum_\alpha V_{j\alpha}(q=0) p_\alpha n_j \\ &\quad + \frac{1}{2} \sum_{\alpha\beta} V_{\alpha\beta}(q=0) p_\alpha p_\beta. \end{aligned} \quad (\text{A6})$$

The effect last three (the Hartree) terms of Eq. (A6) may be calculated by noting that

$$\begin{aligned} \lim_{q \rightarrow 0} V_{ij}(q) &= \lim_{q \rightarrow 0} \frac{e^2}{2\epsilon q} [1 - (1 - e^{-qd_{ij}})] \\ &= \left(\lim_{q \rightarrow 0} \frac{e^2}{2\epsilon q} \right) - \frac{e^2}{2\epsilon} d_{ij} \equiv (\infty) - \frac{e^2}{2\epsilon} d_{ij}, \end{aligned} \quad (\text{A7})$$

where (∞) denotes the formally divergent part in the last line of Eq. (A7). The last three (the Hartree) terms of Eq. (A6) become

$$(\infty) \frac{1}{2} (n_1 + n_2 - p_F - p_B)^2 + \frac{e^2 d}{2\epsilon} (p_F - n_1)(n_2 - p_B) \quad (\text{A8}) \\ + \frac{e^2 D_F}{2\epsilon} p_F (n_1 + n_2 - p_B) + \frac{e^2 D_B}{2\epsilon} p_B (n_1 + n_2 - p_F).$$

Requiring the first term of Eq. (A8) to not diverge imposes charge neutrality: $n_1 + n_2 = p_F + p_B$. From Gauss's law, the Hartree energy [Eq. (A8)] may therefore be written, up to an overall constant, as

$$\frac{\epsilon}{2} [E_{12}^2 d + E_F^2 D_F + E_B^2 D_B], \quad (\text{A9})$$

where E_{12} is the electric field between layers 1 and 2, E_F is the electric field between the front gate and layer 1, and E_B is the electric field between the back gate and layer 2.

Equation (A9) is just the electric field energy per unit area for the sample; we drop the last two terms since they may be regarded as constants for fixed p_F and p_B . The ground-state energy per unit area may thus be written as

$$\frac{\mathcal{E}_0}{L_x L_y} = \frac{1}{L_x L_y} \sum_{\mathbf{k}s} \varepsilon_k \langle c_{1\mathbf{k}s}^\dagger c_{1\mathbf{k}s} + c_{2\mathbf{k}s}^\dagger c_{2\mathbf{k}s} \rangle \quad (\text{A10}) \\ - \frac{t}{L_x L_y} \sum_{\mathbf{k}s} \langle c_{1\mathbf{k}s}^\dagger c_{2\mathbf{k}s} + c_{2\mathbf{k}s}^\dagger c_{1\mathbf{k}s} \rangle + \frac{e^2 d}{2\epsilon} (n_1 - p_F)^2 \\ - \frac{1}{2(L_x L_y)^2} \sum_{j_1 \mathbf{k}_1 s_1} \sum_{j_2 \mathbf{k}_2 s_2} V_{j_1 j_2} (|\mathbf{k}_2 - \mathbf{k}_1|) \\ \times \langle c_{j_1 \mathbf{k}_1 s_1}^\dagger c_{j_2 \mathbf{k}_2 s_2} \rangle \langle c_{j_2 \mathbf{k}_1 s_2}^\dagger c_{j_1 \mathbf{k}_1 s_1} \rangle.$$

3. Exchange integrals

The exchange integral $I_{\alpha\beta s}(q)$ is defined as

$$I_{\alpha\beta s}(q) = \frac{1}{L_x L_y} \sum_{\mathbf{K}} \Theta(k_{\alpha s} - |\mathbf{K} + \mathbf{q}/2|) \quad (\text{A11}) \\ \times \Theta(k_{\beta s} - |\mathbf{K} - \mathbf{q}/2|),$$

where α and β can be either a or b , and where $k_{\alpha s}, k_{\beta s}$ denote the Fermi wave vectors for particles of spin $s = \uparrow, \downarrow$ in subbands a or b . Note that Eq. (A11) implies that $I_{\alpha\beta s}$ is $1/(2\pi)^2$ times the shaded area shown in Fig. 18, where for concreteness \mathbf{q} is taken to be in the $\hat{\mathbf{x}}$ direction.

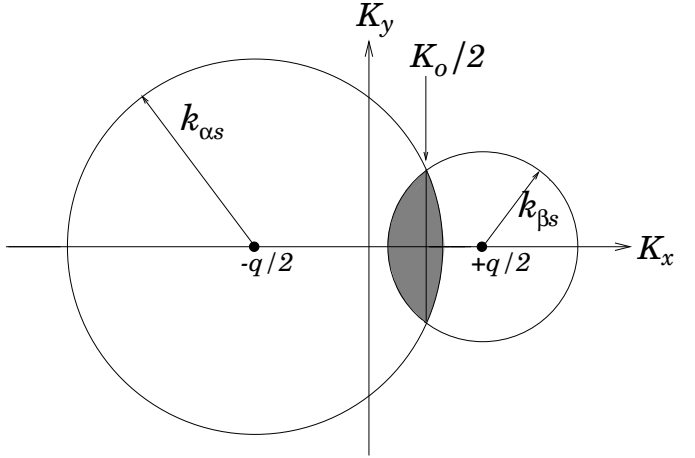


FIG. 18. The quantity $I_{\alpha\beta s}(q)$ is proportional to the area of the shaded region of overlap between two circular Fermi surfaces of radii $k_{\alpha s}$ and $k_{\beta s}$, which are centered at $K_x = \pm q/2$. The circular Fermi surfaces intersect at $K_x \equiv K_0/2$.

Let the quantity $K_0/2$ equal the value of K_x at which the Fermi circles of radius $k_{\alpha s}$ and $k_{\beta s}$ intersect:

$$K_0 = (k_{\alpha s}^2 - k_{\beta s}^2)/q = 4\pi(n_{\alpha s} - n_{\beta s})/q. \quad (\text{A12})$$

Then

$$I_{\alpha\beta s}(q) \equiv [n_{\beta s} \Theta(k_{\alpha s} - k_{\beta s} - q) + n_{\alpha s} \Theta(k_{\beta s} - k_{\alpha s} - q)] \quad (\text{A13}) \\ + \Theta(k_{\alpha s} + k_{\beta s} - q) \Theta(q - |k_{\alpha s} - k_{\beta s}|) \\ \times \frac{1}{\pi} \{ n_{\alpha s} [\cos^{-1} \left(\frac{q + K_0}{2k_{\alpha s}} \right) \\ - \left(\frac{q + K_0}{2k_{\alpha s}} \right) \sqrt{1 - \left(\frac{q + K_0}{2k_{\alpha s}} \right)^2}] \\ + n_{\beta} [\cos^{-1} \left(\frac{q - K_0}{2k_{\beta s}} \right) \\ - \left(\frac{q - K_0}{2k_{\beta s}} \right) \sqrt{1 - \left(\frac{q - K_0}{2k_{\beta s}} \right)^2}] \}.$$

When $\beta = \alpha$, then $k_{\beta s} = k_{\alpha s}$, $K_0 = 0$, and Eq. (A13) becomes

$$I_{\alpha\alpha s}(q) \equiv n_{\alpha s} \Theta(2k_{\alpha s} - q) \quad (\text{A14}) \\ \times \frac{2}{\pi} \left[\cos^{-1} \left(\frac{q}{2k_{\alpha s}} \right) - \left(\frac{q}{2k_{\alpha s}} \right) \sqrt{1 - \left(\frac{q}{2k_{\alpha s}} \right)^2} \right],$$

and the first exchange integral in Eq. (23) may be carried out explicitly:

$$-\frac{1}{2L_x L_y} \sum_{\mathbf{q}} V_{11}(q) I_{\alpha\alpha s}(q) = -\frac{8}{3\sqrt{\pi}} \frac{e^2}{4\pi\epsilon} n_{\alpha s}^{3/2}. \quad (\text{A15})$$

Equation (A15) is just the exchange energy per unit area for a uniform spin-polarized two-dimensional electron gas of areal density $n_{\alpha s}$.

4. Interlayer exchange parameter

A key quantity in our discussion of the effects of interlayer exchange in double-layer systems is the interlayer exchange parameter Γ , defined by

$$\Gamma \equiv \frac{1}{L_x L_y} \sum_{\mathbf{q}s} \left[\frac{V_{11}(q) - V_{12}(q)}{e^2 d / 2\epsilon} \right] \times \left[\frac{I_{aas}(q) + I_{bbs}(q) - 2I_{abs}(q)}{(n_a - n_b)^2} \right], \quad (\text{A16})$$

which is positive and a monotonically decreasing function of the interlayer separation d :

$$0 < \Gamma(d > 0) < \Gamma(d \rightarrow 0), \quad (\text{A17})$$

when the subband densities are regarded as fixed. We note that in the three-component phase ($p = 3$), unlike the ($p = 1, 2, 4$) phases, the equilibrium subband densities change with d , so that according to Eq. (46),

$$\lim_{d \rightarrow \infty} \Gamma_{\text{eq}}(p = 3) \propto \frac{1}{(n_a - n_b)^2 d} \propto \frac{d}{a_0} \rightarrow \infty, \quad (\text{A18})$$

when $p_F = p_B$, in apparent disagreement with Eq. (A17). We stress that the inequality in Eq. (A17) is true only when the subband densities $n_{\alpha s}$ are regarded as fixed, which is not the case in Eq. (A18).

The interlayer exchange parameter Γ is important because it determines when SILC is possible (for $\zeta < 1 - \Gamma_1$ and $p = 1$) – i.e., when $\sin \theta \neq 0$. It also determines the value of the pseudospin Stoner enhancement factor I (which depends on Γ_0). Γ affects the state of the system (e.g., layer densities and Eisenstein ratio R_E) whenever $\sin \theta \neq 0$.

a. Inequality

Using the inequality

$$e^2 d / 2\epsilon > V_{11}(q) - V_{12}(q), \quad (\text{A19})$$

which is true for $d > 0$, it follows from Eq. (A16) that for $d > 0$,

$$\begin{aligned} \Gamma &< \frac{1}{L_x L_y} \sum_{\mathbf{q}s} \left[\frac{I_{aas}(q) + I_{bbs}(q) - 2I_{abs}(q)}{(n_a - n_b)^2} \right] \\ &= \sum_s \frac{(n_{as} - n_{bs})^2}{(n_a - n_b)^2} = \Gamma(d \rightarrow 0), \end{aligned} \quad (\text{A20})$$

where we have used the fact that

$$\lim_{d \rightarrow 0} \frac{[V_{11}(q) - V_{12}(q)]}{e^2 d / 2\epsilon} = 1 \quad (\text{A21})$$

and

$$\begin{aligned} &\frac{1}{L_x L_y} \sum_{\mathbf{q}s} [I_{aas}(q) + I_{bbs}(q) - 2I_{abs}(q)] \\ &= \frac{1}{(L_x L_y)^2} \sum_{\mathbf{q}\mathbf{K}s} [\Theta(k_{as} - |\mathbf{K} + \mathbf{q}/2|) - \Theta(k_{bs} - |\mathbf{K} + \mathbf{q}/2|)] \\ &\quad \times [\Theta(k_{as} - |\mathbf{K} - \mathbf{q}/2|) - \Theta(k_{bs} - |\mathbf{K} - \mathbf{q}/2|)] \\ &= \sum_s \left\{ \frac{1}{L_x L_y} \sum_{\mathbf{k}} [\Theta(k_{as} - k) - \Theta(k_{bs} - k)] \right\}^2 \\ &= \sum_s (n_{as} - n_{bs})^2. \end{aligned} \quad (\text{A22})$$

Thus the condition

$$(n_{a\uparrow} - n_{b\uparrow})(n_{a\downarrow} - n_{b\downarrow}) \geq 0 \quad (\text{A23})$$

is sufficient to guarantee that $\Gamma < 1$.

Equation (A22) is true at finite temperature when $I_{\alpha\beta s}(q)$ is generalized appropriately. This is because

$$\lim_{d \rightarrow 0} [V_{11}(q) - V_{12}(q)] = \frac{e^2 d}{2\epsilon} \quad (\text{A24})$$

is independent of the wave vector q . We may write

$$\begin{aligned} \Gamma &= \frac{1}{(L_x L_y)^2} \sum_{\mathbf{k}_1, \mathbf{k}_2, s} \left[\frac{V_{11}(|\mathbf{k}_2 - \mathbf{k}_1|) - V_{12}(|\mathbf{k}_2 - \mathbf{k}_1|)}{e^2 d / 2\epsilon} \right] \\ &\times \left\{ \frac{\left(\langle a_{\mathbf{k}_2 s}^\dagger a_{\mathbf{k}_2 s} \rangle - \langle b_{\mathbf{k}_2 s}^\dagger b_{\mathbf{k}_2 s} \rangle \right) \left(\langle a_{\mathbf{k}_1 s}^\dagger a_{\mathbf{k}_1 s} \rangle - \langle b_{\mathbf{k}_1 s}^\dagger b_{\mathbf{k}_1 s} \rangle \right)}{(n_a - n_b)^2} \right\}, \end{aligned} \quad (\text{A25})$$

which generalizes Γ to finite temperatures. In the limit $d \rightarrow 0$, Eq. (A24) shows that Γ approaches

$$\begin{aligned} &\frac{1}{(n_a - n_b)^2} \sum_s \left[\frac{1}{L_x L_y} \sum_{\mathbf{k}} \left(\langle a_{\mathbf{k}s}^\dagger a_{\mathbf{k}s} \rangle - \langle b_{\mathbf{k}s}^\dagger b_{\mathbf{k}s} \rangle \right) \right]^2 \\ &= \frac{1}{(n_a - n_b)^2} \sum_s (n_{as} - n_{bs})^2 \\ &\rightarrow \begin{cases} 1, & p = 1 \quad (n_{a\uparrow} = n_T) \\ 1, & p = 2a \quad (n_{a\uparrow} = n_{b\uparrow} = n_T/2) \\ 1, & p = 3 \quad (n_{a\uparrow} = n_{a\downarrow} = n_{b\uparrow} = n_T/3) \\ 1/2, & p = 2b \quad (n_{a\uparrow} = n_{a\downarrow} = n_T/2) \\ 1/2, & p = 4 \quad (n_{a\uparrow} = n_{a\downarrow} = n_{b\uparrow} = n_{b\downarrow} = n_T/4) \end{cases}. \end{aligned} \quad (\text{A26})$$

Empirically, we find that within the MFA, the spins in subbands a and b are either completely unpolarized (at higher densities) or fully polarized (at sufficiently low densities.) Therefore the only possible MFA configurations of spin and pseudospin that would not satisfy the inequality in Eq. (A23) and that might therefore have $\Gamma > 1$ would be three-component ($p = 3$) states in which subband a (the majority subband) is spin-unpolarized and subband b (the minority subband) is spin-unpolarized:

$$n_{a\uparrow} = n_{a\downarrow}, n_a > n_{b\uparrow} > n_{b\downarrow} = 0. \quad (\text{A27})$$

b. Pseudospin-unpolarized Γ

It is useful to define and evaluate

$$\Gamma_0 \equiv \lim_{n_a \rightarrow n_b} \Gamma. \quad (\text{A28})$$

We begin our calculation of Γ_0 by noting that

$$\begin{aligned} I_{aas}(q) + I_{bbs}(q) - 2I_{abs}(q) &= \quad (\text{A29}) \\ &\frac{1}{L_x L_y} \sum_{\mathbf{K}} [\Theta(k_{as} - |\mathbf{K} + \mathbf{q}/2|) - \Theta(k_{bs} - |\mathbf{K} + \mathbf{q}/2|)] \\ &\quad \times [\Theta(k_{as} - |\mathbf{K} - \mathbf{q}/2|) - \Theta(k_{bs} - |\mathbf{K} - \mathbf{q}/2|)] \\ &\approx \frac{(k_F \Delta n / n_T)^2}{L_x L_y} \sum_{\mathbf{K}} \delta(k_F - |\mathbf{K} + \mathbf{q}/2|) \\ &\quad \times \delta(k_F - |\mathbf{K} - \mathbf{q}/2|) \\ &= \left(\frac{k_F}{2\pi} \frac{\Delta n}{n_T} \right)^2 \frac{\Theta(1-x)}{x\sqrt{1-x^2}}, \end{aligned}$$

where $\Delta n \equiv (n_a - n_b) \rightarrow 0$, $k_F = \sqrt{4\pi n_T/p}$ is the Fermi wave vector per layer for the state with p components ($p = 2, 4$), and $x \equiv q/2k_F$. Using Eq. (A29), we obtain

$$\begin{aligned} \Gamma_0 &= \frac{2}{p} \frac{2/\pi}{e^2 d/2\epsilon} \int_0^1 dx \frac{[V_{11}(2k_F x) - V_{12}(2k_F x)]}{\sqrt{1-x^2}} \quad (\text{A30}) \\ &= \frac{2}{p} \frac{2}{\pi z} \int_0^{\pi/2} d\theta \frac{(1 - e^{-z \sin \theta})}{\sin \theta}, \end{aligned}$$

where $z = 2k_F d$, and the second line is obtained by the substitution of variables $x = \sin \theta$. It is straightforward to obtain $\Gamma_0(z)$ for small $z \rightarrow 0$ by expanding the last line of Eq. (A30) in powers of z ,

$$\lim_{z \rightarrow 0} \Gamma_0(z) = \frac{2}{p} \left[1 - \frac{1}{\pi} z + \frac{1}{12} z^2 \right], \quad (\text{A31})$$

up to second order in z .

Obtaining Γ_0 for $z \rightarrow \infty$ is more cumbersome. One way to proceed is to define a cutoff ϵ that satisfies

$$\frac{1}{z} \ll \epsilon \ll 1 \quad (\text{A32})$$

so that $\sin \theta \approx \theta$ for $\theta < \epsilon$ and $z \sin \theta \gg 1$ for $\theta > \epsilon$. Then

$$\begin{aligned} \Gamma_0 &\approx \frac{2}{p} \frac{2}{\pi z} \left[\int_0^\epsilon d\theta \frac{(1 - e^{-z\theta})}{\theta} \right. \\ &\quad \left. + \int_\epsilon^{\pi/2} d\theta \frac{1}{\sin \theta} \right]. \quad (\text{A33}) \end{aligned}$$

The first integral in Eq. (A33) may be carried out using the identity^{41,42}

$$\int_0^R dt \frac{(1 - e^{-t})}{t} = \ln(R) + \gamma + \int_R^\infty dt \frac{e^{-t}}{t}, \quad (\text{A34})$$

where $\gamma \approx 0.5772$ is Euler's constant, and $R \equiv z\epsilon \rightarrow \infty$, so that the last term of Eq. (A34) can be dropped for large R . The second integral in Eq. (A33) is well known:⁴³

$$\int d\theta \frac{1}{\sin \theta} = \ln[\tan(\theta/2)]. \quad (\text{A35})$$

Now, $\tan(\epsilon/2) \approx \epsilon/2$ for $\epsilon \ll 1$, so that the logarithmically divergent ($\sim \ln \epsilon$) parts of the two integrals in Eq. (A33) cancel each other, leaving

$$\lim_{z \rightarrow \infty} \Gamma_0 = \frac{2}{p} \frac{2}{\pi z} [\ln(2z) + \gamma]. \quad (\text{A36})$$

c. Pseudospin-polarized Γ

We now compute

$$\Gamma_1 \equiv \lim_{n_a \rightarrow n_T} \Gamma. \quad (\text{A37})$$

When the double-layer system is pseudospin polarized so that $n_a = n_T$, then $I_{bbs}(q) = I_{abs}(q) = 0$, and it follows from Eqs. (A14) and (A16) that

$$\begin{aligned} \Gamma_1 &= \frac{1}{p} \frac{16}{\pi z} \int_0^1 dx (1 - e^{-zx}) [\arccos(x) - x\sqrt{1-x^2}] \quad (\text{A38}) \\ &= \frac{1}{p} \frac{32}{3\pi z} [1 - S(z)], \end{aligned}$$

where $z \equiv 2k_F d$, and

$$\begin{aligned} S(z) &= \frac{3}{2} \int_0^1 dx e^{-zx} [\arccos(x) - x\sqrt{1-x^2}] \quad (\text{A39}) \\ &= \frac{3\pi}{4z} \left\{ 1 - \frac{2}{z} [I_1(z) - L_1(z)] \right\} \\ &\rightarrow \begin{cases} 1 - (3\pi/32)z + (1/15)z^2 - (\pi/256)z^3, & z \rightarrow 0 \\ 3\pi/4z, & z \rightarrow \infty \end{cases} \end{aligned}$$

so that

$$\Gamma_1(z) \rightarrow \frac{1}{p} \begin{cases} 1 - (32/45\pi)z + (1/24)z^2, & z \rightarrow 0 \\ (32/3\pi)/z - 8/z^2, & z \rightarrow \infty \end{cases} \quad (\text{A40})$$

Here I_1 and L_1 are modified Bessel and modified Struve functions of the first kind, respectively.^{44,45}

$$I_n(z) = i^{-n} J_n(iz), \quad L_n(z) = i^{-(n+1)} H_n(iz), \quad (\text{A41})$$

where J_n is the ordinary Bessel function of order n , and H_n is the Hankel function of order n .

Obtaining Eq. (A39) is somewhat involved. The first part of the integral in the first line of Eq. (A39) can be obtained by writing

$$\int_0^1 dx e^{-zx} \arccos(x) = \int_0^1 dx e^{-zx} \left[\frac{\pi}{2} - \arcsin(x) \right], \quad (\text{A42})$$

and using the identity⁴⁶

$$\begin{aligned} & \int_0^1 dx e^{-zx} \arcsin(x) \\ &= \frac{\pi}{2z} [I_0(z) - L_0(z) - e^{-z}], \end{aligned} \quad (\text{A43})$$

which corrects a misprint in Eq. (4.551.1) of Ref. 41. One then obtains

$$\begin{aligned} & \int_0^1 dx e^{-zx} \arccos(x) \\ &= \frac{\pi}{2z} [1 + L_0(z) - I_0(z)], \end{aligned} \quad (\text{A44})$$

The second part of the integral in the first line of Eq. (A39) can be obtained by writing

$$\begin{aligned} & \int_0^1 dx e^{-zx} x \sqrt{1-x^2} = -\frac{\partial}{\partial z} \int_0^1 dx e^{-zx} \sqrt{1-x^2} \quad (\text{A45}) \\ &= -\frac{\partial}{\partial z} \left[1 - \int_0^1 dx \frac{ze^{-zx}}{\sqrt{1-x^2}} \right] \\ &= \frac{\pi}{2} \frac{\partial}{\partial z} \left[\frac{L_1(z) - I_1(z)}{z} \right], \end{aligned}$$

and by using the identities⁴⁷

$$\begin{aligned} \frac{\partial}{\partial z} \left[\frac{I_1(z)}{z} \right] &= \frac{I_2(z)}{z} \\ \frac{\partial}{\partial z} \left[\frac{L_1(z)}{z} \right] &= \frac{L_2(z)}{z} + \frac{2}{3\pi} \end{aligned} \quad (\text{A46})$$

to obtain

$$\int_0^1 dx e^{-zx} x \sqrt{1-x^2} = \frac{1}{3} + \frac{\pi}{2z} [L_2(z) - I_2(z)] \quad (\text{A47})$$

Combining Eqs. (A44) and (A47) and using the identities⁴⁸

$$\begin{aligned} I_0(z) - I_2(z) &= \frac{2I_1(z)}{z} \\ L_0(z) - L_2(z) &= \frac{2L_1(z)}{z} + \frac{2z}{3\pi} \end{aligned} \quad (\text{A48})$$

gives the second line of Eq. (A39). The third line of Eq. (A39) follows from power series (for small z) and asymptotic (for large z) expansions of $I_1(z)$ and $L_1(z)$.⁴⁹

We note that for the same value of p , $\Gamma_1(z) \leq \Gamma_0(z)$ for all z . This may be seen by the substitution of variables $x = \sin \theta$ in Eq. (A38):

$$\begin{aligned} \Gamma_1(z) &= \frac{2}{p} \frac{2}{\pi} \int_0^{\pi/2} d\theta \frac{(1 - e^{-z \sin \theta})}{z \sin \theta} \\ &\times \{\sin(2\theta) [(\pi - 2\theta) - \sin(2\theta)]\} \leq \Gamma_0(z), \end{aligned} \quad (\text{A49})$$

where Γ_0 is expressed as an integral over θ in the last line of Eq. (A30). However, for differing values of p ,

$\Gamma_1(p=1) > \Gamma_0(p=2)$ for $0 < z < z_c \approx 44.09$. Both $\Gamma_1(p=1)$ and $\Gamma_0(p=2)$ are plotted in Fig. 19. For $z > z_c$ (not shown), $\Gamma_1(p=1) < \Gamma_0(p=2)$.

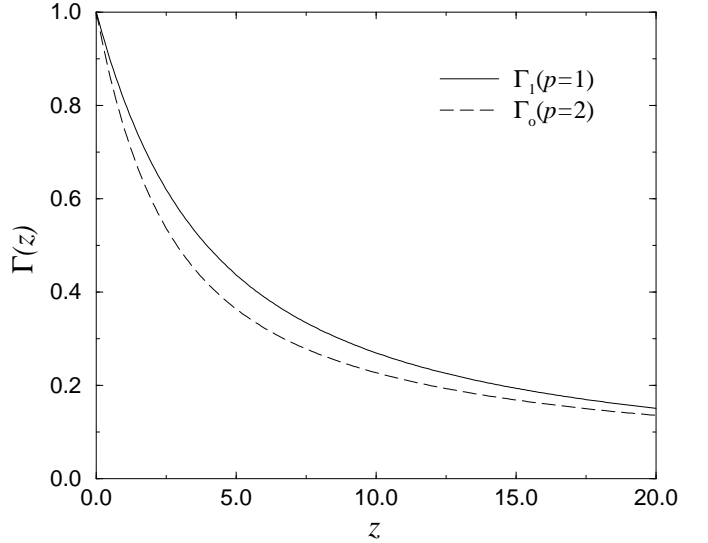


FIG. 19. $\Gamma_1(p=1)$ (solid curve) and $\Gamma_0(p=2)$ (dashed curve) as a function of $z = 2k_Fd$. For $0 < z < z_c \approx 44.09$, $\Gamma_1(p=1) > \Gamma_0(p=2)$.

5. Stoner enhancement factor

We now outline our calculation of the Stoner interaction parameter for $t \rightarrow 0$. Consider a two- or four-component state with equal subband densities (pseudospin unpolarized), $n_a = n_b = n_T/2$. For small $t \rightarrow 0$, imagine moving a small amount of charge $\Delta n/2$ from subband b to subband a , $n_a \rightarrow n_T/2 + \Delta n/2$, $n_b \rightarrow n_T/2 - \Delta n/2$, so that $(n_a - n_b) = \Delta n$, and calculate the change in the total energy [Eq. (23)] as $\Delta n \rightarrow 0$. The effect of the change of densities on the last term of Eq. (23) may be calculated by using Eq. (A30). The change in the energy per unit area due to Δn as $\Delta n \rightarrow 0$ is then given by

$$\begin{aligned} \frac{\Delta \mathcal{E}_0}{L_x L_y} &= \frac{(\Delta n)^2}{p \nu_0} - t \Delta n - \frac{1}{\sqrt{\pi p}} \frac{e^2}{4\pi\epsilon} \frac{(\Delta n)^2}{\sqrt{n_T}} \\ &+ \frac{e^2 d}{2\epsilon} \left(\frac{\Delta n}{2} \right)^2 \Gamma_0. \end{aligned} \quad (\text{A50})$$

Minimizing $\Delta \mathcal{E}_0 / L_x L_y$ with respect to Δn to solve for Δn and using the definition Eq. (55) of the Stoner enhancement I gives

$$\begin{aligned} I &= \frac{\nu_0 e^2}{2\pi\epsilon k_F} \left(1 - p \frac{\pi}{4} k_F d \Gamma_0 \right) \\ &= \frac{\nu_0}{\pi} \left\{ 2V_{11}(2k_F) - \int_0^1 dx \frac{[V_{11}(2k_F x) - V_{12}(2k_F x)]}{\sqrt{1-x^2}} \right\}, \end{aligned} \quad (\text{A51})$$

which is just the first line of Eq. (56). Equation (A51) is equal to the $t \rightarrow 0$ limit of the Stoner interaction pa-

parameter calculated in the GRPA, given in Eq. (14) of Ref. 23.

6. Intersubband gap

The subband transfer energy Δ_{ab} for the pseudospin-polarized ($n_a = n_T$) $p = 1$ or $p = 2b$ phase is defined as the MFA energy required to move a particle from the occupied a subband to the (otherwise empty) b subband:

$$\Delta_{ab} = \frac{\delta}{\delta n} \left(\frac{\mathcal{E}_0}{L_x L_y} \right), \quad (\text{A52})$$

where $\delta\mathcal{E}_0$ denotes the change of \mathcal{E}_0 under

$$\begin{aligned} n_{a\uparrow} &\rightarrow (1/p)(n_T - \delta n), & n_{b\uparrow} &\rightarrow \delta n, \\ n_{a\downarrow} &\rightarrow (1 - 1/p)(n_T - \delta n), & n_{b\downarrow} &= 0, \end{aligned} \quad (\text{A53})$$

where $\delta n \ll n_T$, and $n_{b\downarrow} = 0$ reflects the fact that at low densities ($n_b = \delta n \rightarrow 0$), subband b will be spin-polarized. In order to calculate Δ_{ab} we first compute

$$\begin{aligned} &\frac{\delta}{\delta n} \sum_s [I_{aas}(q) + I_{bbs}(q) - 2I_{abs}(q)] \quad (\text{A54}) \\ &= \frac{\delta}{\delta n} \frac{1}{L_x L_y} \sum_{\mathbf{K}} [\Theta(k_{as} - |\mathbf{K} + \mathbf{q}/2|) - \Theta(k_{bs} - |\mathbf{K} + \mathbf{q}/2|)] \\ &\quad \times [\Theta(k_{as} - |\mathbf{K} - \mathbf{q}/2|) - \Theta(k_{bs} - |\mathbf{K} - \mathbf{q}/2|)] \\ &\approx \frac{\delta}{\delta n} \frac{2}{L_x L_y} \sum_{\mathbf{K}s} \Theta(k_{as} - |\mathbf{K} + \mathbf{q}/2|) [\delta k_{as} \delta(k_{as} - |\mathbf{K} - \mathbf{q}/2|) \\ &\quad - \Theta(\delta k_{bs} - |\mathbf{K} - \mathbf{q}/2|)] \\ &\approx \frac{\delta}{\delta n} \frac{1}{2\pi^2} \sum_s \left[\delta k_{as} \int d^2 K \Theta(k_{as} - |\mathbf{K} + \mathbf{q}|) \delta(k_{as} - |\mathbf{K}|) \right. \\ &\quad \left. - \Theta(\delta k_{bs} - |\mathbf{K}|) \right] \\ &= \frac{\delta}{\delta n} \frac{1}{2\pi^2} \sum_s [2k_{as} \delta k_{as} \arccos(q/2k_{as}) \Theta(2k_{as} - q) \\ &\quad - \pi(\delta k_{bs})^2 \Theta(k_{as} - q)] \\ &= - \left[\frac{2}{\pi} \Theta(1-x) \arccos(x) + 2\Theta(1/2-x) \right], \end{aligned}$$

where $k_{as} = \sqrt{4\pi n_{as}}$ so that

$$\delta k_{as} = -(2\pi/k_F)\delta n_{as}, \quad \delta k_{b\uparrow} = -\sqrt{4\pi\delta n}, \quad (\text{A55})$$

and $k_F = \sqrt{4\pi n_T/p}$. In order to obtain the last line of Eq. (A54), we expanded the bracketed terms to first order with respect to δn , and defined $x \equiv q/2k_F$.

The subband transfer gap is then given by

$$\begin{aligned} \Delta_{ab} &= -\frac{2n_T}{p\nu_0} + 2t \sin \theta + \frac{4}{\sqrt{\pi}} \frac{e^2}{4\pi\epsilon} \sqrt{n_T/p} \quad (\text{A56}) \\ &\quad - \frac{e^2 d n_T}{2\epsilon} \cos \theta (\cos \theta - \zeta) \\ &\quad - \frac{\sin^2 \theta}{4} \frac{e^2 k_F}{2\pi\epsilon} \left\{ \frac{[e^{-z/2} - (1-z/2)]}{z/2} \right. \\ &\quad \left. + \frac{2}{\pi} \int_0^1 dx (1 - e^{-zx}) \arccos(x) \right\}, \end{aligned}$$

where $\zeta = (p_F - p_B)/n_T$ and $z = 2k_F d$. Equation (A56) is expressed in dimensionless form in Eq. (105).

* Present address: Department of Materials Science and Engineering, University of Arizona, Tucson, AZ 85721.

¹ *The Quantum Hall Effect* (Springer-Verlag: New York, 1990), edited by R. E. Prange and S. M. Girvin, and references therein.

² *Perspectives in Quantum Hall Effects* (Wiley: New York, 1997), edited by S. Das Sarma and A. Pinczuk, and references therein.

³ J. P. Eisenstein, G. S. Boebinger, L. N. Pfeiffer, K. W. West, and S. He, Phys. Rev. Lett. **68**, 1383 (1992);

⁴ Y. W. Suen, L. W. Engel, M. B. Santos, M. Shayegan, and D. C. Tsui, Phys. Rev. Lett. **68**, 1379 (1992).

⁵ S. Q. Murphy, J. P. Eisenstein, G. S. Boebinger, L. N. Pfeiffer, and K. W. West, Phys. Rev. Lett. **72**, 728 (1994).

⁶ K. Yang, K. Moon, L. Zheng, A. H. MacDonald, S. M. Girvin, D. Yoshioka, and S. C. Zhang, Phys. Rev. Lett. **72**, 732 (1994).

⁷ K. Moon, H. Mori, K. Yang, S. M. Girvin, A. H. MacDonald, L. Zheng, D. Yoshioka, and S. C. Zhang, Phys. Rev. B **51**, 5138 (1995).

⁸ K. Yang, K. Moon, L. Belkhir, H. Mori, S. M. Girvin, A. H. MacDonald, L. Zheng, and D. Yoshioka, Phys. Rev. B **54**, 11 644 (1996).

⁹ See S. M. Girvin and A. H. MacDonald, “Multicomponent Quantum Hall Systems: The Sum of Their Parts and More”, in *Perspectives in Quantum Hall Effects* (Wiley: New York, 1997), edited by S. Das Sarma and A. Pinczuk, and references therein.

¹⁰ J. P. Eisenstein, L. N. Pfeiffer, and K. W. West, Phys. Rev. B **50**, 1760 (1994); J. P. Eisenstein, L. N. Pfeiffer, and K. W. West, Phys. Rev. Lett. **68**, 674 (1992).

¹¹ M. B. Pogrebinskii, Fiz. Tekh. Poluprovodn **11**, 637 (1977) [Sov. Phys. Semicond. **11**, 372 (1977)]; P. J. Price, Physica B+C **117/118**, 750 (1983); Lian Zheng and A. H. MacDonald, Phys. Rev. B **48**, 8203 (1993).

¹² F. Bloch, Z. Phys. **57**, 545 (1929).

¹³ A. H. MacDonald, Surf. Sci. **229**, 1 (1990).

¹⁴ A. H. MacDonald, P. M. Platzman, and G. S. Boebinger, Phys. Rev. Lett. **65**, 775 (1990), L. Brey, *ibid.* **65**, 903 (1990); H. Fertig, Phys. Rev. B **40**, 1087 (1989).

¹⁵ P. Paul Ruden and Zhiqiang Wu, Appl. Phys. Lett. **59**, 2165 (1991).

¹⁶ A. H. MacDonald, Phys. Rev. B **37**, 4792 (1988).

¹⁷ Lian Zheng, M. W. Ortalano, and S. Das Sarma, Phys. Rev. B **55**, 4506 (1997); S. Das Sarma, M. W. Ortalano, and Lian Zheng, Phys. Rev. B **58**, 7453 (1998).

¹⁸ S. Conti and G. Senatore, Europhys. Lett. **36**, 695 (1996).

¹⁹ Y. Katayama, D. C. Tsui, H. C. Manoharan, and M. Shayegan, Surf. Sci. **305**, 405 (1994); Y. Katayama, D. C. Tsui, H. C. Manoharan, S. Parihar, and M. Shayegan, Phys. Rev. B **52**, 14817 (1995).

²⁰ X. Ying, S. R. Parihar, H. C. Manoharan, and M. Shayegan, Phys. Rev. B **52**, R11611 (1995).

²¹ I. S. Millard, N. K. Patel, M. Y. Simmons, E. H. Linfield, D. A. Ritchie, G. A. C. Jones, and M. Pepper, Appl. Phys.

- Lett. **68**, 3323 (1996).
- ²² S. J. Papadakis, J. P. Lu, M. Shayegan, S. R. Parikh, and S. A. Lyon, Phys. Rev. B **55**, 9294 (1997).
- ²³ L. Świerkowski and A. H. MacDonald, Phys. Rev. B **55**, R16017 (1997).
- ²⁴ K. S. Singwi, M. P. Tosi, R. H. Land, and A. Sjölander, Phys. Rev. **176**, 589 (1968).
- ²⁵ Lerwen Liu and A. H. MacDonald, in preparation.
- ²⁶ T. Jungwirth and A. H. MacDonald, Phys. Rev. B **53**, 9943 (1996).
- ²⁷ G. Ortiz, M. Harris, and P. Ballone, Phys. Rev. Lett. **82**, 5317 (1999).
- ²⁸ F. Rapisarda and G. Senatore, Aust. J. Phys. **49**, 161 (1996).
- ²⁹ S. Shapira, U. Sivan, P. M. Solomon, E. Buchstab, M. Tischler, and G. Ben Yoseph, Phys. Rev. Lett. **77**, 3181 (1996).
- ³⁰ A. R. Hamilton, M. Y. Simmons, F. M. Bolton, N. K. Patel, I. S. Millard, J. T. Nicholls, D. A. Ritchie, and M. Pepper, Phys. Rev. B **54**, R5259 (1996). We are very grateful to A. R. Hamilton for providing us with the numerical data used in Fig. 6.
- ³¹ S. R. Renn, Phys. Rev. Lett. **68**, 658 (1992); Kun Yang, Phys. Rev. B **58**, R4246 (1998).
- ³² A. Stern, S. Das Sarma, M. P. A. Fisher, and S. M. Girvin, Phys. Rev. Lett. **84**, 139 (2000).
- ³³ Y. B. Kim and A. J. Millis, preprint cond-mat/9611125.
- ³⁴ S. Sakhi, Phys. Rev. B **56**, 4098 (1997).
- ³⁵ I. Ussishkin and A. Stern, Phys. Rev. B **56**, 4013 (1997).
- ³⁶ N. E. Bonesteel, I. A. McDonald, and C. Nayak, Phys. Rev. Lett. **77**, 3009 (1996); N. E. Bonesteel, Phys. Rev. B **48**, 11484 (1993).
- ³⁷ I. Ussishkin and A. Stern, Phys. Rev. Lett. **81**, 3932 (1998).
- ³⁸ F. Zhou and Y. B. Kim, Phys. Rev. B **59**, R7825 (1999).
- ³⁹ M. P. Lilly, J. P. Eisenstein, L. N. Pfeiffer, and K. W. West, Phys. Rev. Lett. **80**, 1714 (1998).
- ⁴⁰ I. B. Spielman, J. P. Eisenstein, L. N. Pfeiffer, and K. W. West, preprint cond-mat/0002387.
- ⁴¹ *Table of Integrals, Series, and Products*, I. S. Gradshteyn and I. M. Ryzhik (Academic Press, New York, 1980).
- ⁴² *Table of Integrals, Series, and Products*, (Ref. 41) Eqs. (8.212.1) and (8.211.1).
- ⁴³ *Table of Integrals, Series, and Products*, (Ref. 41), Eq. (2.526.1).
- ⁴⁴ *Table of Integrals, Series, and Products*, (Ref. 41), Eq. (8.406.3).
- ⁴⁵ *Table of Integrals, Series, and Products*, (Ref. 41), Eq. (8.550.2).
- ⁴⁶ *Table of Integrals, Series, and Products*, (Ref. 41); Equation (4.551.1) of Ref. 41 is incorrect as printed. The correct formula may be obtained by using Eqs. (8.431.4) and (8.551.2) of Ref. 41, and is given in Eq. (A43) of the Appendix.
- ⁴⁷ *Table of Integrals, Series, and Products*, (Ref. 41), Eqs. (8.486.3) and (8.553.3).
- ⁴⁸ *Table of Integrals, Series, and Products*, (Ref. 41), Eqs. (8.486.1), (8.550.2), and (8.553.4) express the first order modified Bessel (I_1) and modified Struve (L_1) functions in terms of the corresponding zeroth and second order functions.
- ⁴⁹ *Table of Integrals, Series, and Products*, (Ref. 41), Eqs. (8.447.2) and (8.550.2).